Aids to navigation design and review: Phase I report
Kennedy, Allison; Raman-Nair, Wayne; Williams, Christopher; Seo, Dong Cheol

National Research Council Canada   Conseil national de recherches Canada

NATIONAL RESEARCH COUNCIL CANADA
OCEAN, COASTAL AND RIVER ENGINEERING

Aids to Navigation Design and Review Phase I Report

Technical Report

Allison Kennedy, Wayne Raman-Nair, Christopher Williams and Dong Cheol Seo

December 2013

Canada

Report Documentation Form

NRC·CNRC Ocean, Coastal and River Engineering – Génie océanique côtier et fluvial

Report Number: OCRE-TR-2013-048

Program Arctic Technologies		Project Number A1-003893		Publication Type Technical Report
Title (and/or other title) Aids to Navigation Design and Review - Phase I Report				
Author(s) – Please specify if necessary, corporate author(s) and Non-NRC author(s) Allison Kennedy, Wayne Raman-Nair, Christopher Williams and Dong Cheol Seo				
Client(s) Canadian Coast Guard				
Key Words (5 maximum) navigation risk, maneuvering, squat, sea-keeping			**Pages** 154	**Confidentiality Period** N/A
Security Classification UNCLASSIFIED	**Distribution** UNLIMITED	**How long will the report be Classified/Protected?** N/A		
Limited Distribution List (mandatory when distribution is Limited)				

Date:	VER #	Description:	Prepared by:	Check by:
19/12/2013	1	Initial draft report sent to client	AK	CCG
07/04/2014	2	Client comments addressed	AK	
Click here to enter a date.				
Click here to enter a date.				
Click here to enter a date.				
Click here to enter a date.				
Click here to enter a date.				
Click here to enter a date.				

Anne Barker
Program Lead

Signature

Director of R & D

Signature

NRC – OCRE Addresses

Ottawa
1200 Montreal Road, M-32
Ottawa, ON, K1A 0R6

St. John's
P.O. Box 12093, 1 Arctic Avenue
St. John's, NL, A1B 3T5

National Research Council Canada   Conseil national de recherches Canada

Canada

National Research Council Canada
Conseil national de recherches Canada

Ocean, Coastal and River Engineering
Génie océanique, côtier et fluvial

Aids to Navigation Design and Review
Phase I Report

OCRE-TR-2013-048

Allison Kennedy, Wayne Raman-Nair, Christopher Williams and Dong Cheol Seo

December 2013

Executive Summary

Purpose
This report summarizes the results of the work completed in Phase I of the CCG-funded project: Aids to Navigation Design and Review. In general, this project involves the development of a tool to help quantify navigational risk to support the design of marine short range navigational aid systems. Phase I of this project includes a review of currently available guidelines and tools for the design of navigational aid systems and waterways, as well as the preliminary development of the Navigational Risk Identification Module (NRIM).

Content and Structure
Section 1 introduces this investigation and describes its main elements. Section 2 provides a review of existing guidelines and tools that support the design and review of marine navigational aid systems. Section 3 outlines the preliminary development of the NRIM in terms of an assessment of methods to predict squat, a review of wave induced heave and pitch prediction as well as details of maneuvering model development. Section 4 outlines the vessel and channel parameters used in Phase I of this investigation. Section 5 presents preliminary comparisons of Phase I NRIM output with the outputs from the Kitimat study; this includes ship zig-zag and turning circle performance, effects of wind, waves and shallow water, squat and heave and pitch predictions, and, a discussion of the discrepancies found. Section 6 outlines the work proposed for Phase II including narrow-channel and bank-proximity effects, two-way traffic, overtaking and passing effects. Section 6.6 summarizes questions posed for the work of Phase II. Appendix A provides the details for the ship maneuvering model and explains how the trajectory of the ship is simulated. Appendix B provides the details for how the wave-induced motions of ships are estimated; examples are provided for a VLCC including comparisons with the outputs of the Kitimat study. Appendix C provides the details for how ship squat is predicted by 16 different formulae for open-water conditions, and, by seven formulae for confined-waterway conditions; comparisons are made with limited full-scale measurements in the Panama Canal.

Conclusions
During this preliminary investigation there were a number of potential methods explored that predict ship hydrodynamic derivatives (required by the maneuvering model), ship squat and wave induced motions. The Phase I review was not exhaustive since there were a large number of formulations available in the literature, that could be used to predict the aforementioned parameters. Based on those that were reviewed, certain methods did demonstrate more promising attributes than others in terms of their usefulness in NRIM for the open water case. For hydrodynamic derivative prediction, the empirical equations presented by Clarke [1], when used in the Phase I maneuvering model, compared reasonably well to the simulated data provided in the Kitimat study. Another positive attribute of these equations is that they have shallow water correction factors available. In terms of wave induced motions, the predictions using the empirical formulation by Jensen [2] followed the trend of predictions with the strip-theory method and provide a relatively un-complex and

analytical equation for prediction. The strip-theory method provides a more accurate prediction by considering the detailed geometry of hull form and compares well to ShipMo3D predictions. The assessment of ship squat, as detailed in Appendix C, considered a number of empirical relationships, some of which correlated closely with measured data.

A positive attribute of all of the aforementioned formulations is that they require only basic (non-complex) input relating to the ship or channel. In addition, the use of such methods would require minimal computation time and would not require expertise for problem set-up. This type of formulation may be better suited to the problem at hand as opposed to complex methods which require difficult input and lengthy computational time. Validation of these methods against full or model scale data would allow for a more thorough assessment of their performance.

Contents

List of Figures

List of Tables

List of Acronyms

AMCSD Analysis Module of Climatological Site Data

BEM Boundary Element Method

CCG Canadian Coast Guard

CFD Computational Fluid Dynamics

DOF degree of freedom

DOFs degrees of freedom

DRDC Defence Research and Development Canada

DGPS Differential Global Positioning System

GPS Global Positioning System

GUI Graphical User Interface

IACS International Association of Classification Society

JTP Joint Tanker Project

LCG Longitudinal Centre of Gravity

MDA Minimum Depth Allowance

MMG Mathematical Modelling Group

NRC National Research Council Canada

NRIM Navigational Risk Identification Module

OCRE Ocean, Coastal and River Engineering portfolio

OEB Ocean Engineering Basin

PIANC Permanent International Association of Navigation Congresses

PMM Planar Motion Mechanism

RAO Response Amplitude Operator

VLCC Very Large Crude Carrier

1　INTRODUCTION

This report provides details Phase I of a project, undertaken by the National Research Council Canada (NRC) of Canada, that aims to develop a numerical tool to support the Canadian Coast Guard (CCG) process for the design and review of marine Aids to Navigation systems. The first component of Phase I involved a review of existing design guidelines and support tools. A comprehensive review of the CCG Procedures Manual for the design and review of marine short-range aids to navigation systems as well as the waterway design guidelines developed by PIANC was completed. This was complemented by a detailed review of two numerical tools that could provide design support. The first, a tool developed primarily by the Japan Institute of Navigation, was identified by the CCG during initial project discussions. The second was a tool developed by FORCE Technology which is the source of the simulated data that was provided to NRC by the CCG for comparison and validation of Phase I work.

The second component of Phase I involves the preliminary development of a numerical tool, labelled as the Navigational Risk Identification Module (NRIM), to support the CCG Navigational Aid System design and review process. The NRIM is designed to provide output as specified by CCG. The development of NRIM is supported by findings from the review of existing guidelines and potential support tools. The NRIM is comprised of two main components: the Minimum Depth Allowance (MDA) model and the maneuvering model. Each component is developed independently and reported separately in this document. The description of NRIM development includes a discussion of preliminary NRIM capabilities, required input and assumptions.

The third component of Phase I involves providing the output from preliminary NRIM and maneuvering model for a specified scenario. The NRIM output is compared to simulated data provided by the CCG. Details of these comparisons are provided as well as a discussion of possible justifications for discrepancies. Subsequently, details of the CCG requested NRIM output are discussed in relation to the Phase I output. In some instances, the Phase I NRIM output provides only a component of a requested parameter. For example, preliminary NRIM can output squat, heave and pitch motions, which are considered in the computation of MDA. However, preliminary NRIM does not consider any safety factor that may be applied to the MDA calculation. In these cases, potential additions to the Phase I NRIM output are described to allow for full investigation of the parameters.

The final section of this report includes a summary of details relating to proposed Phase II NRIM development. Phase II development was summarized in the project proposal and designed to achieve the desired NRIM output as requested by CCG. Through Phase I development, findings and insight relating to the tasks involved in Phase II have been identified and are summarized for consideration. The details provided in this report should lead group discussions between the CCG working group and NRC project team, to effectively

align efforts for Phase II NRIM development.

2 REVIEW OF EXISTING LITERATURE AND TOOLS

A review of select design guidelines and tools was conducted during Phase I. This review allowed for the investigation of areas of the navigational aid system design and review which MDA could support and the identification of empirical relations and computational methods that could support the development of NRIM.

2.1 Design Guidelines

There were two design guidelines reviewed in detail during Phase I. The first was the CCG guidelines for design and review of marine navigational aid systems [4]. The second was PIANC guidelines for the design of ports and channels [5]. The review of these guidelines resulted in a better understanding of current means to assess navigational threat and identify areas that NRIM could support.

2.1.1 CCG Guidelines

The CCG Procedures Manual for Design and Review of Short-Range Marine Aids to Navigation, referred to hereafter as CCG Guidelines, describe the procedure of design and review in four distinct steps, which include: 1. basic site review, 2. preliminary hazard identification and threat rating, 3. needs analysis, 4. operational analysis. The basic site review involves the collection of data relevant to the site including historical environmental data, bathymetry, existing navigational aids and types of vessels that use the site. Data collected from step one is consolidated on the site data sheet and the procedures for data collection are summarized in Chapter 2 of the CCG Guidelines. Step two, the preliminary hazard identification and threat rating, involves the assessment of an initial rating on the severity of each threat. The results of the preliminary rating of each unique threat are summarized on the preliminary threat rating sheet and the procedures for assessing the preliminary threat rating are reviewed in Section 3 of the CCG Guidelines. The needs analysis, step three, involves the rating of composite threats, identifying generic types of navigational aids to reduce these threats, and assessing how the potential and currently existing navigational aids reduce threats. The procedures for the needs analysis are summarized in Chapter 4 of the CCG Guidelines and the results of the assessment are compiled in the needs matrix. The final step, operational analysis, involves conducting an operational based assessment of site-specific requirements to compliment the results of the previous steps. This step is completed separately for open and confined waters and the procedures are summarized in Chapter 5 and Chapter 6 of the CCG Guidelines, respectively. The operational analysis involves consultations with waterway users by which any questions arising from the previous steps can be confirmed.

In general, NRIM can support the processes involved in step numbers two and three. In terms of the preliminary threat rating, step two, NRIM will allow for the direct assessment

and quantification of benchmark values to represent the threat ratings for many of the threats outlined on the preliminary threat rating sheet. The specific benchmark values that NRIM can assist in quantifying include: non-threatening under keel clearance value and the "significant" and "highly significant" limits representing the distance from other vessel when passing, minimum channel width, angle of turn in channel, wind speed, current speed along track and current speed across track. Currently these benchmark values are provided on the generic preliminary threat rating form and change for the different ranges of vessel length, beam, draft and gross tonnage considered. These benchmark values resulted from consultation with experienced navigators.

To exemplify the use of MDA to assess and quantify the preliminary threat rating benchmark values, let's consider the non-threatening under keel clearance benchmark. This benchmark ranges between $3\,m$ and $15\,m$, pending on the basic vessel particulars. To assess this value for a particular vessel category, NRIM could be used to simulate the MDA using a wide range of vessel speeds and environmental conditions. This would give an idea of how the MDA varies with different environmental conditions and vessel speeds and indicate the maximum MDA requirement. The MDA requirement calculated using NRIM includes the vessel draft, squat and wave induced heave and pitch (at this stage). The MDA calculation includes additional consideration than the calculation used in the CCG Guideline which includes only vessel draft, maximum wave height and the safety factor (non-threatening under keel clearance benchmark). Since the MDA computation is a more thorough computation involving coupled effects of environmental and vessel parameters, it would result in less uncertainty and may result in a decision for a lower safety factor value. The safety factor could be selected by adding a percentage of the maximum MDA computed by NRIM.

The support that NRIM could provide step number three, the needs analysis, relates to defining the composite threat rating. This support is both indirect and direct. Indirectly, the composite threat analysis makes use of the preliminary threat ratings in the assessment. As described in the previous paragraphs, NRIM can be used to assess the preliminary threat rating benchmarks and therefore have an impact on the composite threat rating. Another way that NRIM would support step three is by considering the environmental conditions that are unique to the given waterway and using them to help define the threats specific to the site. NRIM could be used to simulate specific maneuvers through a defined section of the waterway to determine the performance in different environmental conditions. In terms of the composite threats highlighted on the needs matrix form, NRIM could directly support rating of: sea conditions, proximity of hazards, complexity of track, and diminished room to maneuver.

In general, NRIM can be used as a numerical design tool to complement the use of CCG guidelines for the design and review of marine short range aids to navigation systems. By doing this, the overall design and review process becomes less prescriptive. The use of

NRIM will allow for the design of a navigational system that is uniquely tailored to a given waterway, set of environmental conditions, and vessels. This type of design is impossible using only a set of prescriptive based regulations. A performance based approach will help reduce the risk of over designing a navigational aid system which could lead to reduced costs for the CCG.

Besides those mentioned above, there are other areas of the design and review process that NRIM could support, such as the selection of type of navigational aid and positioning of the aids. This would have to be examined further and would involve the implementation of empirical relations involving the detection of drift, such as those used in the Japanese Tool (Japanese Port Authority). These equations only examine detection of drift through floating buoys, an anchored lit spar, or through GPS or DGPS. Therefore, implementation of these, or similar equations would only support the selection, design and positioning of drifting buoys and an anchored spar, other navigational aids would not be considered. There could be other empirical relations existing in the literature that consider other types of navigational aids. The investigation of this type of equation, and integration into NRIM is beyond the scope of the current project. However, this could be investigated in the future based on CCG recommendation.

2.1.2   PIANC Guidelines

The Permanent International Association of Navigation Congresses (PIANC) in coordination with the International Association of Ports and Harbours, has developed a set of guidelines to support the design of channels and ports. The guideline, entitled "Approach Channels: A Guide for Design," was published in June, 1997 [5]. An updated version of this document is under preparation by PIANC and was expected for publication in the first or second quarter of 2012 (PIANC Presentation [6]). The updated publication could not be located through a literature search and may have a delayed release date. These updates could not be obtained for inclusion in this review. The PIANC guidelines involve the design of a channel or port as opposed to design of navigational aid system. However, the general guidelines in terms of identification of navigational hazards are common to both processes. In addition, the PIANC guidelines focus on ports and channels as opposed to general waterways. The methodology for waterway design in PIANC involves an initial concept design supplemented later with a detailed design. The concept design makes use of generic guidelines based on experimental results and operational guidance from vessel navigators. The detailed design makes use of computer based design tools such as programs to simulate vessel maneuvering and identify and quantify risk.

Support for Navigational Aid System Design

The PIANC guidelines contain insight that could be used to support the CCG design and review of marine aids to navigation procedures. Two key areas of support are described

below. In short, the first area of support relates to using the generic guidance summarized in PIANC, to make a preliminary threat rating for scenarios in which there is limited data. This could be incorporated into NRIM in the future if this is of interest to CCG. The second area of support relates to integrating some of the listed empirical formula into NRIM to allow for consideration of different scenarios.

To elaborate on the first area of support, the PIANC guidelines also provide generic guidance on certain aspects of the design. For example, for concept design concerning the minimum depth allowance the guideline indicates that a depth to draft ratio of 1.10 is commonly used across the globe as a minimum. This includes a safety margin and is related to calm sea conditions. A value of 1.3 is indicated for channels with wave action. Similarly, the guidelines indicate that a vessel turning radius in calm water will be in the range of one to two times the vessel length in deep water. In shallow water, the turning radius is indicted to be approximately 5 or more times the vessel length. These details arise from the result of a study involving a single screw/single rudder container ship operating in different water depths. These types of generic values could be used by CCG to enable a conservative threat rating for scenarios in which little to no data is available relating to the vessel particulars or environmental conditions. The preliminary NRIM requires the input of data relating to the environment, vessel particulars and channel geometry to allow for investigation of threat for a given scenario. In cases where this information is not available, it may be appropriate to use generic guidelines to obtain a preliminary threat rating. This type of general guidance could be integrated into NRIM so that it could be selected to provide guidance for scenarios with limited data.

The PIANC guidelines provide relatively simple formulations for the calculation of certain parameters such as the required bank clearance. Currently NRIM is not equipped with formula to compute bank loads and thus it cannot predict the effects of a bank on maneuvering. This will be considered in Phase II in terms of a review of empirical relations to compute bank loading that are existing in the literature. The generic PIANC guidance relating to vessel speed and environmental conditions could be added as an alternative to allow for calculation of a conservative guideline. In addition, general guidance is provided to assess additional maneuvering lane requirements for different channel bottom types: smooth and soft, smooth and hard and rough and hard. This insight could be incorporated into NRIM during Phase II as a conservative measure since a detailed investigation of this effect was not proposed for consideration.

Another area of support from the PIANC guidelines relates to the examination of threat benchmark values. There is some operational guidance provided in PIANC that could help to define the vessel settings to use when assessing the threat benchmarks for select parameters. The threat benchmarks are the values that denote a significant or highly significant threat, and can be examined using NRIM. For example, NRIM can be used to investigate the turning performance of a vessel in a given channel parameter, but cannot

define what constitutes a significant threat. It is obvious that if the vessel turn is larger than the available channel turning radius at certain environmental conditions, then this is a significant threat. However, what constitutes a moderate threat may be harder to define. The PIANC guidelines indicate that a turn should never be designed for 100% rudder angle as this leaves no reserve for correction against environmental forces. Instead, the guidelines reference operational guidance from ship-handlers that indicate a comfort zone when turning at rudder angle between 15 and 20% of the maximum rudder angle. Therefore, for waterways in which there are turns that require a larger rudder angle, this may relate to a threat.

2.2   Design Tools

There were two design tools investigated in detail during Phase I. The first is the Japanese Fairway tool which provides select output in support of the design of a channel or waterway. The second is the FORCE Technology simulator which can assess fast time maneuvering scenarios and output the trajectories indicating vessel performance. This review is aimed to identify any components of the existing tools that could be used to support NRIM development.

2.2.1   Japan Fairway (2010)

A review of the Japanese tool [7] was conducted to investigate three key items: the basic output of the tool, how the basic output is calculated, the overall capabilities of the tool, and how the tool compares to CCG desired output as well as NRIM Phase I.

Basic Output of Japanese Tool & Details of Methodology

The Japanese has three output parameters which include: the MDA, the minimum channel width and the radius of turning circle. Details of the methodology and equations used to calculate these parameters are provided below.

Calculation of MDA

The MDA is calculated by adding together the vessel draft, squat, the maximum of heave plus pitch (bow sink) or heave plus roll (bilge keel sink) and a parameter referred to as the "allowance of depth."

$$MDA = d + Squat + Max(heave + pitch, heave + roll) + allowance\ of\ depth$$

The parameter d is the maximum vessel draft in still water. The allowance of depth accommodates for the list of a vessel due to a large rudder angle to alter the course. This parameter is calculated based on a simple relation to the vessel draft. For vessel drafts less than or equal to 10 m the allowance of depth is set to 0.5 m and for larger vessel

drafts it is set to 0.05 multiplied by the draft. There is no reference provided as to where this relationship originated.

For: d $\leq$ 10 m; allowance of depth = 0.5 m

d > 10 m; allowance of depth = 0.05 $\cdot$ d

The squat is calculated using a single equation that was formulated by Yoshimura, 1986 [8]. This equation is used to estimate the vessel squat for all scenarios considered. The reference for this squat formulation was provided but the paper was only available in Japanese. Therefore, details relating to the data from which this squat formula was derived is still unknown. If the equation was derived using model scale tests of one specific hull form or channel configuration it may introduce error when used to predict the squat for scenarios that greatly differ from this case. The squat formula is a function of the vessel draft, waterway depth, vessel length, breadth and speed as well as the block coefficient. The calculation does not consider the width of the waterway and it is uncertain if it was defined for open or narrow waterways.

The bow sink due to heave and pitch (heave + pitch) is estimated using a plot of the ratio of heave to wave amplitude versus a function of vessel length. Documentation indicates that this graphic was defined by the Very Large Crude Carrier (VLCC) study group. No further detail on this reference is provided. The data presented on the graphic is based on a block coefficient of 0.7, Froude number of 0.1 and deep water.

The bilge sink due to heave and roll (heave + roll) is estimated using an empirical equation by Honda, 1998 [9]. This parameter is only considered when the natural rolling period is nearly equal to the meeting period between the vessel and wave. In all other conditions it is assumed that the bow sink is larger than the bilge sink. The Honda equation is a function of the significant wave height, vessel breadth and maximum vessel rolling angle.

In the Japanese tool, there is no additional depth allowance added to account for different vessel bottom shape, such as a flat or round bottom. When predicting the bilge keel sink due to wave-induced motion, the flat bottom is applied resulting in a conservative result. Moreover, the Japanese tool does not add a component to the MDA to account for vessel heeling due to course change or maneuvering effects.

In the Spanish ROM guidelines, section 7.2.3.8, which is not reviewed in this report, a factor to account for the heeling effect during turning is described. The theoretical background behind this factor relates to the balance between centrifugal force and restoring force. However, the calculation of this factor requires many parameters including: turning radius, speed, centre of gravity, centre of buoyancy, draft, and the area of moment of inertia. This may be impractical to calculate within NRIM unless these values are known for each vessel considered. In addition, the frequency in which this factor is applicable may be small since it is only relevant for flat bottomed vessels.

Calculation of Minimum Channel Width

The minimum channel width is calculated using a de-coupled approach. The parameters considered for one-way traffic include the width required to compensate for wind, current and yaw, the width required for the detection of drift and the width to accommodate for the effect of bank suction. The drift angle due to wind is calculated by taking a sum of the forces and moments in sway and yaw respectively. The fluid forces on the hull and rudder are calculated using empirical relationships for the hydrodynamic derivatives defined by Hirano (1985) and Fujii (1961) [10]. The hydrodynamic derivatives are a function of the vessel particulars. The wind forces are approximated using empirical formula defined by Yamano, 1997[11]. The equations are solved for the drift angle caused by wind forces.

The drift angle caused by current loads is calculated by considering the geometry of the direction of vessel speed and cross current speed. The resulting computation defines the current induced drift angle as the arctan of the current component in the sway direction divided by the vessel speed. The total drift angle due to current and wind is then calculated by summing the two values. The width required to compensate for wind and current is then found using geometry of the ship drift angle as well as the length and breadth of the vessel.

The drift sideways due to ship yaw is calculated by integrating the yaw angle over the yawing period and multiplying this by the vessel speed. For this calculation the vessel yaw period and maximum yaw angle must be known. In cases that these are unknown, general values are provided for use. The width required to accommodate for the effect of bank suction is found based on works by Kijima and Qing (1983) [12] and Kijima and Nonaka (1981) [12]. Again, a summation of forces and moments is considered which includes the fluid forces on the hull and rudder (represented by the hydrodynamic derivatives) and the bank forces. The bank forces are calculated using an empirical relation by Kijima and Qing (1983) [12]. This equation uses a dimensionless value of side thrust and moment coefficient which can be found from plots of the coefficient at different ratios of distance between the vessel and channel wall as well as the vessel length. The sum of forces and moments are solved to determine the rudder angle and drift angle and the required width to account for the bank effect is found using geometry along with the calculated drift angle.

The width required for the detection of drift is calculated using equations derived by the West Japan port operation study group. These equations are specific to the method used to identify or detect drift whether it arise from lit buoys, an elevated post light, radar or GPS (and DGPS). These are relatively simple computations based on the vessel particulars and features of the drift identification source. This width accounts for any error in the methods of drift identification.

The total minimum channel width is calculated by summing the width required due to the effects of wind, current and yaw, the width required due to the bank effect and the width to accommodate for detection of drift.

Calculation of Turning Circle Radius

The radius of turn is calculated based on an empirical equation that contains a coefficient for "index of turning" which was calculated based on results of simulations that were done using the MMG model. The hydrodynamic coefficients for the hull and rudder used in these simulations are again those by Hirano (1985) [10] and Fujii (1961) [13]. A database of the indices of turning for different vessel types was summarized so that when the tool can select the most relevant index when calculating the turning radius for a given scenario. The simulations were run in shallow water, with zero wind and 20 degrees of rudder angle.

Comparison of Japanese Tool Output to CCG Requirements and NRIM Phase I and Phase II

In general, the Japanese tool has the capability to provide output for the scenario in which the parameters of the channel, vessel and operation are known, similar to the capability of preliminary NRIM Phase I. It also has the capability to calculate output for scenarios in which there is limited information relating to the vessel and no information on the environment or speed. These are basic calculations using only the vessel length and draft. Reference to where these guidelines originated are not provided. NRIM currently does not have this capability but it could be introduced if it is desirable to CCG. A further capability of the Japanese tool relates to its ability to assess existing waterways in terms of the navigational aids that are already in place, when calculating the minimum channel width. This is included by considering the method for detecting drift in a waterway and applying the relevant drift formulation. This functionality would allow one to consider the minimum channel width based on the assistance of different navigational aids to determine vessel drift. NRIM does not currently have this capability since at this stage it considers only the coupled effects of wind and current and the resulting global and local motions. This capability could be considered in Phase II. It would be relatively simple to implement the same equations for the detection of drift that are employed by the Japanese tool. If further investigation as to their validity and generality are required, or a literature review to determine if more applicable formulations exist, this may require additional effort would be out of scope of the current project.

The capabilities of the Japanese tool and NRIM are summarized in Table 1 and compared to the output requested by CCG. In general the Japanese tool provides an estimate for 5 of the 8 requested CCG items. NRIM Phase I also provides an estimate of 5 of the eight items, though not all of the same items as the Japanese Tool. Phase II NRIM is planned to provide an estimate for all of the 8 CCG requested items plus have the capability to consider other non-requested items as described in Table 1.

Table 1: Assessment of Japanse Tool

Output and/or Capability	Japanese Tool	NRIM Phase I	NRIM Phase II	CCG Requested
Minimum Depth Allowance	Yes	Yes	Yes	Yes
Limiting Channel Width (one way traffic)	Yes	Yes	Yes	Yes
Limiting Channel Width (two way traffic)	Yes	No	Yes	Yes
Limiting Channel Width (over taking traffic)	Yes	No	Yes	Yes
Advance and Transfer	No	Yes	Yes	Yes
Crash Stop Distance	No	Yes*	Yes*	No
Zig Zag Performance	No	Yes	Yes	No
Minimum Settle Up Distance	No	Yes	Yes	Yes
Radius of Turn	Yes	Yes	Yes	Yes
Impact of Data on results	No	No	Yes	Yes
Provide guidance for scenario with unknown environmental conditions, vessel particulars (besides length and draft), and vessel speeds	Yes	No	No†	No

* This capability is currently built into the NRIM but it requires information on vessel resistance and engine powering
† Not planned for inclusion in Phase II NRIM however; could be investigated if time permits and if desirable by CCG

In general, the Japanese tool largely calculates parameters based on empirical equations relating to uncoupled responses of vessel motions. This results in relatively simple computations that can be done quickly using limited input data. The output from NRIM is based on coupled motions of a vessel as output from numerical simulations of the vessel response to the effects of vessel speed, wind, waves and current. Many of the NRIM computations are more general than those applied in the Japanese Tool, providing the flexibility to consider different scenarios without the introduction of error. For example, the strip theory approach for the computation of wave induced heave and pitch can have different boundary conditions to represent different channel geometries and vessel particulars. In comparison, the method used to calculate wave induced heave and pitch in the Japanese Tool is specific to a particular vessel shape, speed and channel configuration.

Though NRIM uses less general and more complex methods of calculation that the Japanese Tool it can be packaged such that it has a low computation time and provide alternatives which require general-type input parameters.

2.2.2 SimFlex Navigator (FORCE Technology)

The SimFlex Navigator [14] is a tool developed by FORCE Technology which simulates ship maneuvering. The tool can be used to simulate turning circles, zig-zag manoeuvers, as well as acceleration and stopping runs in different wind, current and wave conditions. The simulation can be run in realtime or fast time mode. When ran in realtime, the vessel is controlled by the user. When the simulation is ran in fast-time the vessel is controlled by the numerical navigator. The numerical navigator is a component of the simulation that incorporates human error as a random function with a given standard deviation. The numerical navigator can follow a pre-defined course with a given speed over ground. Another attribute of the fast-time simulator relates to an add-on tool referred to as "Replay." This tool can complete a statistical analysis from the results of a group of simulations, which can be used to support decision making.

The model behind the FORCE technology simulator is the DEN-MARK 1, a mathematical model that was developed in-house at FORCE Technology. There was little information found in the public domain relating to the mathematics behind the maneuvering model or the specific equations used in its development. FORCE technology maneuvering models are frequently used operationally in both fast time and real time simulators to investigate the maneuvering of different vessels and for training purposes.

It is possible to simulate the motions of any ship using the SimFlex Navigator provided that adequate data is obtained. FORCE technology has developed an additional tool, the SimFlex ShipYard, which allows users to develop their own ship models to be used in the SimFlex Navigator. The input required to model a new ship includes hydrodynamic data, environmental forcing data, mechanical forcing data and data relating to the navigational

instruments. In addition, a 3DOFs model of the vessel and superstructure is also required.

The FORCE technology fast-time simulator has a number of desirable attributes that would support the CCG process of identification and quantification of navigational risk as well as the overall design and review process for marine navigational aid systems. However, the large data input requirements for the development of a new vessel model may limit the applicability of the tool in supporting CCG needs. The key limiting attribute of this tool in terms of its use to support CCG needs relate to the duration of time required to build a single ship model for simulation. A more generic model that requires only input of general ship particulars, such as the Japanese Tool or the NRIM, are better suited to provide a relatively quick investigation of risk to a range of ships.

3   PHASE I NRIM DEVELOPMENT

3.1   Minimum Depth Allowance

3.1.1   Squat Assessment Details

The purpose of this section is to present the results of a preliminary investigation into the capabilities, applicability, advantages, disadvantages and limitations of each of the various formulae (in the open literature) which are available for predicting the changes in sinkage and trim (squat) when a ship enters a confined waterway. Definitions are provided along with diagrams which are associated with the geometrical, ship and hydrodynamic parameters used in the formulae. The details for 15 different formulae are provided, along with an assessment of their applicability to a ship traveling in: (i) unrestricted uniform-depth shallow-water conditions, (ii) a trapezoidal canal, and, (iii) a trenched channel. Some formulae provide estimates only for bow squat, others can estimate stern squat and the change in trim angle.

A comparison was made with published full-scale measurements of squat for four ships operating in the Panama Canal. A preliminary sensitivity analysis was performed to determine how sensitive the predictions are to assumptions concerning the values of the various ship and channel parameters. An attempt was made to see if likely variations of the channel parameters during the full-scale measurements in the Panama Canal could account for the spread in the measurements of ship squat. Based on the preliminary squat assessment, suggestions for further investigation during Phase 2 are made.

The details and results of the preliminary squat assessment are presented in Appendix C.

3.1.2   Wave-induced Heave and Pitch Consideration

Wave excitation is the most fundamental environmental load on a floating body. Ship motion in waves is one of important performance criteria, because it is strongly related with the workability and safety of the ship. Even a ship which moves in a restricted area can be excited by waves. Obviously, wave load and its effect, usually referred to as wave-induced motion or sea-keeping performance, has to be considered to assess MDA.

Empirical Method of Wave-induced Motion

Wave-induced motion is generally the interaction between wave and ship. So, the shape of submerged body is most important parameter to determine the wave-ship interaction. Apparently, the prediction has to consider the specific hull geometry such as bow, stern and bilge-keel. However, it is not easy to take account of the detailed shape in the design phase. As a result, several simple empirical methods are suggested to provide a rough

prediction of wave response.

Among various empirical formulae of wave-induced motion, three methods are reviewed in this report; a)Japan Fairway Design guidance [7], b)Jenson(2004) [2] and c)IACS JTP rule [15]. The specific equations and procedures are described in Appendix B.2. The features of these three formulae can be summarized as Table 2.

Table 2: Comparison Table between Empirical Methods of Wave-induced Motion

	Japan Fairway	Jenson(2004)	IACS JTP
Input	Ship Length	Ship Length	Ship Length
		Ship Beam Width	
		Ship Draft	Ship Draft
		Ship Block Coeff.	Ship Block Coeff.
		Ship Speed	Ship Speed
	Ship GM †		
	Wave Period	Wave Period	
	Wave Heading	Wave Heading	
	Wave Height	Wave Height	
Outcome	Bow Sink Amp. Factor	Heave RAO	Pitch Angle
	Bilge Sink Amp. Factor	Pitch RAO	Roll Angle
Note	No Eq. of Bow Sink Calc.‡	No Roll Prediction	No Wave Consideration
			No Heave Prediction

† *Distance between center of gravity and metacentre*
‡ *Instead of equation, graph is provided*

As shown in Table 2, only a few parameters are necessary for estimation. Its calculation procedure is easy and straight forward. However, it is clear that the result of empirical formula has uncertainties because it can not consider the specific hull shape. Moreover, these formulae adopt several assumptions to allow for simplification of the problem. The first assumption is that the water is deep enough. Secondly, water area is assumed as open sea. These two assumption can cause an additional uncertainty when applying the empirical formula to a confined channel. As a result, it is important to identify the application limit.

Numerical Method for Wave-induced Motion

For more accurate prediction, the numerical method should be used instead of the empirical method. For a wave related problem, strip method or 3-dimensional panel method is widely implemented instead of general CFD tool to avoid high computational costs. In this

project, strip method is implemented to estimate wave-induced motion in open sea and restricted channel. The detailed theory and numerical scheme is described in Appendix B.3 and B.4.

Compared with the empirical method, numerical analysis requires detailed information on the hull shape. As well, the numerical method requires a larger computing time than the relatively instantaneous empirical computation. For example, the calculation time of the developed strip method software is summarized in Table 3.

Table 3: Example of Strip Method Calculation Time

Analysis input	No of wave freq.	11
	No of sections	27
	No of grids per section	650
Computing time		193 min.

3.2   Maneuvering Model

This section describes the results of a literature review relating to maneuvering models to help guide the selection of methods to incorporate into NRIM. The Phase I NRIM maneuvering model is then described in general and a brief discussion of its performance is provided. A detailed description of the Phase I maneuvering model is provided in the Appendix A.

3.2.1   Maneuvering Model Literature Review

There are a number of different recognized methods available to predict the maneuvering performance of a vessel. These methods differ in terms of the amount of effort required, the accuracy of results and the computational time required for predictions. Typical methods include: model testing, empirical computation, system identification, and CFD. There are also hybrid methods that have been published (e.g. model by Toxopeus [16]) which combine two or more of the aforementioned methods to obtain the desired output.

In general, there tends to be a link between the amount of effort (and cost) required and the accuracy of the results. Model testing is the most costly of the options and has a high level of accuracy in comparison with the other methods. The CFD method takes a large amount of effort and computing power. On the upside, CFD methods have been demonstrated to provide good results. System identification is a method of model optimization based on maneuvering trajectories from model or full scale tests. This is a relatively low-cost option but the accuracy results pend on the quantity and quality of the trajectories available for optimization. Prediction using existing empirical methods is relatively quick, easy and inexpensive. There has been extensive work completed in the area of empirical modeling

resulting in a number of documented and published models. A downfall of empirical predictions of maneuverability is that the accuracy is generally limited by the assumptions made in the model. A detailed description of the advantages and disadvantages of each method is provided in the proceedings of the 25th International Towing Tank Conference [17].

After considering all the prediction methods outlined above, it has been decided that the method that would work best to fulfil the needs of CCG is an empirical approach. This method would allow NRC to consider multiple vessels in different channel configurations in the relatively short project timeline. The use of other more complex methods would both extend the project delivery date and increase the project cost.

Selection of Mathematical Model

The use of an empirical method requires the use of a set of mathematical equations to represent a vessel maneuvering in a given waterway. A mathematical model based on the equations of motion is commonly used and is selected for use in this project. There are two general approaches to represent the loads on a given vessel within the mathematical model. The first is a whole vessel approach, which considers the overall loads on the entire vessel. The second is a modular approach, which considers the distinct loads on different sections of the vessel. The most common example of each approach are the Abkowitz model [18] and the Mathematical Modelling Group (MMG) model [19]. The Abkowitz model considers the global loads on the vessel in its entirety. The MMG model is modular in nature and considers the forces on the hull, rudder and propeller independently. When comparing the two, the Abkowitz model requires more complex hydrodynamic derivatives than the MMG model and is used in published literature less frequently. In general a modular approach is less sensitive to the choice of maneuvering coefficients [17] in comparison to a whole vessel approach. These considerations lead to the selection of the MMG model for NRIM development.

The MMG model was originally proposed in 1976 by the Mathematical Modeling Group. To compute the forces and moments one must first calculate the hydrodynamic derivatives pertaining to the vessel of interest. These can be found using existing empirical or semi-empirical formulae that relate the hydrodynamic derivatives to the general particulars of a given ship. A number of this type of equations have been developed and published. A relatively recent study conducted by Toxopeus [20], investigated the performance of a number of different empirical and semi-empirical equations used to compute the hydrodynamic derivatives. There were four different methods investigated including those by Kijima, et al. [21], Vassalos et al. [22], Clarke et al. [1] and Norrbin [23]. The formulations by Clarke compare relatively well to the values found experimentally for each vessel type considered. These equations directly relate the hydrodynamic coefficients to the principal particulars of a given vessel and are an improvement to methods based on flat-plate and slender body theory [1]. The Clarke equations are based on a linear regression analysis using over 70

experimental measurements of hydrodynamic derivatives for a wide range of different ship types.

The hydrodynamic derivatives are unique to the waterway that they were defined based on. The Clarke equations were derived from experimental data of vessels operating in deep water. Therefore, their applicability to shallow water scenarios may introduce additional errors. Complimentary equations were developed by Sheng [24] which corrected the Clarke, deep-water hydrodynamic equations and made them applicable to shallow water. This shallow-water correction is based on basic hull parameters of a given vessel. Since the Clarke equations appeared reasonable when compared to measured results, are related directly to basic hull parameters and have an available correction method for application to shallow water; they were selected for use for Phase I NRIM development.

The article by Toxopeus [20] also examined an approach to determine the hydrodynamic coefficients using a hybrid semi-empirical/CFD method as well as a method using just CFD. In general the hydrodynamic derivatives measured by these methods were much closer to the experimental measurements than those determined using the semi-empirical or empirical equations. In particular, the CFD based derivatives were often very close to the measured derivatives. However, the level of effort required to compute the hydrodynamic derivatives using these methods is much higher than what is required for a semi-empirical approach. The use of this method would require expertise in the area of CFD and would not be easily packaged into NRIM. However, it would be possible for NRC to compute hydrodynamic coefficients for select vessels using CFD to add to the NRIM database. This is outside of the scope of the current project but could be investigated in terms of required effort during Phase II for inclusion in the project report.

3.2.2   Phase I Maneuvering Model Description and Details

The simulation model is based on standard maneuvering equations of motion as outlined in Appendix A. The solution of these equations is achieved via the appropriate numerical tools in *MATLAB*[TM] [25]. There were two distinct maneuvering models considered in Phase I. The first model is two dimensional and considers a constant forward speed. The second model is three dimensional and accepts input relating to the engine setting. The speed can change throughout a maneuvering simulation with a given engine setting in the 3DOFs model. The maneuvering model requires the following inputs (propulsive and thruster forces only required for 3DOFs model):

- Environmental data

  - Water depth, wind speed and direction, current speed and direction

- Ship's main particulars and data

  – Beam at waterline, length at waterline, draft, block coefficient, displacement, rudder area, rudder lift coefficient, projected areas exposed to wind and current, drag coefficients for wind and current, moment of inertia about vertical axis through ship's waterplane centre, location of centre of gravity relative to ship centre, propulsive forces at various settings, thruster forces.

• Maneuvering Coefficients (Hydrodynamic Derivatives)

  – Details of the meaning of these coefficients are elucidated in Appendix A.

The maneuvering coefficients can be determined for a particular vessel either through model testing (Planar Motion Mechanism (PMM)), sea trials, or by using CFD codes to emulate the PMM tests. For this study, we have used the coefficients presented by Clarke et al. [1] which were derived from analytical and empirical methods. These coefficients depend on hull geometry and are to be regarded as valid about a nominal operating surge speed. This is also evident from the derivation presented in Appendix A. The hydrodynamic coefficients used here must therefore be considered as approximations to the coefficients appropriate to the vessels of interest to the Canadian Coast Guard. We note further that Clarke provides shallow water corrections to these coefficients. Verification of these corrections can be performed by CFD studies.

3.2.3   Maneuvering Model Output and Performance

We remark that the simulations were compared to the results of sea trials performed by another client, the details of which we are not at liberty to report. General ship's particulars were used to estimate the hydrodynamic coefficients for sway and yaw based on the work of Clarke et al. [1]. The following additional parameters were estimated: hydrodynamic coefficients in surge, location of centre of mass, propeller thrust, drag coefficients for wind and current. The results of a simulation with 35 degree rudder angle to starboard compare well with the sea trials.

3.3   Decision on Shallow and Open Water

Generally, if the ratio of the water depth to the ship's draft (H/T) is around 1, it can be considered as "shallow water." However, there is no absolute criterion, because various naval architectural problems are based on very different backgrounds. For the free surface wave problem (e.g. wave-induced motion), when the ratio of the water depth to the wave length is smaller than 0.05, it is considered as shallow water. On the other hand, when evaluating the squat effect, the ratio of the water depth to the ship's draft is the important parameter to assess the water depth. Furthermore, every empirical formula for the squat prediction has its own criterion of what is considered shallow water. As a result, NRIM will automatically choose the proper (shallow or deep water) model considering the given

conditions and theoretical background. In other words, the user does not need to input into NRIM weather the scenario being assessed is in shallow or deep water. Instead, NRIM will internally decide this and select the appropriate empirical relations, based on the criterion around which the relations were formulated.

The term "open water" indicates that there is no obstacle in the water way. In contrast, a confined (or restricted) channel describes a channel which contains an obstacle, such as a close proximity bank. Similar to the discussion on shallow versus deep water, the empirical equations considered in NRIM to account for narrow channel effects each have different significant parameters that consider the significance of narrow-channel effects. As such, the narrow channel versus open water distinction will be made internally, within NRIM.

It should be noted that the distinction between open water and narrow channels, as well as deep water versus shallow water, is based on the significance of the effect of narrow channels or shallow water on the parameter being predicted. Therefore, pending on the empirical relation selected within NRIM to compute the parameter of interest, the effect may vary.

4   PHASE I SCENARIO DETAILS

The scenario to consider for Phase I development of NRIM was based on the availability of comparative data to support validation of model output. The CCG has provided NRC with access to a collection of reports that detail a comprehensive study that was conducted to investigate a set of tanks operating in waterways through Kitimat, British Columbia. The primary report entitled: "Maneuvering Study of Escorted Tankers to and from Kitimat," [3] assessed the maneuvering performance of four tankers. A secondary report entitled "Section 3.6: Special Underkeel Clearance Survey," [26] considered the MDA requirement for the largest of the tankers reviewed in the maneuvering study. A third report entitled "Appendix F: Additional Maneuvering Results and Parameters," [27] provided additional maneuvering simulations for the tankers.

The primary maneuvering report provided simulated results for each of the four independent tankers in deep open water. The report documented simulated results of the following maneuvers: turning circles, speed acceleration maneuvers and zig-zag maneuvers. There was also crash stop data provided but this is not considered in the Phase I comparison since limited propulsive information was available to feed into the NRIM. The supplementary report containing the content of Appendix F, provided simulated results of the tankers turning circle in open, shallow water. The shallow water turning circle was simulated for a water depth of 25.32 m. The MDA assessment, as detailed in the Section 3.6 supplementary report, was carried out for shallow, open water, similar to certain portions of the Kitimat channels under consideration. Considerations of squat were computed at a range of different shallow water depths between 30 and 50 m.

4.1   Vessel Details

For Phase I, the largest vessel considered in the Kitimat study, a loaded VLCC (VLCC 3219), was selected for investigation. This vessel was selected for two key reasons. The first reason was that there were ample maneuvering results available from the primary and secondary maneuvering reports for this particular vessel. The maneuvering results were output from a FORCE technology simulator. This type of simulator has been used operationally for many years and was used in the Kitimat study to investigate the maneuvering performance of tankers. The second reason for selecting this particular vessel is that there were considerations into the MDA for this vessel provided in the Section 3.6 supplementary report. As part of the Kitimat study, only the largest tanker (VLCC 3219) was investigated for MDA requirements and therefore, there was no comparative data available for the other three tankers considered in the study. The general particulars of the Phase I vessel are summarized in Table 4.

Though this vessel was selected for demonstration in Phase I, it is important to note that the preliminary NRIM, developed in Phase I can presently be used to investigate maneuvering

Table 4: Phase I Vessel Particulars - VLCC 3219

Parameter	Value
Length Overall (m)	346.8
Length between Perpendiculars (m)	336
Breadth moulded (m)	60.5
Draft fore/aft (m)	21.0/21.0
Displacement (m^3)	373172
Block Coefficient	0.87
Frontal Wind Area (m^2)	1060
Lateral Wind Area (m^2)	4100

and MDA parameters for any vessel type, size and shape, given that the empirical relations are accepted by CCG.

4.2   Channel Geometry

The channel geometry was selected based on the channel configurations for which comparative data existed. The maneuvering results and the MDA considerations from the Kitimat study were computed in relation to two different channel configurations. The majority of the maneuvering results were presented for deep, open water while the MDA calculations were performed for shallow, open water. There were some maneuvering results, turning circles, provided for the shallow, open water case. Therefore, for Phase I development two different channel geometries are considered: shallow/open water and deep/open water. It is important to note that the maneuvering performance and MDA requirements will change based on the channel geometry they are operating in. The channel configurations considered in Phase I are summarized in Table 5.

Table 5: Phase I Channel Details

Assessment Type	Channel Geometry Details
Maneuvering	Deep, open water
Maneuvering	Shallow, open water
MDA	Shallow, open water

It is to be noted that though these channel configurations were considered for the comparison and review of output, NRIM currently has the capability to consider other geometries for MDA calculation, when using the strip theory approach. Using this approach, NRIM can currently be used to investigate MDA in narrow channels, deep water or channels with sloping sides. For maneuvering considerations, NRIM does not yet have the ability to con-

sider the bank effect, i.e. the effect of narrow channels.

5 PHASE I NRIM OUTPUT

The output from Phase I NRIM, for the scenarios described in Section 4, are provided and compared with the results from the Kitimat study. Discussions on additional input and considerations that may be required to compliment NRIM output in order to obtain CCG required parameters are also provided.

5.1 Comparison with Kitimat Study

The Phase I NRIM output for the scenarios of interest are presented and compared to the results presented in the Kitimat study. Details of all parameters relating to each scenario (e.g. channel configuration, vessel speed, rudder angle, etc.) are provided as well as discussions on the result of each comparison.

5.1.1 Maneuvering Performance

NRIM was used to simulate specific maneuvering scenarios relating to VLCC 3219 that were represented in the Kitimat study maneuvering report (FORCE Technology, 2010) [3]. The majority of the maneuvering simulations from the Kitimat study were based on deep, open water conditions. All comparisons in this report are based on the open water case: one in shallow water and the remaining in deep water. The simulated results in the Kitimat study were performed using the FORCE Technology fast time simulator. The simulations included a number of different maneuvers, such as: zig-zags, turning circles, and acceleration runs. The NRIM simulated results are compared to the FORCE technology simulator output for each of the aforementioned maneuvers. The simulation inputs including vessel speed, engine setting, rudder angle and environmental conditions, are summarized for each particular maneuver. The simulated results are then compared in terms of distance travelled, and differences between the results are examined.

Zig-Zag Performance (Open/Deep Water)

The zig-zag maneuver, as presented in the Kitimat maneuvering report, involved a succession of rudder angle changes from port to starboard. Initially, the rudder was set to 10 degrees port. When the heading of the vessel reached 10 degrees port the rudder angle was switched to 10 degrees starboard. Then, when the vessel heading reached 10 degrees starboard, the rudder angle is again changed to 10 degrees port, and the run is continued until the heading again reaches 10 degrees port and the rudder angle is reversed. This simulation was conducted at the vessel service speed of 15 $knots$. There was no wind or current loading included in the simulation. The simulated results from the Kitimat report and from NRIM are presented in Fig. 1.
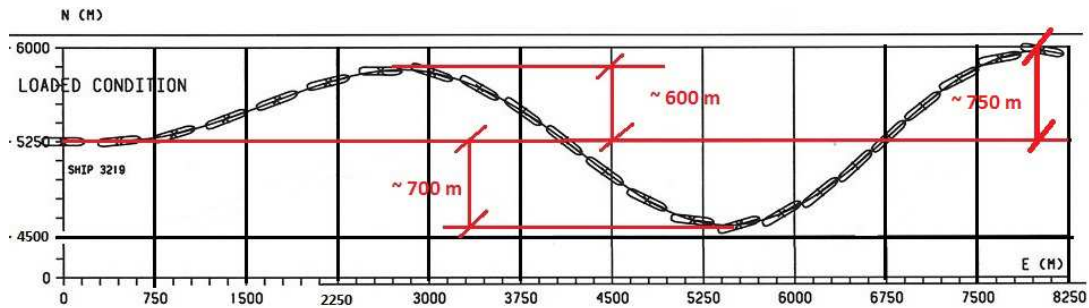
Figure 1: Kimimat Study Zig-Zag Maneuver (Adapted from FORCE Technology [3])
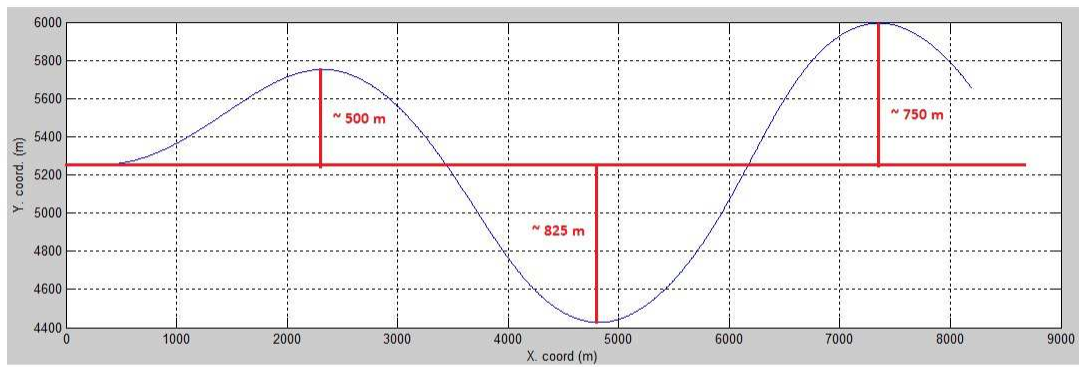
Figure 2: NRIM Zig-Zag Maneuver

The two simulations compare relatively well on the y-coordinate extremes of the first, second and third turn. NRIM predicts a little lower for the first port-turn (500 m versus 600 m) and then a little higher for the extreme of the starboard turn (825 m versus 700 m). The second port turn extreme compares very well with both predictions from the FORCE Technology simulator and NRIM both equal to 750 m.

In terms of the maximum forward distance travelled (x-coordinate) the FORCE Technology simulator predicts a distance of approximately 8000 m. At this same point, i.e. at the lateral maximum of the second port turn, the NRIM predicts a distance of approximately 7400 m.

Turning Circle Performance

There were two deep water turning circle simulations presented in the Kitimat study maneuvering report, both relating to a starboard rudder angle of 35 degrees. The first simulation was run with full engine power and the second simulation involved the engine running at an rpm that related to 10 $knots$. Since these runs were not held at constant forward speed and instead were set to constant engine settings, the three degree of freedom NRIM maneuvering model was required and used.

The FORCE technology simulator predicted similar results for both turning scenarios. For each, the advance was approximately 3300 m and the transfer was approximately 1100 m. The NRIM simulations produced similar results for both scenarios as well. In both instances, the transfer was predicted to be 1200 m (100 m larger than the FORCE technology predictions). For the full engine power case, the NRIM predicted an advance of 3125 m while for the 10 $knots$ engine setting run resulted in an advance prediction of 3100 m. These predictions were lower than the FORCE technology simulator predictions by 175-200 m. The results of the FORCE technology and NRIM simulations for each of the turning circle scenarios are presented in Fig. 3 and 4.
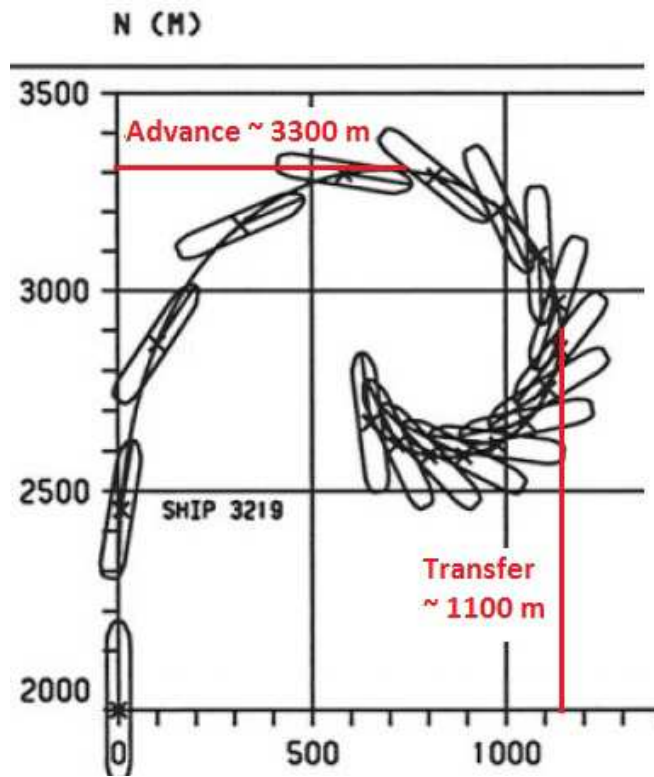
(a) Kitimat Study (Adapted from FORCE Technology [3])
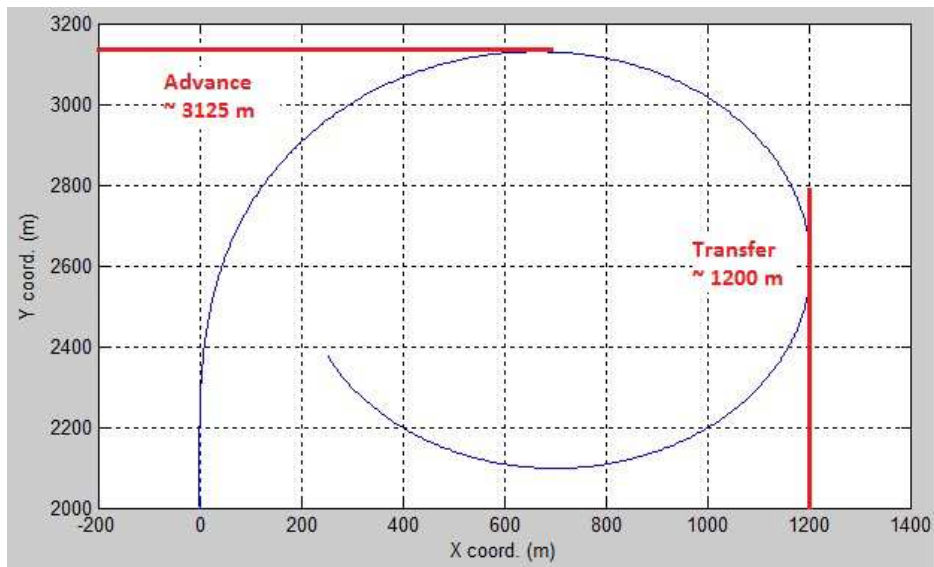
(b) NRIM

Figure 3: Turning Circle 1 - Engine at Full Power
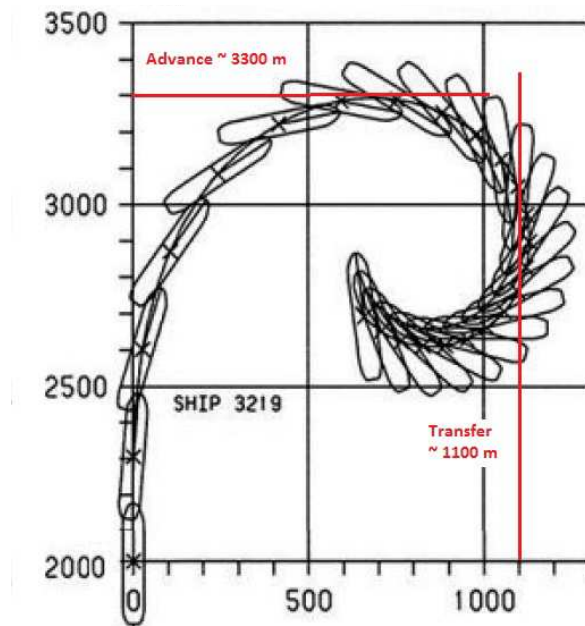
(a) Kitimat Study(Adapted from FORCE Technology [3])
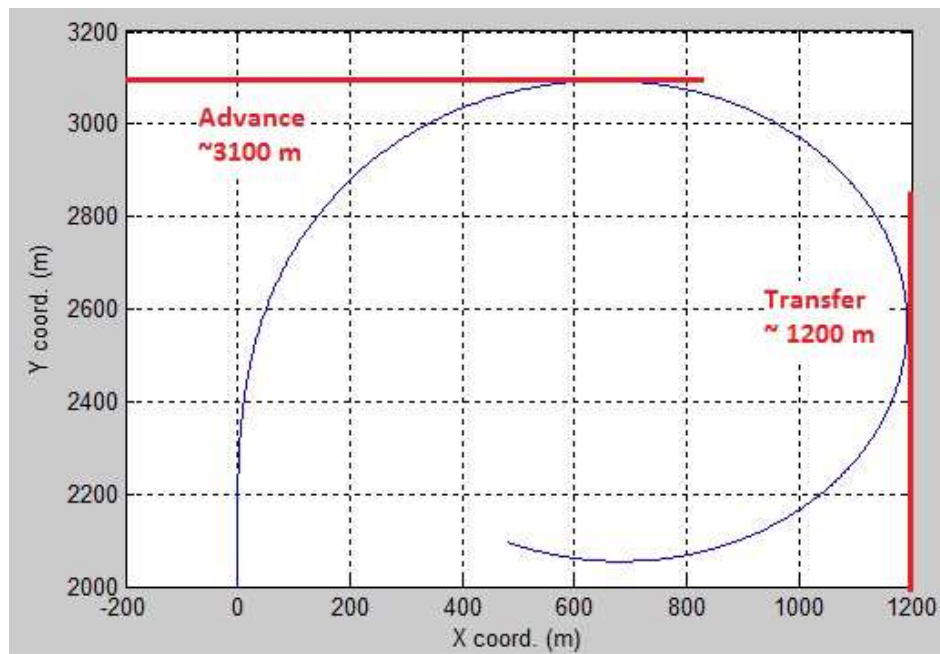
(b) NRIM

Figure 4: Turning Circle 2 - Engine Setting for 10 knots Forward Speed

Effect of Wind

A simulation was presented in which the effect of wind was investigated. In this simulation the wind speed was set to 30 knots and directed towards the port side of ship (beam wind). The rudder angle was set to zero degrees and the vessel speed to 8 knots. These parameters did not change throughout the simulation. The run time for this simulation was indicated to be five minutes. Since the forward speed was maintained at a constant value throughout the run, the two degree of freedom maneuvering model was used for NRIM simulation. The FORCE Technology simulated results indicated an overall forward distance of approximately 1000 m and a lateral offset of approximately 50 m. The NRIM simulation indicated a forward distance of approximately 1250 m and a lateral offset of around 40 m. When comparing these two sets of output we see that NRIM predicted a larger forward distance (by approximately 250 m) and a smaller lateral offset (by approximately 10 m). Both simulations indicated that the vessel turned into the wind during the run. The simulated results from both the FORCE Technology simulator and NRIM are provided in Fig. 5.
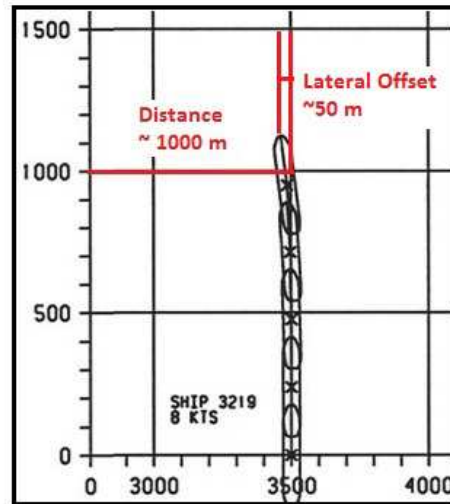
(a) Kitimat Study (Adapted from FORCE Technology [3])
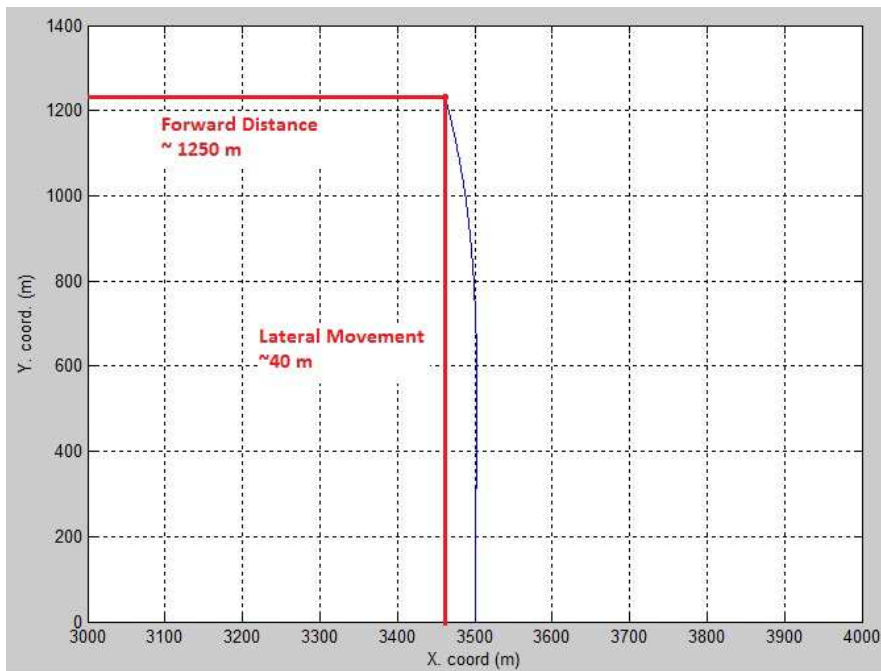
(b) NRIM

Figure 5: Effect of Wind Maneuver

Shallow Water Performance

The Kitimat study did provide results for a simulation conducted to investigate a shallow water turning circle for VLCC 3219. These results were provided in Appendix F of the Kitimat study (Force Technology, 2006) [27]. The water depth was set at 25.32 m and the rudder angle was 35 degrees in the starboard direction. The engine was set such that the initial speed was 8.6 $knots$. The NRIM maneuvering model makes use of empirical relations to correct the hydrodynamic derivatives for the shallow water effect. These empirical correction equations were developed by Sheng (1981) [24] and are described in Appendix 2 of the Clarke paper (Clarke, 1982) [1]. The corrections are indicated to be applicable in conditions at or above H/T = 1.2, where H is the water depth and T is the vessel draft. VLCC 3219 has a draft of 21.0 m and the case of water depth equal to 25.32 m relates to a H/T value of exactly 1.2. The NRIM maneuvering model was used to represent this scenario and the result, in terms of advance and transfer, were on the order of 10 times larger than those from the FORCE technology simulator. These large predictions may be due to the fact that the H/T ratio was too close to the threshold value implied by Clarke (1982) [1].

The NRIM maneuvering model was run again for this scenario but with the water depth increased slightly to 28 m, relating to a H/T ratio of 1.33. In this case, the results from the NRIM simulation compared reasonably well with the output from the FORCE technology simulator. The results from these two simulations are presented in Fig. 6. The FORCE simulation predicted an advance of approximately 1300 m which the NRIM advance prediction was slightly lower, approximately 1200 m. The transfer predictions compared very well with the FORCE technology simulation indicating a transfer of 1550 m and the NRIM predicting a transfer of 1500 m. The results of these comparisons indicate that the NRIM maneuvering model could be used to approximate the performance in shallow water but the H/T value should not be less than approximately 1.35. If a scenario arises in which the H/T value is below 1.35 then NRIM could still be used to provide a reasonable prediction of the maneuvering parameters if the water depth that is entered into the model is raised to meet the threshold requirement.
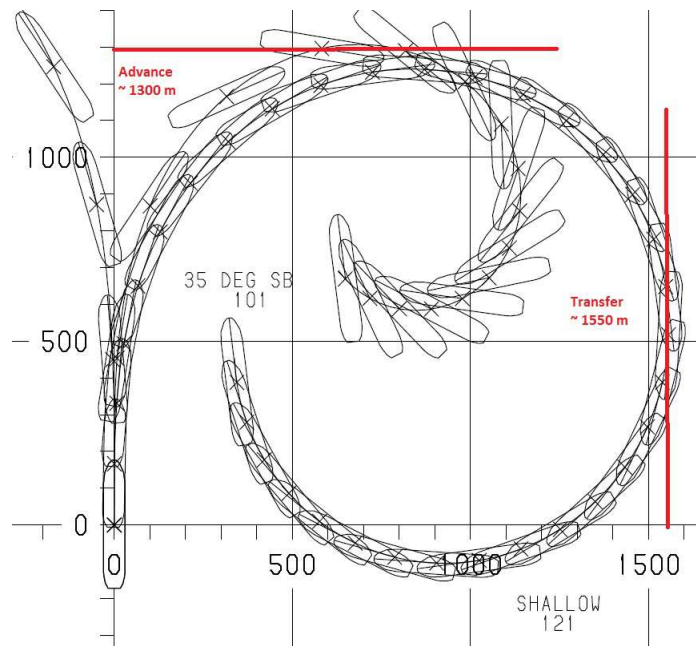
(a) Kitimat Study (Adapted from FORCE Technology [27])
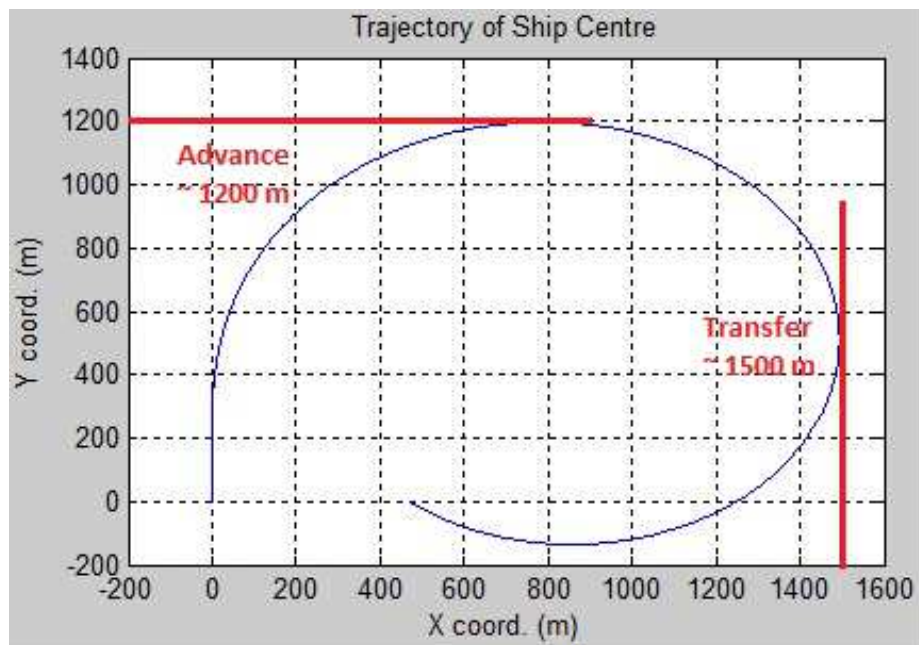
(b) NRIM

Figure 6: Turning Circle in Shallow Water

Discussion of Discrepancies

To use the three degree of freedom maneuvering component of NRIM information relating to the propulsive force created by the engine, in the surge direction, is required. In addition, the damping coefficient for the hull and rudder is required to enable computation of hull resistance at different vessel forward speeds. The three degrees of freedom (3DOFs) model is required when the vessel speed changes throughout the run and an engine setting is specified. The 3DOFs model was used to investigate the turning circle maneuvers, since the speed was denoted to vary throughout each run (shallow and deep water turns). For these simulations, the vessel resistance was calculated using the Holtrop-Mennen method [28]. The propulsive force was set equal to the vessel resistance at the given speed. The hull damping coefficient was then approximated using the below relation, while substituting in the calculated resistance and solving for C_D.

$$R = \frac{1}{2}\rho A C_D u^2$$

Where:

R is the vessel resistance

ρ is the density of water

A is the wetted hull area

C_D is the friction drag coefficient for the hull

u is the vessel forward speed

The Holtrop-Mennen method is a common approach that is described well in the literature [28]. This method of determining hull resistance via Holtrop-Mennen and then approximation of C_D using the above formulation, could be integrated into NRIM and used for scenarios in which no data relating to the propulsive forces for the vessel of interest are known. If the vessel propulsive force at different forward speeds was known, this data could be used instead of the approximations using the aforementioned method. Using actual propulsion data would reduce the overall uncertainties in the simulated predictions. The approximation of vessel resistance, propulsive forcing and damping coefficient may have led to some of the discrepancies between the FORCE technology simulations and the NRIM results.

Another source of uncertainty in the NRIM maneuvering simulations results from the prediction of hydrodynamic derivatives. The hydrodynamic derivatives are approximated using empirical relations by Clarke [1] in both the two and three degree of freedom models. To reduce this error the hydrodynamic derivatives could be measured experimentally to define actual values for specific scenarios. The experimentation to define hydrodynamic derivatives could involve model testing or computational testing using CFD. This may be something to consider for certain high risk scenarios in order to reduce the uncertainty

involved in simulated results, but would be outside the scope of the current project.

There are other parameters involved in the maneuvering computations that were esti-
mated. The Longitudinal Centre of Gravity (LCG), for example, was not provided in the
Kitimat reports but is required in the NRIM maneuvering model. The LCG was assumed to
be located at 20 m aft of the ship centre. This assumption was based on the LCG of typical
VLCC in this size range and the comparison of results with the provided data. All of the
parameters in the NRIM maneuvering component that were estimated for the simulations
performed in Phase I are summarized in Table 6. In general, the estimated parameters
were selected based on known values for a similar type and size of ship, data published in
the literature or calculated using an empirical relation. If true values of these parameters
were known these values could be entered into NRIM to reduce error.

Table 6: Estimated Parameters in NRIM Phase I Output

Parameter Details	Value for VLCC 3219	Source of Estimation
Hydrodynamic Derivatives	Many	Clarke (1982)
Rudder lift coefficient	0.3	Published Data
Rudder factor	3	Clarke (1982) Appendix 1
Projected area of ship exposed to lateral current flow	$L \cdot T$	Geometry - Conservative
Drag coefficient for current flow in lateral (beam) direction	1.2	In Literature - for Cylindrical Shape
Normal and axial wind drag coefficients	1.0 (both)	In Literature - for Cubic Shape
Propulsive Force	Various	Holltrop-Mennen (1982)
Longitudinal Centre of Gravity (LCG)	-20	Literature / Model Performance

Overall, the NRIM maneuvering output compared reasonably well with the FORCE Tech-
nology simulated results. Primarily, the source of discrepancies is associated with the
uncertainties involved in the input parameters, as detailed above. Since the FORCE tech-
nology simulator has been used operationally for many years and is well validated, this
comparison indicated that the NRIM maneuvering component is effectively capturing the
maneuvering behavior of the vessel at hand. Differences in some of the maneuver dis-
tances may be due to the prediction methods used to approximate the parameters dis-
cussed above. These predictive methods can be further investigated in Phase II based on
CCG recommendation.

5.1.2   Squat Comparisons

The under keel clearance assessment conducted as part of the Kitimat study considered a single squat formulation by Eryuzlu [29]. The preliminary squat investigation conducted in Phase I, as described in Appendix C of this report, considers the Eryuzlu formulation and compares it to the output of other squat prediction methods. In both the Kitimat under keel clearance study [27] and the Phase I squat investigation, predictions were made for VLCC 3219 and the open, shallow water case. The input parameters used in the Phase I squat analysis are defined in Appendix C.5. A curve of predicted squat value versus vessel speed is provided, from which it can be observed that the Eryzulu predictions (those from Phase I and those from the Kitimat study), are relatively low in comparison to the other predicted values. The Kitimat under keel clearance study reports that the Eryzulu equation is exclusively used by the CCG and hence this formulation should be further investigated in Phase II to obtain a complete understanding of the vessel types and channel configurations on which it is based.

5.1.3   Heave and Pitch Comparisons

In Kitimat study[26], dynamic motion in open sea is assessed using IACS JTP rule. General specification of ship is as follows.

Table 7: General Specification of Generic VLCC

Length [m]	345.3
Draft [m]	23.1
Beam [m]	58.1
Volume [m^3]	369,128.0
Block Coeff.	0.8

To compare the result of the developed strip method tool, specific VLCC shape data is required in addition to general dimensions of the ship in Table 7. A generic VLCC was created by NRC as shown in Fig. 7. This generic VLCC was designed to have the same basic particulars as outlined in Table 7 so that it could be used in the strip theory method to provide output to compare with the Kitimat data.

As mentioned in Kitimat study, $15m$ of significant wave height is applied to the calculation. As mentioned before, IACS JTP rule does not provide the heave prediction. The heave RAO is assumed as 1.5. Fig. 8 shows estimation results including two empirical formulas as well; Japan Fairway Guideline and Jensen's method.

As shown in Fig.8, the empirical formulae predict larger values than the output of the strip theory method. The results from the empirical formulas may be conservative to account for
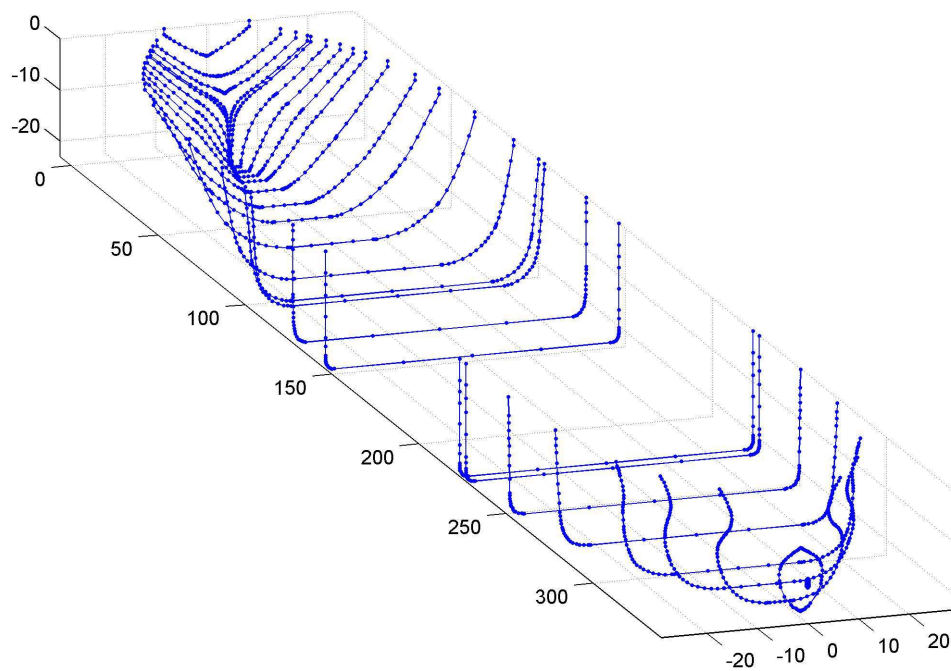
Figure 7: Hull Shape of Generic VLCC for Comparative Study
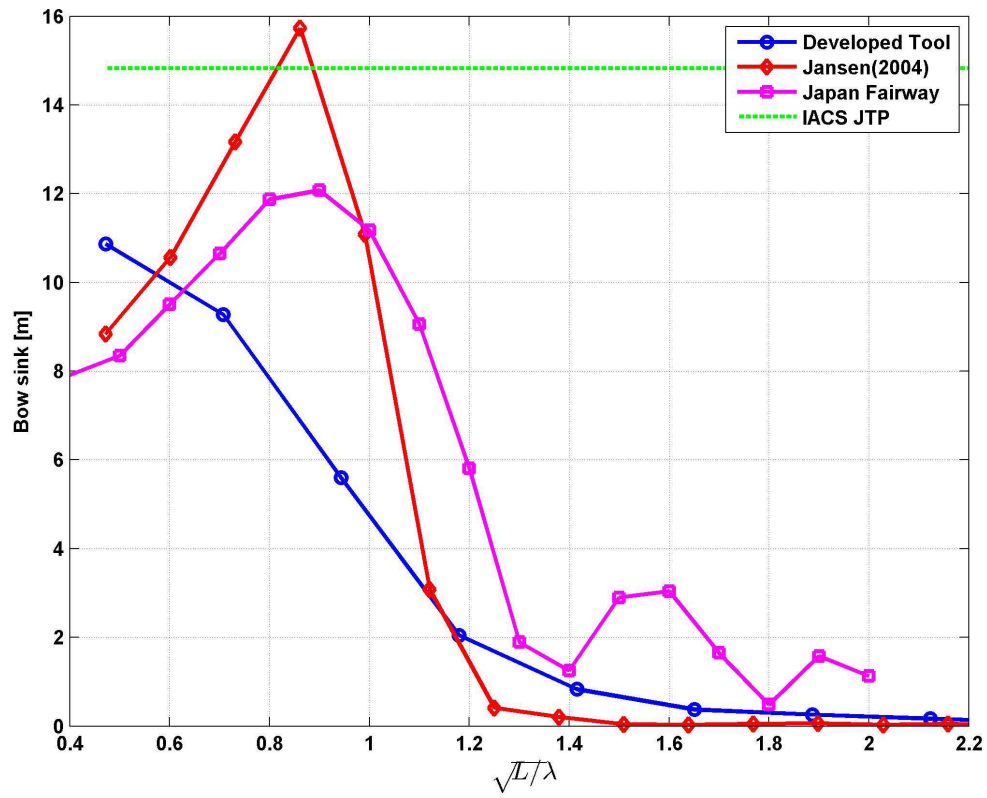
Figure 8: Bow Sink in $15m$ of Significant Wave Heights with Quatering Sea, $130°$ (L: Ship Length, λ : Wave Length)

the fact that the equations do not consider the unique hull features (just the basic param-
eters are required) Obviously, this difference related with the insufficient hull consideration
in empirical formulas. As mentioned in Appendix B.2.2, Jensen's method assumes that
the ship is a box shaped barge, which can cause a larger pitch motion eventually. Japan
Fairway also assumes that single typical response graph can represent every kind of ship.
Thus, the typical response should be selected in conservative manner. As a result, it is
supposed that those empirical formulas should give a conservative result. This is also ob-
served in International Association of Classification Society (IACS) JTP rule. It provides
only one single maximum value for structure designing.

As mentioned in Kitimat study, dynamic response in open sea is too severe for ships in
coastal areas, considering milder sea condition. Another wave condition is selected in Kiti-
mat study: $2m$ of wave height and 2.5 to 5 sec of wave period. When applying this coastal
wave condition, strip method as well as two empirical formulas: Japan Fairway Guideline
and Jensen's method, gives very small prediction which is negligible in MDA calculation.
This does not means that wave-induced motion is not important in MDA calculation. It is
noted that wave-induced motion can be negligible in mild or calm water area. More precise
study on wave environment in objective areas should be conducted.

5.2   Additional Considerations for CCG Required Output

This section describes the NRIM output requested by the CCG as described in the pro-
posal for this project. This output is compared to the current NRIM capabilities to highlight
existing gaps and review additional considerations that are required to fill these gaps.

5.2.1   Minimum Depth Allowance

The components of MDA that are considered and calculated by Phase I NRIM include
heave, pitch and squat. Other factors that may affect the MDA requirement include roll
and the vessel draft. The vessel draft can easily be added to NRIM computation of heave,
pitch and squat, to estimate the minimum depth allowance. The vessel roll is thought to
be relatively insignificant in comparison to the other parameters mentioned. However, if
CCG would like consideration of this parameter under certain conditions, for example the
existence of fin-stabilizers, it could be investigated in Phase II in terms of existing empir-
ical relations. Possible empirical relations were identified in the Phase I literature review.
Alternatively, a safety factor could be added to the NRIM computation to account for the
potential effects of this parameter and other anomalies. The Phase I NRIM can assess the
MDA in the following manner:

Minimum depth allowance

MDA is eventually related with vertical motion of the ship. Usually, the important parameters can be categorized as Fig. 9. The characteristics of these parameter can be summarized as Table 8
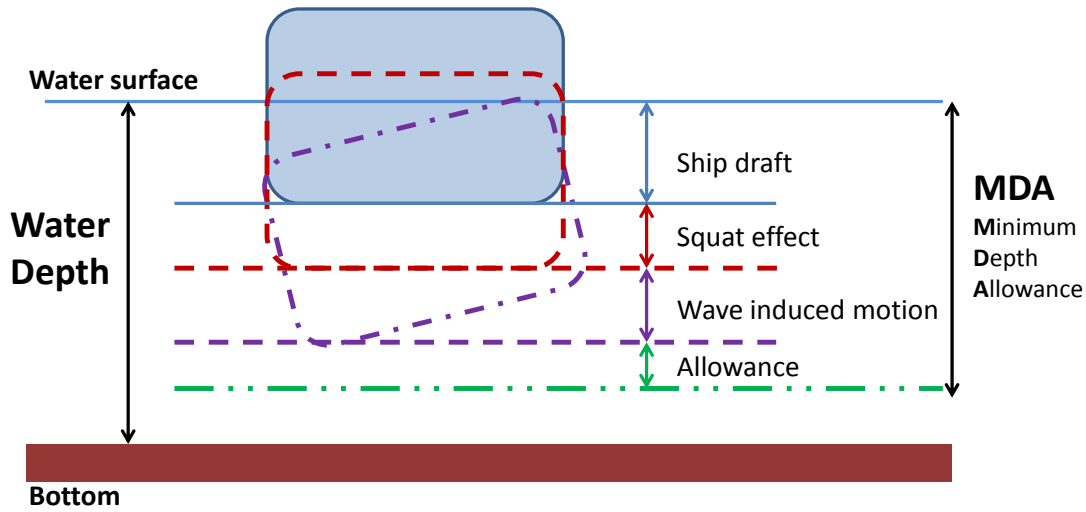
Figure 9: Minimum Depth Allowance

Table 8: MDA Parameters and Characteristics

Parameter	Related Concern	Operation Controllability
Ship Draft	Ship Characteristics	No
Squat Effect	Water Depth	No
	Ship Speed	Yes
Wave Induced Motion	Ship Characteristics	No
	Wave Height	No
Depth Allowance	Operational Experience	No

Obviously, ship draft is the most important parameter, because at least, water depth should be bigger than the draft. It is a fixed parameter when assessing MDA.

Secondly, squat is an important phenomenon which is frequently observed in shallow water operation. For scenarios in which the water depth is a concern, slower speed can reduce

MDA requirement.

The third parameter is wave-induced motion. Wave response is usually determined by the hull shape. As well, this dynamic effect strongly depends on wave characteristics such as wave period and height. It is not easy to control or reduce the dynamic motion during the operation. However, in coastal area, wave height and period is usually much smaller that open sea. Thus, the contribution of wave-induced motion becomes smaller due to small wave excitation. For the big vessel such as VLCC and container ship, it might be negligible considering the small relative wave length. For small vessels such as fishing boats, it is obvious that the wave-induced motion is still worth consideration because the resonance frequency of the small ship can be close to the wave frequency in coastal area.

Final component of MDA is depth allowance. Depth allowance can cover a lot of uncertainties during the operation. Thus, this parameter should be considered in the operational aspect. Depth allowable margin needs to be assessed by experts with sufficient experiences.

For a efficient calculation, two different MDA models can be considered.

For severe wave condition

$$MDA = ShipDraft + SquatEffect + WaveInducedMotion + DepthAllowance$$

- 1st step: Wave-induced motion is predicted by Jenson's method

- 2nd step: For 1st step MDA > water depth, wave-induced motion is predicted by numerical method like the developed strip method tool

For mild wave condition

$$MDA = ShipDraft + SquatEffect + DepthAllowance$$

For mild wave condition such as coastal areas, wave-induced motion can be negligible. In addition to wave height, wave period is also important parameter to decide if wave condition is severe or not. For conventional VLCC, the mild wave condition can be determined in terms of the relative wave length as equation 1 considering heave and pitch RAO becomes negligible around 2.

$$\sqrt{L/\lambda} > 2$$

where:

L: ship length [m]

λ: wave length [m]

(1)

Example of Wave Input for MDA Calculation

In Phase 1 NRIM, the module of wave-induced motion is based on the RAO concept. This RAO is the characteristic function of the specific ship, which describes the motion acting on unit amplitude of wave height. As a result, the expected motion can be calculated by multiplying the wave amplitude by the RAO value. Multiple sets of waves can be considered within NRIM. The following cases are representative examples of MDA consideration. However, for more realistic predictions, detailed wave information input, like case 4, is advisable.

- Case 1

    - Input: wave height
    - Output: maximum heave and pitch and its corresponding wave conditions like wave period (or frequency) and heading

- Case 2

    - Input: wave height and period (or range of periods)
    - Output: maximum heave and pitch and its corresponding wave heading

- Case 3

    - Input: wave height and heading (or range of headings)
    - Output: maximum heave and pitch and its corresponding wave period

- Case 4

    - Input: wave height, heading and period (or ranges of periods and headings)
    - Output: maximum heave and pitch

5.2.2   Minimum Channel Width

The preliminary NRIM can provide insight into the determination of minimum channel width for a one-way vessel in open water. Phase I NRIM simulations can be run with different wind and current to define the maneuvering lane requirements against the effect of these environmental conditions and vessel yaw. These simulations will be improved to consider the bank effect / effect of narrow channels in Phase II. Another enhancement will be the consideration of two-way and overtaking traffic. Based on the review of different waterway design guidelines and simulation tools, there are additional parameters that may affect the minimum channel width calculation besides those previously mentioned.

The Japanese Tool considers a width requirement to account for lags in the detection of drift. There are different empirical equations provided to compute this requirement pending

on the source of drift detection available to the vessel. If the only means of detecting drift is through the use of buoys, the additional width is calculated based on the buoy positioning, distance from buoys and other features of the buoy set up. In this case the extra width requirement can be quite large. In cases where the vessel is equipped with GPS or DGPS, simple guidance based on the breadth of the ship is provided. In the case of a DGPS the extra width requirement due to lag in detection of drift is 50% of the vessel breadth. These types of guidelines can be added to NRIM such that the required additional width is simply added to the width requirement due to wind and current forcing, if this is of interest to CCG. A detailed review of formula to account for drift detection is beyond the project scope. However, if CCG can provide NRC with such formula or agree to use the Japanese methods, this can be added to NRIM with little effort.

The PIANC guidelines consider yet another parameter in the calculation of minimum channel width, the bottom surface type. For this consideration, an extra width value, based on "a percentage of the vessel breadth", is simply added to the channel width requirement if the channel bottom is a certain type. This value is relatively small, having a maximum of 20% of the vessel breadth. Also, the bottom type consideration is only relevant when the water depth is low. PIANC guidelines indicate that the effect can be neglected when the water depth is greater than 1.5 times the vessel draft. Again, this requirement can be easily added to NRIM if CCG is accepting of the PIANC estimation methods.

Another consideration of the PIANC guideline is the maneuvering lane width requirement against the effects of wave. Wave forcing is not included in the maneuvering component of NRIM, only the MDA module. In terms of maneuvering, wave forcing may be relatively small in sheltered and narrow channels. The Japanese tool also doesn't include a channel width consideration relating to the effect of waves. The PIANC guidelines suggest that an additional width be considered for cases in which the wave height is larger than 1 meters and the wave length is equal to or greater than the length of the vessel. This addition can be up to 3 times the breadth of the vessel for cases of high speed and when the wave height is larger than 3 m. This project did not include the integration of wave loading into the maneuvering model, but these general guidelines could be added to NRIM if requested.

5.2.3   Radius of Turn, Advance and Transfer

The angle of turn can currently be investigated by NRIM, for the open water case. This investigation considers the effects of wind and current as well as vessel speed and rudder angle. The input requires vessel speed or engine setting, wind speed and direction, current speed and direction, and rudder angle. From the result of this type of simulation one can easily identify the radius of turn, advance and transfer. It is expected that the consideration of wave induced loading may be irrelevant here since wave heights will be small in an enclosed channel.

To investigate the radius of turn, advance and radius for scenarios involving narrow channels the bank effect should be considered. The maneuvering coefficients for narrow channels depend on bank proximity and water depth. These coefficients can be determined either through model tests or CFD software. Alternatively, they can be approximated using existing empirical relations. The ability to assess radius of turn, advance and transfer in waterways with narrow channels (using existing empirical relations) will be implemented in Phase II.

5.2.4   Minimum Settle Up Distance

NRIM can currently be used to investigate maneuvers in which the rudder angle changes at preset points through the simulation. The result of this type of simulation was presented in Figure 2 and supports the determination of minimum settle up distance at different wind, current, vessel speed and rudder angle settings. Again, this type of simulation is currently only applicable to the open water case since the bank-effect will not be integrated until Phase II.

A potential way to integrate this capability into a user friendly GUI would be to allow NRIM to accept a text file that defines the rudder angle at different time intervals through the run. In this case the rudder angle would be defined as a user-specified function of time. For standard runs (i.e. other maneuvers besides those to investigate the minimum settle-up distance) the single value of rudder angle can be entered directly into the GUI.

6   PHASE II DEVELOPMENT

The following sections describe the different components of Phase II development and summarize the findings from the Phase I literature review that could support these developments. In addition, a summary of questions or queries from the NRC project team, relating to Phase II development, are listed. These questions could be discussed in future meetings with the CCG working group to help direct Phase II NRIM developments.

6.1   Narrow Channel Maneuvering - Bank Effect

The Phase I NRIM development did not include the effect of narrow channels in the maneuvering model. The effect of narrow channels can be investigated in the MDA considerations when using the strip-theory approach and when using the empirical relations (if accepted by CCG). Further investigations are required in Phase II as to how to integrate the effect of narrow channels (the bank effect) into the maneuvering model. The literature review in Phase I provided some options and highlighted different methods to be considered in terms of their compatibility to the NRIM maneuvering model, their validity and the complexity of their input requirements. Two potential methods include that used by the Japanese Tool and that suggested by the PIANC design guidelines.

The Japanese Tool uses empirical equations by Kijima (1981 [30], 1983 [12]) to predict the forces and moments applied by a bank or channel wall on the hull of a vessel. These equations could be integrated into the NRIM maneuvering code to allow for a simulation that includes the forcing caused by a bank/channel wall. These equations make use of dimensionless coefficients of force and moment that arise from experimental data. The details of the experimentation used to define these values are not well understood at this stage. Further investigation is required to determine if this approach is applicable to all vessels and conditions and to define the limitations and benefits in general.

The PIANC guidelines, in the concept design stage, add an additional percentage onto the required channel width, if the vessel is in close proximity to a bank. The additional width percentage is based on only the speed of the vessel and gets larger as the vessel speed increases. This approach would be easy to compute within NRIM but the source of this guidance is not well understood. If this approach were used in NRIM, it would not be integrated into the maneuvering model but simply added to the output of the maneuvering simulation to account for the bank effect. In other words, the simulated path would not be modified but the output of minimum channel width requirement would be increased to accommodate for the forces applied by a bank or narrow channel. Since the concept design PIANC approach is relatively simple, it may be conservative. A comparative analysis was conducted between the results of the Japanese Tool output and PIANC requirements (Japan Institute of Navigation, 2009) [7] which indicated that PIANC requirements are more conservative.

These methods, and others found in the literature, will be reviewed in more detail during Phase II to select the best option for integration into NRIM. Phase II integration of the bank effect will be based on existing empirical methods that are available in the literature. If validation of the approximated coefficients found using these predictive measures are required for certain specific scenarios, the unique narrow-channel maneuvering coefficients could be investigated through CFD or model testing, as an add-on to this project.

6.2   Two Way Traffic, Overtaking Vessels and Passing Vessels

The investigation of two-way traffic as well as overtaking and passing vessels will commence in Phase II of NRIM development. Similar to the narrow channel/bank effect, methods for consideration of two-way traffic and overtaking/passing vessels were identified in the Phase I literature review. Overtaking vessels relate to two vessels transiting in the same direction at different speeds. In this case the vessel at the rear has a higher speed than the vessel at the front and the rear vessel "overtakes" the front vessel to become the leading vessel. Passing vessels relate to two vessels travelling in opposite direction, both coming to a point where they meet side by side prior to passing one another. These terms are used relatively consistently in the literature.

In both the PIANC guidelines and the Japanese tool, basic maneuvering distances were required for each of the independent vessels and then additions were made to account for overtaking and passing vessels. In the Japanese tool, empirical relationships were used to compute the forces and moments due to over-taking and passing vessels. In both the overtaking and passing case, the formulas were based on reports by Kijima (1984 [31] and 2002 [32]. These equations should be investigated further in Phase II to determine their applicability for integration into the NRIM. Limited details are provided in the Japanese Tool documentation relating to the development or basis of these equations and therefore the actual papers are required for review. The Japanese Tool literature does indicate that the equation presented to compute the overtaking forces and moments is for the shallow water case (Water Depth / Vessel Draft = 1.2 or below). Therefore, this equation may not be applicable for deep water and additional methods may be required.

The PIANC concept design method deals with passing distance in two-way traffic similar to how it dealt with the bank/narrow channel clearance requirements. An additional width was simply added to the width requirement if passing in two-way traffic was applicable. This width was based on a percentage of the basic maneuvering width which increased with vessel speed. The PIANC concept design guidelines did not provide considerations for the overtaking case. It may be that the considerations of the passing case are intended to cover both the passing and overtaking scenarios.

The previously described methods, along with additional relations described in the litera-

ture, will be reviewed in further detail in Phase II in order to identify the optimal method to include in NRIM. It should be noted that to model maneuvering scenarios involving passing vessels (two-way traffic), the effects of the hydrodynamic interactions between the vessels must be considered. The use of existing empirical formulations will be implemented in Phase II but we cannot comment on their validity without further investigation.

6.3   Implementation of Other Vessels

The number of vessel types that can be considered in NRIM is dependent on the level of detail and in effect level of precision, required for model development. At this stage, any vessel type or size can be simulated using the maneuvering model component of NRIM, given that the approach to approximation of hydrodynamic derivatives (hull and rudder coefficients) is sufficient. As presented in Section 5.1, the maneuvering output for the Kiti-mat scenario using the approximated hydrodynamic derivatives, compared relatively well to the FORCE Technology data. If a better approximation of hydrodynamic derivatives is required then this would require either CFD testing or model scale testing, which is beyond the scope of the current project. CFD testing could be considered for scenarios of great concern to CCG in the future, to define better approximations for hydrodynamic derivatives and provide a closer approximation of vessel maneuvering.

There are currently two maneuvering methods available in NRIM. The first is a two degrees of freedom (2DOFs) model and relates to a pre-set forward speed. Using this approach the engine setting is not considered, but the speed can be pre-set to change at defined times throughout the simulation. For this 2DOFs model there is no information required relating to the propulsion system and ship resistance. The other maneuvering method is three degrees of freedom (3DOFs) and considers a defined engine setting. In a simulation using the 3DOFs model, the vessel speed can change as a result of the external forces and the speed is not forced as in the case of the 2D model. This method requires information relating to the propulsive force from the ship engine and the vessel resistance curve. To use this method the CCG would need to provide NRC with this data so that it can be integrated into the model for a specific vessel. Alternatively, the approximate methods of estimating vessel resistance at a given speed and using this to define a propulsive force (as described in Section 5.1.1) can be used.

As for the MDA component of NRIM, again, multiple vessel types can be considered if the level of approximation is adequate for CCG requirements. The squat prediction is based on empirical equations from the literature. However, the wave induced heave and pitch can be computed using two different methods. The first uses strip theory and requires a table of offsets detailing the vessel geometry. Using this method, the boundary conditions can be modified, representing shallow or deep water and wide or narrow channels. This simulation provides relatively accurate results, based on our comparison with measured data however, the simulation requires approximately 1 hour to run. The second option

involves the use of empirical relations to investigate the wave induced heave and pitch. There were two empirical relations considered in Phase I and they compared reasonably well to the available data. However, they are less accurate than predictions using the strip-theory approach. When using the empirical relation method to compute wave induced heave and pitch, only basic parameters of the vessel geometry are required. Therefore, any number and type of vessel can be simulated. However, it must be cautioned that as the vessels of interest sway from the vessels considered in the development of these empirical relations, the errors in prediction may increase. Additional investigation to explore existing empirical relations to compute heave and pitch, their limitations and strengths, will be conducted in Phase II to confirm the best equations to use in NRIM. It is important to note that these two methods are not mutually exclusive and can both be available in NRIM. In cases where the CCG has data relating to the ship offsets, it may be best to select the strip theory approach. But in cases in which there is limited information available relating to the vessel geometry, the empirical approach can be selected to provide an approximation of heave and pitch.

6.4   Probabilistic Capabilities

Once all deterministic modelling is complete, NRIM will be enhanced to enable probabilistic computations and analysis. The application of probabilistic methods will allow for the computation of the following items in relation to the output of both the maneuvering and MDA models:

- Plots of probability distributions.
  - From these plots, the user will be able to extract values for any given confidence level.
  - For example, the turn radius calculation could be run using the full range of relevant input parameters to determine the range of resulting turn radius values (relevant to the environmental conditions of the given area), from which you can see the highest 10%, 20%, and etc.

- Text files summarizing the distributions of all input and output data.
  - This file will indicate the mean and standard deviation of all output and corresponding input as well as the distribution (e.g. normal) of each parameter.

- Plots representing the influence of input variables (such as wind speed, current speed, vessel speed, etc.) on output parameters.
  - The user will have the ability to select which output to evaluate and which input parameters to consider in the given evaluation.

– For example, the turn radius output could be assessed to determine the effect that wind speed has on the results.

The updated version of NRIM will be designed such that the environmental input data can be loaded from a CSV text file that contains raw data in a fixed tabular form (e.g. date and data columns). The CCG environmental database, AMCSD, is capable of exporting environmental data in this format as per the AMCSD guideline. In the case of limited available input data, a mean and standard deviation could be used as input where a normal distribution would be fit. It will also be possible to run a probabilistic simulation that considers a range in different vessel settings such as rudder angle and forward speed.

In all cases, the probabilistic approach will provide the user with an indication of how the output varies in relation to the variability of a combination of local environmental conditions and vessel settings.

6.5   Development of GUI

The final step of NRIM development will be the design of a Graphical User Interface (GUI) to house the maneuvering, MDA and probabilistic modules. The GUI will allow for a user friendly means of using the NRIM so that it can be manipulated and interpreted by the end user. The interface will enable a user to select and enter parameters through custom forms, save and restore sessions, and save and view output results.

The GUI will also be configured such that it requests a user specified safety margin as either a set-value or a percentage value. For example, when one selects to compute the MDA, the option would be presented to input a safety margin as a percentage or a set value. When the option to enter the safety margin as a percentage is selected, the user will be given the choice of setting the safety margin as any given percentage of the calculated MDA. When the option to enter the safety margin as a set value is selected the user must input the desired safety margin in units of length (meters, feet, etc.; whichever preferred by CCG). The selected safety factor should be based on operational insight and as such, the NRC will not provide any recommendation as to the appropriate value.

The GUI will also provide the user with the option to calculate the defined output for a given waterway using either a deterministic or probabilistic approach. If a deterministic approach is selected, the user will be asked to input a single value for each environmental input parameter in order to calculate the defined output. These single input values could relate to the mean, maximum or minimum conditions relevant to a given waterway. If a probabilistic approach is selected, the user will be asked to provide historic environmental input data relevant to the given waterway.

6.6 Questions for Working Group

MDA Related

1. Based on the findings presented from the preliminary squat investigation, could the CCG working group please confirm whether they would prefer a single squat formula (model) for use in NRIM to represent all types of ships which operate in all Canadian waters, or, whether a number of different squat formulae (models), each unique to a set of ship types and/or waterway types is preferred.

   - The second method may be less prone to error since certain formulations are defined based on a select set of ship types and/or channel configurations and may be more suited to make predictions relating to these parameters.

   - A number of the formulations considered in the preliminary squat investigation could be integrated into NRIM, but more research to help validate some of these equations may be required in Phase II (pending on CCG requests).

   - Using the second method, NRIM could internally select the most appropriate squat formulation based on the user definition of vessel type and channel configuration.

2. After reviewing the results of the Phase I squat investigation, would the CCG like to pursue:

   - An investigation of additional squat prediction methods, i.e. those using regression type analysis that were not considered in Phase I, or are you satisfied with selecting methods from those considered in the Phase I assessment?

   - If CCG would like investigation into squat prediction methods that use a regression analysis it will be necessary for the CCG to provide NRC with access to full scale data from the St. Lawrence Seaway, taken in 2005. These measurements were made by Gharbi et al. which were used in the regression analysis by Beaulieu et al., as mentioned briefly in the Squat Review presented in Appendix C. This subject can be discussed in the project review meeting prior to Phase II development.

3. After reviewing the results of the Phase I squat investigation, would the CCG like to pursue:

   - Validation of the squat predictive equations for the shallow/open water case or the trenched channel case? If so, CCG would have to provide NRC with full-scale data for validation of such scenarios

   - In particular, the equations by Eryuzlu et al., 1994 [29], were validated by data that are owned by the CCG. Further investigation would allow NRC to perform a comparison of predicted squat values using the available formulations to the full-scale measurements, such as was done for the trapezoidal canal case.

4. Right now, the empirical relations detailed in Appendix B can be used to approximate the heave and pitch for any vessel type and size or the strip-theory method could be used to determine the heave and pitch for the VLCC 3219 case only. Does the CCG have the vessel offsets for other vessels that they would like included for assessment in the strip-theory method during Phase II? Recall that this approach considers more detail of the vessel geometry and thus may be less conservative and have a higher accuracy, but has a higher computation time.

Maneuvering Model Related

5. Based on the CCG review of Phase I maneuvering performance (as documented in this report), do you feel satisfied to proceed with the proposed method for hydrodynamic derivative estimation (i.e. those by Clarke [1])?

6. When considering the effects of narrow channels and overtaking/passing vessels, is the CCG group satisfied with using either hydrodynamic coefficient estimation methods available in the literature and/or other methods available in the literature (such as those presented in PIANC which would not be integrated within the maneuvering model, but added to the output) to predict the added width (ect.) required to account for these effects?

7. Detailed consideration of empirical relations that investigate width requirements to accommodate for lags in detection of drift, wave effect on maneuvering and the effects of channel bottom type are not included in this project. If CCG would like the NRIM tool to output a minimum channel width value that considers these parameters the generic guidance from PIANC and/or the Japanese Tool may be able to be added during Phase II. In this case, an additional width would be added to the NRIM simulated output (which considers the drift and yaw due to the coupled effects of wind and current at different speeds) in the final minimum width computation.

8. Should the three degree of freedom maneuvering model (surge, sway and yaw) be packaged into NRIM? The model is currently programmed but if this type of simulation is not necessary, then perhaps it can be left out of the NRIM package. The 3DOFs model allows for investigation of vessel performance with different engine settings (and varying speed) while the 2DOFs model considers constant speed. The 2DOFs and 3DOFs models can mutually exist within NRIM such that the 3DOFs model is called upon only when necessary.

Probabilistic Method and/or GUI Development Related

9. If it is preferred that NRIM contain multiple squat formulae (some more suitable for select scenarios), should the GUI provide a choice of averaging across multiple formulae at each vessel speed? Should the plots of predicted squat versus vessel

speed include (i) the mean curve and (ii) a band of width plus-and-minus one standard deviation based on the range of predicted values at each vessel speed?

Related to Potential Future Work−Beyond Scope of Current Project

10. NRC could develop unique squat formulations for select high-risk scenarios (i.e. one squat formulation directly related to a specific vessel type and channel type). Development of these equations could be based on regression analysis of model scale and/or full-scale data, analytical assessment of scenario particulars, or CFD and BEM analysis. This type of investigation may be out of scope of the current project (pending on the availability of data in the literature) but could be completed as an add-on after project completion.

11. For the purpose of determining hydrodynamic derivatives (maneuvering coefficients), are the CCG interested in experimentally defining certain derivatives for select high risk cases, as opposed to predicting them using the current NRIM empirical relation approximation methods? This would likely reduce the error in the defined coefficients and increase the accuracy of the maneuvering model output. This could be completed in a future add-on Phase to this project after which the hydrodynamic derivatives would be added to NRIM. The hydrodynamic derivatives could be defined experimentally using two methods available at the NRC:

   - Perform model tests using the planar motion PMM for specific scenarios
   - Use computational fluid dynamics software (CFD)

References

[1] D. Clarke, P. Gedling, and G. Hine, "The application of manoeuvering criteria in hull design using linear theory," The Royal Institution of Naval Architects, Tech. Rep., 1982.

[2] J. J. Jensen, A. E. Mansour, and A. S. Olsen, "Estimation of ship motions using closed-form expressions," *Ocean Engineering*, vol. 31, pp. 61–85, 2004.

[3] FORCE Technology, "Maneuvering study of escorted tankers to and from Kitimat:Part 2, Main report," TERMPOL TDR, Tech. Rep. B23-19, 2010.

[4] Canadian Coast Guard, "Procedures manual for the design and review of marine short-range aids to navigation systems," Canadian Coast Guard, TP9677E, Tech. Rep., 1989.

[5] PIANC, "Approach channels a guide for design," Final report of the joint Working Group PIANC and IAPH, Tech. Rep., June 1997.

[6] M. McBride and HR Wllingford Ltd., "Approach channels (a guide for design): Progress of marcom working group 49." [Online]. Available: http://www.pianc.org.uk/documents/seminars/25Nov11/mark-mcbride.pdf

[7] Japan Institute of Navigation Standard committee, "Design standard for fairway in next generation," 2004.

[8] Y. Yoshimura, "Mathematical model for the manoeuvring ship motion in shallow water," *Journal of the Kansai society of naval architects, Japan*, vol. 200, March 1986.

[9] *Outline of ship handling (5th edition)*.   SEIZANDOSHOTEN, 1998.

[10] M. Hirano, J. Takasina, S. Moriya, and Y. Nakamura, "An experimental study on maneuvering hydrodynamic forces in shallow water," *Transactions of the west-Japan society of naval architects*, vol. 69, 1985.

[11] T. Yamano and Y. Saito, "An estimation method of wind force acting on ship's hull," *Journal of the Kansai society of naval architects, Japan*, vol. 228, 1997.

[12] K. Kijima and H. Qing, "Manoeuvring motion of a ship in the proximity of bank wall," *Journal of The Society of Naval Architects of Japan*, vol. 162, 1983.

[13] H. Fujii and T. Tuda, "Experimental researches on rudder performance," *Journal of the Society of Naval Architects of Japan*, vol. 110, 1961.

[14] FORCE Technology, "Simflex Navigator," 2013. [Online]. Available: http://www.forcetechnology.com/en/Menu/Products/Maritime-ship-simulators/Ship-simulator-systems/

[15] International Association of Classification Societies, "Common structural rules for dou-ble hull oil tankers," January 2006.

[16] S. Toxopeus and S. Lee, "Comparison of maneuvering simulation programs for sim-man test cases," SIMMAN, Tech. Rep., 2008.

[17] ITTC, "The maneuvering committee-final report and reccommendations to the 25th ITTC," International Tow Tank Committee, Fukoka, Tech. Rep., 2008.

[18] M. Abkowitz, "Stability and motion control of ocean vehicles," The Massachusetts In-stitute of Technology (M.I.T.), Tech. Rep., 1989.

[19] A. Ogawa and H. Kasai, "On the mathematical model of maneuvering motion of ships," *International Shipbuilding Progress*, vol. 25, Issue Number 292, pp. 306 – 319, 1978.

[20] S. L. Toxopeus, "Deriving mathematical manoeuvring models for base ship hulls using viscous flow calculations," *Journal of Marine Science and Technology*, vol. 14, pp. 30–38, 2009.

[21] K. Kijima, Y. Nakiri, and Furukawa, "On a prediction method for ship manoeuvrability," Proceedings of the international workshop on ship manoeuvrability, Tech. Rep., 2000.

[22] D. Vassalos, S. Park, and B. Lee, "Developing a manoeuvring design capability for naval vessels," Proceedings of the PRADS practical design of ships and other floating bodies conference, Tech. Rep., 1995.

[23] N. Norrbin, "Theory and observations on the use of a mathematical model for ship maneuvering in deep and confined waters," Meddelanden, SSPA No. 69, Tech. Rep., 1971.

[24] Z. Sheng, "Contribution to the discussion of the maneuverability committee report," Proceedings of the 16th International Towing Tank Conference (ITTC), Tech. Rep., 1981.

[25] MathWorks Inc., "Matlab documentation," 2012. [Online]. Available: http://www. mathworks.com/help/matlab/

[26] Northern Gateway Pipelines Inc, "Section 3.6: Special underkeel clearance survey, TERMPOL survey and studies," Tech. Rep., January 2010. [Online]. Available: https://docs.neb-one.gc.ca/ll-eng/llisapi.dll/fetch/2000/90464/90552/384192/620327/ 624798/691974/B23-7_-_TERMPOL_Surveys_and_Studies_-_Section_3.6_-_ Special_Underkeel_Clearance_Survey_A1Z6J1.pdf?nodeid=691993&vernum=-2

[27] FORCE Technology, "Appendix F: Maneuvering study of escorted tankers," TERMPOL TDR, Tech. Rep. B23-27, 2006.

[28] J. Holtrop and G. Mennen, "An approximate power prediction method," International Shipbuilding Progress, Tech. Rep., 1982.

[29] N. E. Eryuzlu, , and R. Hausser, "Experimental investigation into some aspects of large vessel navigation in restricted waterways," *Proceedings of the Symposium of Aspects of Navigability of Constraint Waterways Including Harbor Entrances*, pp. 1–15, 1978.

[30] K. Kijima and K. Nonaka, "Ship's manoeuvrability in restricted water," The Society of Naval Architects of Japan 3rd Manoeuvrability of Ship Symposium, Tech. Rep., 1981.

[31] K. Kijima, "Yasukawa manoeuvrability of ships in narrow waterway," *Journal of The Society of Naval Architects of Japan*, no. 156, 1984.

[32] C. Lee and K. Kijima, "On the safe navigation including the interaction forces between ship and ship," *Transactions of the west-Japan society of naval architects*, no. 104, pp. 63–74, 2002.

[33] K. McTaggart, "Shipmo3d version 3.0 user manual for computing ship motion in the time and frequency domains," DRDC Atlantic, Tech. Rep., November 2011.

[34] T. Kim and Y. Kim, "Numerical study on floating-body motions in finite depth," *International Journal of Ocean System Engineering*, vol. 2, pp. 176–184, 2012.

[35] O. M. Faltinsen and T. Svensen, "Incorporation of seakeeping theories in cad," 1990.

[36] T. I. Fossen, *Marine Control Systems*.   Marine Cybernetics, 2002.

[37] *Practical Ship Hydro Dynamics*.   Butterworth-Heinemann, 2000.

[38] 22nd ITTC Manoeuvring Committee, "Final report and recommendations (1999)," Tech. Rep., 1990.

[39] E.O.Tuck, "Shallow-water flows past slender bodies," *Journal of Fluid Mechanics*, vol. 26, pp. 81–95, 1966.

[40] T.Constantine, "On the movement of ships in restricted waterways," *Journal of Fluid Mechanics*, pp. 247–257, 1960.

[41] M. J. Briggs, M. Vantorre, K. Uliczka, and P. Debaillon, *Prediction of Squat for Under-keel Clearance*.   World Scientific, 2009, ch. 26, pp. 723–774.

[42] J. T. Tothill, "Ships in restricted channels: A correlation of Model Tests, Field measurements and Theory," NRC Mechanical Engineering, Tech. Rep. MB-264, January 1966.

[43] ——, "Ships in restricted channels: A correlation of model tests, field measurements and theory," *Marine Technology*, pp. 111–128, April 1967.

[44] M. J. Briggs, "Ship squat predictions for ship/tow simulator," US Army Corps of Engineers, Tech. Rep. ERDC/CHL CHETN-I-72, August 2006.

[45] M. J. Briggs, P. J. Kopp, V. K. Ankudinov, and A. L. Silver, "Comparison of measured ship squat with numerical and empirical methods," *Journal of Ship Research*, vol. 57, no. 2, pp. 73–85, June 2013.

[46] K. Ohtsu, Y. Yoshimura, M. Hirano, H. Takahashi, and M. Tsugane, "Design standard for fairway in next generation." Jeju, South Korea: Asia Navigation Conference, October 2006, pp. 20–21.

[47] B. Barrass, *Ship Design for Masters and Mates*, 2004.

[48] B. Barrass and D. R. Derrett, *Ship Stability for Masters and Mates*, 2006.

[49] D. T. Stocks, L. L. Dagget, and Y. Page, "Maximization of ship draft in the St. Lawrence Seaway, Volume 1: Squat study," Tech. Rep. TP13888E, June 2002.

[50] U. M. Guliev, "On squat calculations for vessels going in shallow water and through channels," pp. 17–22, 1971.

[51] B. M. C. Beaulieu, J. Ouarda, and O. Seidou, "Modélisation du surenfoncement des navires marchands qui transitent par le Fleuve Saint-Laurent," INRS-ETE, Québec, QC, Canada, Tech. Rep. R-974, March 2008.

[52] C. Beaulieu, S. Gharbi, T. B. M. J. Ouarda, and O. Seidou, "Statistical approach to model the deep draft ships' squat in the St. Lawrence Waterway," *Journal of Waterway, Port, Coastal and Ocean Engineering*, pp. 80–90, May-June 2009.

[53] C. Beaulieu, S. Gharbi, T. B. Ouarda, C. Charron, and M. A. B. Aissia, "Improved model of deep-draft ship squat in shallow waterways using stepwise regression trees," *Journal of Waterway, Port, Coastal and Ocean Engineering*, vol. 138, pp. 115–121, March 2012.

[54] T. P. Gourlay, "A brief history of mathematical ship-squat prediction, focussing on the contributions of E.O. Tuck," *Journal of Engineering Mathematics*, vol. 70, pp. 5–16, 2011.

[55] "Operating instructions for Japan Fairway 2000."

[56] M. J. Briggs, "Ankudinov ship squat predictions - Part I: Theory, parameters and fortran programs," US Army Corps of Engineers, Tech. Rep. Coastal and Hydraulics Engineering Technical Note CHETN-IX-19, August 2009.

[57] M. J. Briggs and L. Daggett, "Ankudinov ship squat predictions - Part II: Laboratory and field comparisons and validations," US Army Corps of Engineers, Tech. Rep. Coastal and Hydraulics Engineering Technical Note CHETN-IX-20, August 2009.

[58] J. B. Schijf, "17eme congrés de la navigation internationale, section 1 communication 2," Lisbon, 1949.

[59] T. H. Havelock, "Note on the sinkage of a ship at low speeds," *ZAMM*, vol. 19, no. 4, pp. 202–205, August 1939.

[60] S. Dunker, "Analysis of waterway factors on the underkeel clearance of sea-going vessels." Elsfleth/Oldenburg, Germany: 2nd Squat Workshop, 2004, pp. 150–172.

[61] I. H. Vermeer, "The behaviour of a ship in restricted waters," *International Shipbuilding Progress*, vol. 24, no. 280, pp. 323–336, Dec 1977.

[62] I. W. Dand and A. M. Ferguson, "The squat of full ship in shallow water," *Transactions of the Royal Institution of Naval Architects*, vol. 115, pp. 237–255.

[63] K. Eloot, J. Verwilligen, and M. Vantorre, "An overview of squat measurements for container ships in restricted water." Glasgow, UK: SOCW 2008, Sept 2008, pp. 106–116.

[64] T. P. Gourlay and K. Klaka, "Full-scale measurements of containership sinkage, trim and roll," *Australian Naval Architect*, vol. 11, no. 2, pp. 30–36, 2007.

[65] N. Alderf, E. Lefrancois, P. Sergent, and P. Debaillon, "Dynamic ship response integration for numerical prediction of squat in highly restricted waterways," *International Journal for Numerical Methods in Fluids*, vol. 65, pp. 743–763, 2011.

[66] F. Papoulias, "Ship dynamics course notes," 2013. [Online]. Available: http://faculty.nps.edu/vitae/cgi-bin/vita.cgi?p=display_vita&id=1023567943

[67] J. P. Hooft, "The behaviour of a ship in head waves at restricted water depths," *NASA STI/Recon Technical Report N*, vol. 75, p. 22547, Aug. 1974.

[68] B. Morse, S. Michaud, A. Taschereau, and R. Santerre, "Ship squat in shallow and confined channels -The Canadian experience." Elsfleth/Oldenburg, Germany: 2nd Squat Workshop 2004, March 2004.

Appendices

A   MANEUVERING MODEL

A.1   Governing Equations

The governing equations of the maneuvering model are derived with reference to Fig. A.1. We define a fixed inertial frame N with origin at O and X, Y axes in the horizontal plane. The ship has a body-fixed frame B with origin at the ship's centre C. The x axis of frame B is directed along the ship's longitudinal axis as shown, and the y axis is directed towards port. Unit vectors along the x and y axes are denoted by $\vec{i}$ and $\vec{j}$ respectively. The ship's centre C has inertial coordinates (q_1, q_2). The heading angle ψ is here defined as the angle between the body-fixed x axis and the inertial X axis measured anticlockwise from the X axis, and we define $q_3 = \psi$. Let the ship centre C have velocity $\vec{v}_C$ with components u, v in the B frame,i.e.
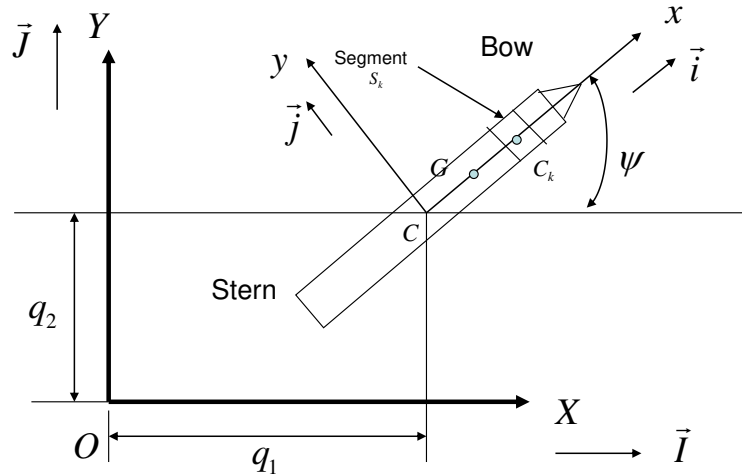
Figure A.1: Configuration

$$\vec{v}_C = u\,\vec{i} + v\,\vec{j} \tag{A.1}$$

The angular velocity of the ship is

$$\vec{\omega} = r\,\vec{k}$$

where $r = \dot{\psi}$ and $\vec{k} = \vec{i} \times \vec{j}$ is the vertical unit vector. Differentiation with respect to time t is denoted by overdots. The centre of mass of the ship is denoted by G and is assumed to lie on the longitudinal axis with x coordinate x_G,i.e. $\overrightarrow{CG} = x_G\,\vec{i}$. The velocity of G is

$$\vec{v}_G = \vec{v}_C + \vec{\omega} \times \overrightarrow{CG} = u\,\vec{i} + (v + rx_G)\,\vec{j}$$

Noting that $\frac{d}{dt}\left(\overrightarrow{i}\right) = \overrightarrow{\omega} \times \overrightarrow{i}$ and $\frac{d}{dt}\left(\overrightarrow{j}\right) = \overrightarrow{\omega} \times \overrightarrow{j}$ we find the acceleration of G is

$$\overrightarrow{a}_G = \frac{d}{dt}\left(\overrightarrow{v}_G\right) = \left(\dot{u} - vr - r^2 x_G\right)\overrightarrow{i} + \left(ur + \dot{v} + \dot{r}x_G\right)\overrightarrow{j} \tag{A.2}$$

The angular acceleration of the ship is

$$\overrightarrow{\alpha} = \frac{d}{dt}\left(\overrightarrow{\omega}\right) = \dot{r}\,\overrightarrow{k} \tag{A.3}$$

Let the sum of all forces and moments acting on the ship (from all sources) be equivalent to a force $\overrightarrow{F}$ at C together with a couple $\overrightarrow{N}$. This is equivalent to a force $\overrightarrow{F}$ at G together with a couple $\overrightarrow{N} + \overrightarrow{GC} \times \overrightarrow{F}$. Let $\overrightarrow{F} = X\overrightarrow{i} + Y\overrightarrow{j}$ and $\overrightarrow{CG} = x_G\overrightarrow{i}$. Then the external force-couple system acting on the ship is equivalent to the force $X\overrightarrow{i} + Y\overrightarrow{j}$ at C together with couple $(N - Yx_G)\overrightarrow{k}$. The equations of motion are

$$X\overrightarrow{i} + Y\overrightarrow{j} = m_0\overrightarrow{a}_G$$
$$(N - Yx_G)\overrightarrow{k} = I_{Gz}\overrightarrow{\alpha}$$

where m_0 is the mass of the ship and I_{Gz} is the moment of inertia of the ship about the vertical (z direction) axis through the centre of mass G. Substituting (A.2) and (A.3) in the equations of motion gives

$$m_0\left(\dot{u} - vr - r^2 x_G\right) \quad = \quad X \tag{A.4}$$

$$m_0\left(ur + \dot{v} + \dot{r}x_G\right) \quad = \quad Y \tag{A.5}$$

$$I_{Gz}\dot{r} \quad = \quad N - Yx_G \tag{A.6}$$

Let I_{Cz} be the moment of inertia of the ship about the vertical axis through C. Then

$$I_{Cz} = I_{Gz} + m_0 x_G^2 \tag{A.7}$$

Using (A.5) and (A.7) we re-write (A.6) as

$$I_{Cz}\dot{r} + m_0 x_G\left(ur + \dot{v}\right) = N \tag{A.8}$$

The governing coupled system of equations consists of (A.4), (A.5) and (A.8). These are the same equations presented by Clarke et al. [1].

A.2   MMG Model

This is a modular model of the external force components (X, Y) and couple N . These are written as (Yoshimura, 2005) [8].

$$X = X_H + X_P + X_R$$
$$Y = Y_H + Y_R$$
$$N = N_H + N_R$$

where the subscripts H, P, R refer to the hull,propeller and rudder respectively. We wish to add force and moment components due to current ,wind and thrusters using subscripts C,W and T respectively, so that

$$
\begin{aligned}
X &= X_H + X_P + X_R + X_C + X_W \\
Y &= Y_H + Y_R + Y_C + Y_W + Y_T \\
N &= N_H + N_R + N_C + N_W + N_T
\end{aligned}
\tag{A.9}
$$

A.3   Forces on Hull in Calm Water

Following Papoulias (Ship Dynamics Course Notes) [66], we express the hydrodynamic forces on the hull as perturbations about a steady forward speed u_0. First assume that the forces are functions of u, v, r and their first time derivatives, i.e.

$$
\begin{aligned}
X_H &= X_H \left(u, v, r, \dot{u}, \dot{v}, \dot{r} \right) \\
Y_H &= Y_H \left(u, v, r, \dot{u}, \dot{v}, \dot{r} \right) \\
N_H &= N_H \left(u, v, r, \dot{u}, \dot{v}, \dot{r} \right)
\end{aligned}
\tag{A.10}
$$

We wish to determine the ship response around an equilibrium condition designated by subscript 0. Expanding (A.10) about the equilibrium state $\left(u_0, v_0, r_0, \dot{u}_0, \dot{v}_0, \dot{r}_0 \right)$ in a Taylor series to first order gives

$$
\begin{aligned}
X_H &= X_0 + (u - u_0) \left(\tfrac{\partial X_H}{\partial u} \right)_0 + (v - v_0) \left(\tfrac{\partial X_H}{\partial v} \right)_0 + (r - r_0) \left(\tfrac{\partial X_H}{\partial r} \right)_0 \\
&\quad + \left(\dot{u} - \dot{u}_0 \right) \left(\tfrac{\partial X_H}{\partial \dot{u}} \right)_0 + \left(\dot{v} - \dot{v}_0 \right) \left(\tfrac{\partial X_H}{\partial \dot{v}} \right)_0 + \left(\dot{r} - \dot{r}_0 \right) \left(\tfrac{\partial X_H}{\partial \dot{r}} \right)_0
\end{aligned}
$$

$$
\begin{aligned}
Y_H &= Y_0 + (u - u_0) \left(\tfrac{\partial Y_H}{\partial u} \right)_0 + (v - v_0) \left(\tfrac{\partial Y_H}{\partial v} \right)_0 + (r - r_0) \left(\tfrac{\partial Y_H}{\partial r} \right)_0 \\
&\quad + \left(\dot{u} - \dot{u}_0 \right) \left(\tfrac{\partial Y_H}{\partial \dot{u}} \right)_0 + \left(\dot{v} - \dot{v}_0 \right) \left(\tfrac{\partial Y_H}{\partial \dot{v}} \right)_0 + \left(\dot{r} - \dot{r}_0 \right) \left(\tfrac{\partial Y_H}{\partial \dot{r}} \right)_0
\end{aligned}
\tag{A.11}
$$

$$
\begin{aligned}
N_H &= N_0 + (u - u_0) \left(\tfrac{\partial N_H}{\partial u} \right)_0 + (v - v_0) \left(\tfrac{\partial N_H}{\partial v} \right)_0 + (r - r_0) \left(\tfrac{\partial N_H}{\partial r} \right)_0 \\
&\quad + \left(\dot{u} - \dot{u}_0 \right) \left(\tfrac{\partial N_H}{\partial \dot{u}} \right)_0 + \left(\dot{v} - \dot{v}_0 \right) \left(\tfrac{\partial N_H}{\partial \dot{v}} \right)_0 + \left(\dot{r} - \dot{r}_0 \right) \left(\tfrac{\partial N_H}{\partial \dot{r}} \right)_0
\end{aligned}
$$

For obvious reasons, the quantities $\left(\tfrac{\partial X_H}{\partial u} \right)_0, \left(\tfrac{\partial X_H}{\partial v} \right)_0, ...,$etc. are called hydrodynamic derivatives. We now make the following observations (Papoulias ,"Ship Dynamics" Course Notes [66])

- Since the state "0" is an equilibrium state, $X_0 = Y_0 = 0, N_0 = 0$.

- Suppose that the equilibrium state is constant surge speed u_0, i.e. $u_0 =$constant, $v_0 = 0, r_0 = 0, \dot{u}_0 = 0, \dot{v}_0 = 0, \dot{r}_0 = 0$.

- Because of port/starboard symmetry, the surge force X_H is independent of $v, \dot{v}, r, \dot{r}$, i.e. $\frac{\partial X_H}{\partial v} = \frac{\partial X_H}{\partial \dot{v}} = \frac{\partial X_H}{\partial r} = \frac{\partial \dot{X}_H}{\partial \dot{r}} = 0$

- Because of port/starboard symmetry, the sway force Y_H is independent of $u, \dot{u}$, i.e. $\frac{\partial Y_H}{\partial u} = \frac{\partial Y_H}{\partial \dot{u}} = 0$

- The yaw moment N_H is independent of $u, \dot{u}$, i.e. $\frac{\partial N_H}{\partial u} = \frac{\partial N_H}{\partial \dot{u}} = 0$

With these observations we write equations (A.11) as

$$X_H = (u - u_0) X_u + \dot{u} X_{\dot{u}}$$
$$Y_H = v Y_v + r Y_r + \dot{v} Y_{\dot{v}} + \dot{r} Y_{\dot{r}}$$
$$N_H = v N_v + r N_r + \dot{v} N_{\dot{v}} + \dot{r} N_{\dot{r}}$$

where we have used the following notation :

$$X_u = \left(\frac{\partial X_H}{\partial u} \right)_0 ; X_{\dot{u}} = \left(\frac{\partial X_H}{\partial \dot{u}} \right)_0 ; Y_v = \left(\frac{\partial Y_H}{\partial v} \right)_0 ; Y_{\dot{v}} = \left(\frac{\partial Y_H}{\partial \dot{v}} \right)_0 , \ldots\ldots\text{etc.}$$

A.4   Forces on Rudder
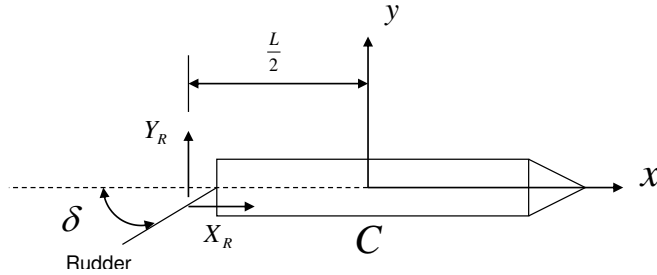
Figure A.2: Rudder Forces

The net force on the rudder is written as $X_R \vec{i} + Y_R \vec{j}$ as shown in Fig. A2. Assuming that X_R passes through C approximately, this is equivalent to a force $X_R \vec{i} + Y_R \vec{j}$ at C with a couple $N_R \vec{k} \equiv Y_R \left(\frac{L}{2} \right) \left(-\vec{k} \right)$, where L is the length of the ship at the waterline. That is, $N_R = -Y_R \left(\frac{L}{2} \right)$. Assume that the rudder force and moment are functions of the rudder angle $\delta(t)$ only and not $\dot{\delta}$ (Papoulias [66]). We can then write

$$X_R(\delta) = (X_R)_{\delta=0} + \left(\frac{\partial X_R}{\partial \delta} \right)_{\delta=0} \delta \simeq 0$$
$$Y_R(\delta) = (Y_R)_{\delta=0} + \left(\frac{\partial Y_R}{\partial \delta} \right)_{\delta=0} \delta = Y_\delta \delta$$
$$N_R(\delta) = (N_R)_{\delta=0} + \left(\frac{\partial N_R}{\partial \delta} \right)_{\delta=0} \delta = N_\delta \delta$$

61

where $Y_\delta = \left(\frac{\partial Y_R}{\partial \delta}\right)_{\delta=0}$ and $N_\delta = \left(\frac{\partial N_R}{\partial \delta}\right)_{\delta=0}$. Since $N_R = -Y_R\left(\frac{L}{2}\right)$ we have

$$N_\delta = \left(\frac{\partial N_R}{\partial \delta}\right)_{\delta=0} = \frac{\partial}{\partial \delta}\left(\frac{-Y_R L}{2}\right)_{\delta=0} = -\frac{L}{2}Y_\delta \qquad \text{(A.12)}$$

A.5 Forces due to Current and Wind

In order to model the distributed current and wind forces on the ship, we divide the hull into n transverse segments S_k $(k = 1, \ldots, n)$ as illustrated in Fig. A1. The centre of segment S_k is C_k and we let $\overrightarrow{CC_k} = d_k\,\overrightarrow{i}$ $(k = 1, \ldots, n)$. The velocity of C_k is

$$\overrightarrow{v}_{C_k} = \overrightarrow{v}_C + \overrightarrow{\omega} \times \overrightarrow{CC_k} = u\,\overrightarrow{i} + (v + rd_k)\,\overrightarrow{j}$$

The current and wind velocities are specified in inertial coordinates (OXY frame) as

$$\overrightarrow{v}_{\text{current}} = v_1^{\text{current}}\overrightarrow{I} + v_2^{\text{current}}\overrightarrow{J} \;\; ; \;\; \overrightarrow{v}_{\text{wind}} = v_1^{\text{wind}}\overrightarrow{I} + v_2^{\text{wind}}\overrightarrow{J}$$

Their components in the body-fixed frame Cxy are given by

$$\begin{pmatrix} v_x^{\text{current}} \\ v_y^{\text{current}} \end{pmatrix} = [C]\begin{pmatrix} v_1^{\text{current}} \\ v_2^{\text{current}} \end{pmatrix} \;\; ; \;\; \begin{pmatrix} v_x^{\text{wind}} \\ v_y^{\text{wind}} \end{pmatrix} = [C]\begin{pmatrix} v_1^{\text{wind}} \\ v_2^{\text{wind}} \end{pmatrix}$$

where matrix $[C]$ is given by

$$[C] = \begin{pmatrix} \cos\psi & \sin\psi \\ -\sin\psi & \cos\psi \end{pmatrix} \qquad \text{(A.13)}$$

For flow in the axial direction (unit vector $\overrightarrow{i}$), we denote the wetted surface area by A_{CA} with associated friction coefficient C_{DA}^{current}. The projected surface area for wind flow in the axial direction is denoted by A_{WA} with associated drag coefficient C_{DA}^{wind}. The densities of seawater and air are denoted by ρ, ρ_{air} respectively. The current and wind forces in the x direction (axial) are then

$$X_C = \frac{1}{2}\rho A_{CA} C_{DA}^{\text{current}}\left|v_x^{\text{current}} - u\right|\left(v_x^{\text{current}} - u\right)$$
$$X_W = \frac{1}{2}\rho_{\text{air}} A_{WA} C_{DA}^{\text{wind}}\left|v_x^{\text{wind}} - u\right|\left(v_x^{\text{wind}} - u\right)$$

The areas of segment S_k exposed to current and wind flow in the beam direction $\left(\text{unit vector } \overrightarrow{j}\right)$ are denoted by $A_k^{\text{current}}, A_k^{\text{wind}}$ with associated normal drag coefficients $C_{DN}^{\text{current}}, C_{DN}^{\text{wind}}$ respectively. Considering the flow velocities relative to the ship segment S_k, we write the forces on S_k due to current and wind as

$$\overrightarrow{F}^{\text{current}/S_k} = \gamma^{\text{current}/S_k}\overrightarrow{j} \;\; ; \;\; \overrightarrow{F}^{\text{wind}/S_k} = \gamma^{\text{wind}/S_k}\overrightarrow{j}$$

where

$$\gamma^{\text{current}/S_k} = \tfrac{1}{2}\rho A_k^{\text{current}} C_{DN}^{\text{current}} \left| v_y^{\text{current}} - v - rd_k \right| \left(v_y^{\text{current}} - v - rd_k \right)$$
$$\gamma^{\text{wind}/S_k} = \tfrac{1}{2}\rho_{\text{air}} A_k^{\text{wind}} C_{DN}^{\text{wind}} \left| v_y^{\text{wind}} - v - rd_k \right| \left(v_y^{\text{wind}} - v - rd_k \right)$$

The y direction current and wind forces are therefore equivalent to forces $Y_C \overrightarrow{j}$ and Y_W $\overrightarrow{j}$ at point C with couples $N_C \overrightarrow{k}$, $N_W \overrightarrow{k}$ where

$$Y_C = \sum_{k=1}^{n} \gamma^{\text{current}/S_k} \quad N_C = \sum_{k=1}^{n} d_k \gamma^{\text{current}/S_k}$$
$$Y_W = \sum_{k=1}^{n} \gamma^{\text{wind}/S_k} \quad N_W = \sum_{k=1}^{n} d_k \gamma^{\text{wind}/S_k}$$

A.6 Thruster Forces

The forces applied by all thrusters can be expressed as a force $Y_T \overrightarrow{j}$ at C and a couple $N_T \overrightarrow{k}$.

A.7 Dimensionless Form of Governing Equations

As mentioned above, we consider perturbations about a steady forward speed u_0. Define the following dimensionless quantities :

$$u' = \frac{u}{u_0}; \ v' = \frac{v}{u_0}; \ r' = \frac{rL}{u_0}; \ t' = \frac{tu_0}{L}$$

where L is the length of the ship at the waterline. Noting that

$$\frac{d}{dt} = \left(\frac{u_0}{L}\right)\frac{d}{dt'}$$

we define

$$\dot{u}' = \frac{d}{dt'}\left(u'\right) = \left(\frac{L}{u_0^2}\right)\dot{u} \ ; \ \dot{v}' = \frac{d}{dt'}\left(v'\right) = \left(\frac{L}{u_0^2}\right)\dot{v} \ ; \ \dot{r}' = \frac{d}{dt'}\left(r'\right) = \left(\frac{L^2}{u_0^2}\right)\dot{r}$$

We note that in the dimensionless form of the equations of motion, the overdot notation refers to differentiation with respect to the dimensionless time t'. Further define

$$m' = \frac{m_0}{\tfrac{1}{2}\rho L^3}; \ I'_{Cz} = \frac{I_{Cz}}{\tfrac{1}{2}\rho L^5}; \ x'_G = \frac{x_G}{L}$$

The dimensionless hydrodynamic derivatives are defined as

$$X'_{\dot{u}} = \frac{X_{\dot{u}}}{\tfrac{1}{2}\rho L^3}; \ X'_u = \frac{X_u}{\tfrac{1}{2}\rho L^2 u_0}; \ X'_P = \frac{X_P}{\tfrac{1}{2}\rho L^2 u_0^2}; \ X'_C = \frac{X_C}{\tfrac{1}{2}\rho L^2 u_0^2}; \ X'_W = \frac{X_W}{\tfrac{1}{2}\rho L^2 u_0^2}$$

$$Y'_{\dot{v}} = \frac{Y_{\dot{v}}}{\tfrac{1}{2}\rho L^3}; \ Y'_{\dot{r}} = \frac{Y_{\dot{r}}}{\tfrac{1}{2}\rho L^4}; \ N'_{\dot{v}} = \frac{N_{\dot{v}}}{\tfrac{1}{2}\rho L^4}; \ N'_{\dot{r}} = \frac{N_{\dot{r}}}{\tfrac{1}{2}\rho L^5}$$

63

$$Y'_v = \frac{Y_v}{\frac{1}{2}\rho L^2 u_0}; \ Y'_r = \frac{Y_r}{\frac{1}{2}\rho L^3 u_0}; \ N'_v = \frac{N_v}{\frac{1}{2}\rho L^3 u_0}; \ N'_r = \frac{N_r}{\frac{1}{2}\rho L^4 u_0}$$

$$Y'_\delta = \frac{Y_\delta}{\frac{1}{2}\rho L^2 u_0^2}; \ N'_\delta = \frac{N_\delta}{\frac{1}{2}\rho L^3 u_0^2} = -\frac{1}{2}Y'_\delta \ \text{(using (A.12))}$$

$$Y'_C = \frac{Y_C}{\frac{1}{2}\rho L^2 u_0^2}; \ N'_C = \frac{N_C}{\frac{1}{2}\rho L^3 u_0^2}$$

$$Y'_W = \frac{Y_W}{\frac{1}{2}\rho L^2 u_0^2}; \ N'_W = \frac{N_W}{\frac{1}{2}\rho L^3 u_0^2}$$

$$Y'_T = \frac{Y_T}{\frac{1}{2}\rho L^2 u_0^2}; \ N'_T = \frac{N_T}{\frac{1}{2}\rho L^3 u_0^2}$$

We substitute (A.9) into the right hand sides of (A.4),(A.5),(A.8) and substitute all parameters in terms of their dimensionless counterparts. This gives the equations of motion in dimensionless form as

$$\begin{aligned}
\left(m' - X'_{\dot{u}}\right)\dot{u}' &= X'_u\left(u' - 1\right) + m'\left(v'r' + (r')^2 x'_G\right) + X'_P + X'_C + X'_W \\
\left(m' - Y'_{\dot{v}}\right)\dot{v}' + \left(m'x'_G - Y'_{\dot{r}}\right)\dot{r}' &= Y'_v v' + (Y'_r - m'u')r' + Y'_\delta\delta + Y'_C + Y'_W + Y'_T \\
\left(I'_{Cz} - N'_{\dot{r}}\right)\dot{r}' + \left(m'x'_G - N'_{\dot{v}}\right)\dot{v}' &= N'_v v' + (N'_r - m'x'_G u')r' + N'_\delta\delta + N'_C + N'_W + N'_T
\end{aligned}$$
$$\text{(A.14)}$$

A.8   Trajectory Simulation

The generalised coordinates are q_1, q_2, q_3 as defined in Fig. A1. We write the velocity of the ship's centre C in inertial coordinates as $\overrightarrow{v}_C = \dot{q}_1\overrightarrow{I} + \dot{q}_2\overrightarrow{J}$. Using (A.1) and the coordinate transformation matrix (A.13) we have the kinematic relations

$$\begin{aligned}
\dot{q}_1 &= u\cos q_3 - v\sin q_3 \\
\dot{q}_2 &= u\sin q_3 + v\cos q_3 \\
\dot{q}_3 &= r
\end{aligned}$$
$$\text{(A.15)}$$

Define the dimensionless quantities

$$q'_1 = \frac{q_1}{L}; \ q'_2 = \frac{q_2}{L}; \ q'_3 = q_3$$

Further define

$$\dot{q}'_1 = \frac{d}{dt'}\left(q'_1\right) = \frac{\dot{q}_1}{u_0}; \ \dot{q}'_2 = \frac{d}{dt'}\left(q'_2\right) = \frac{\dot{q}_2}{u_0}; \ \dot{q}'_3 = \frac{d}{dt'}\left(q'_3\right) = \frac{L\dot{q}_3}{u_0}$$

64

We can then rewrite (A.15) as

$$
\begin{aligned}
\dot{q}_1' &= u' \cos q_3' - v' \sin q_3' \\
\dot{q}_2' &= u' \sin q_3' + v' \cos q_3' \\
\dot{q}_3' &= r'
\end{aligned}
\tag{A.16}
$$

where we note again that the overdots indicate differentiation with respect to the dimensionless time variable t'. Define the 3×1 vector $\{w\} = (u'\ v'\ r')^T$ where the superscript T indicates the transpose. The equations of motion (A.14) can be written in the form

$$
[A]\left\{\dot{w}\right\} = \{f\}
\tag{A.17}
$$

where the 3×3 matrix $[A]$ is given by

$$
[A] = \begin{pmatrix}
m' - X_{\dot{u}}' & 0 & 0 \\
0 & m' - Y_{\dot{v}}' & m'x_G' - Y_{\dot{r}}' \\
0 & m'x_G' - N_{\dot{v}}' & I_{Cz}' - N_{\dot{r}}'
\end{pmatrix}
$$

and the elements of the 3×1 vector $\{f\}$ are given by the right hand side of equation (A.14). Define the 6×1 vector $\{z\} = (q_1'\ q_2'\ q_3'\ u'\ v'\ r')^T$. We then have

$$
\left\{\dot{z}\right\} = \begin{pmatrix} \left\{\dot{q}'\right\} \\ \left\{\dot{w}\right\} \end{pmatrix}
\tag{A.18}
$$

where the 3×1 vector $\left\{\dot{q}'\right\}$ is given by (A.16) and the 3×1 vector $\left\{\dot{w}\right\}$ is found from the solution of (A.17). Equation (A.18) is solved by the MATLAB Runge-Kutta solver "ode45".

B WAVE-INDUCED MOTION

B.1 Introduction

This appendix describes the implemented strip method tool for wave-induced motion in restricted areas. This appendix covers theoretical background and software package summary. Typical result of the developed tool is compared with empirical methods. Finally, the application limit and upgrade plan will be discussed.

B.2 Empirical Method for Wave-induced Motion

Wave-induced motion is one of the performance criteria of the ship. Several empirical methods are suggested to predict wave responses. Those formulae generally assume that the water is deep enough and its boundary is open, where there is nothing to disturb the wave propagation. Apparently, there is a gap between this assumption and restricted area. However, there is no precedent study nor empirical method about the dynamic motion in the restrict areas. Three empirical methods of open sea-way are reviewed in this study.

B.2.1 Fairway Standard of Japan

Related with MDA, Japan Institute of Navigation Standard committee provides a general guidance of wave-induced motion. From the design standard of Japan Fairway(2004) [7], the wave induced motion is considered as two major components. The larger value is applied to the final MDA calculation.

- Bow sink, $D2$ due to heaving and pitching from figure B.1

- Bilge sink, $D3$ due to heaving and rolling from equation B.1

$$D3 = 0.7\frac{H_{1/3}}{2} + \frac{B}{2}\sin\theta \ \ [\text{m}]$$

where:

$H_{1/3}$: significant wave height [m]

B: beam width [m]

$\theta = 7 \cdot 360 \cdot \left(0.35 H_{1/3}/\lambda\right)\sin\psi$

λ: wave length [m]

ψ: encounter wave angle, 0 for headsea

(B.1)

As shown in equation B.1 and figure B.1, the prediction procedure is pretty straight forward. Its input parameter is also simple like general dimensions of the ship. Usually, for a long ship like VLCC, pitch motion gives more significant effect to the vertical displacement. For
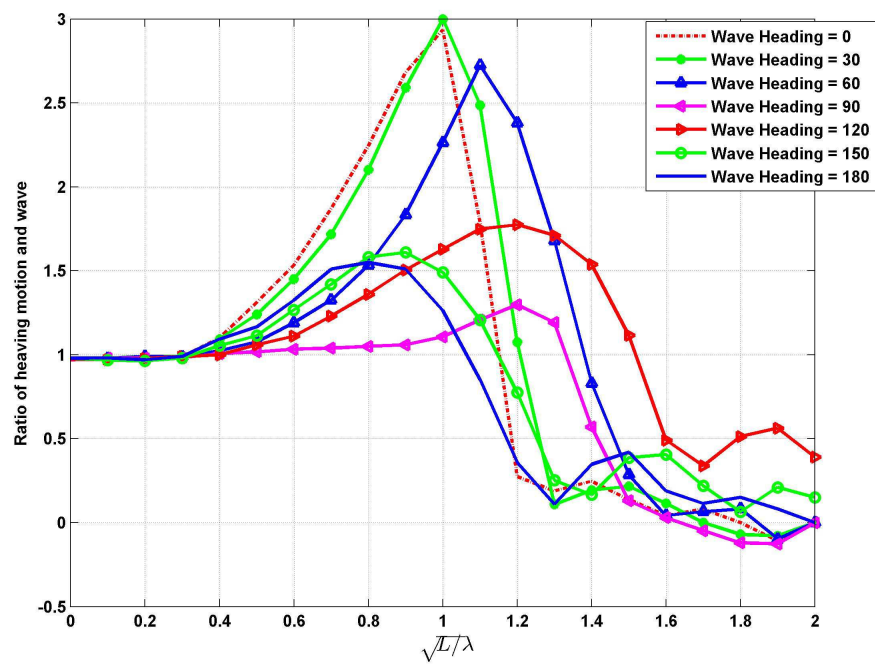
Figure B.1: Ratio of Heave Motion and Wave Amplitude: 10 Sections Regarding VLCC, VLCC Study Group

example, for a general 300 m of VLCC at 10 $konts$, D2 is around 4 and D3 is around 8. So, in the following comparison, pitch and heave coupled motion will be considered for a comparative study.

However, it is noted that the pitch-heave coupled motion in figure B.1 is predicted by one representative graph. There is no variable to consider the different hull shape or vessel type. Obviously, the hull shape of bow and stern strongly affects the pitch response considering the long moment arm of bow and stern section. As a result, the proposed method substantially could have large uncertainties when applied to a wide range of different ship types.

B.2.2   Jensen (2004)

Jensen (2004)[2] also suggested a simple method of wave-induced motion. He assumed that the wave-induced motion of the ship is as same as that of the equivalent box-shaped barge. Using the analytical solution of the box-shaped barge, the dynamic motion of the ship is approximated by equation B.2.

$$\Phi_{heave} = \eta \kappa f \frac{2}{k_e L} \sin \frac{k_e L}{2}$$

$$\Phi_{pitch} = \eta \kappa f \frac{24}{(k_e L)^2 L} \left[\sin \frac{k_e L}{2} - \frac{k_e L}{2} \cos \frac{k_e L}{2} \right]$$

where:

$$\eta = \left(\sqrt{(1 - 2kT\alpha^2)^2 + \left(\frac{A^2}{kB\alpha^3} \right)^2} \right)^{-1}$$

$$k_e = |k \cos \beta|$$

$$\kappa = \exp(-k_e T)$$ (B.2)

$$\alpha = 1 - \frac{U}{\sqrt{gL}} \sqrt{kL} \cos\beta$$

k : wave number

U : ship speed [m/s]

L : ship length [m]

β : relative wave heading [rad], 0 for following sea

g : gravity constant, $9.8 m/s^2$

To consider the different shape between ships and the barge, the equivalent beam width

in equation B.3 is suggested.

$$B = B_0 C_B$$

where:

$$C_B = \frac{\Delta}{LBT}$$ (B.3)

B_0 : ship beam width [m]

T : ship draft [m]

The equivalent beam width is supposed to be useful to capture volumetric characteristic of the ship such as thin or bulky. However, there is the limitation in considering ship flare as well as sharp bow and stern shape which is designed to reduce the fluid interaction. Apparently, the hydrodynamic force on the bow and stern can be over-predicted due to this insufficient hull consideration. Jenson's method is supposed to give more over-estimated pitch motion compared with heave response.

B.2.3   IACS JTP

IACS Joint Tanker Project (JTP) rule (2006) [15] also suggests the prediction method of dynamic ship motion in waves as shown in equation B.4 and B.5. Unlike previous two formulae, the result from this rule is not a ratio or amplification factor corresponding wave height. It gives the dimensional value. Moreover, it is noted that JTP rule does not provide the prediction guidance on heave motion.

Roll angle

$$\theta = \frac{50}{B + 75} \left(1.25 - 0.025 \cdot U_{roll}\right) f_{bk} \ \ [\text{rad}]$$

where:

$$U_{roll} = \frac{2.30 \cdot K_{roll}}{\sqrt{GM}}$$ (B.4)

B: beam width of the ship [m]

f_{bk}: 1 for ships with bilge keel, 1.2 for ships w/o bilge keel

K_{roll}: roll raius of gyration [m], approx. $0.35B$

GM: metacentric height, approx. $0.12B$

69

Pitch angle

$$\varphi = 960 \cdot \frac{V_1}{C_B} \frac{1}{L} \frac{\pi}{180} \ \text{[rad]}$$

where: (B.5)

V_1: cruising speed of the ship [m/s]

C_B: ship block coefficient

L: ship length

JTP rule is basically suggested to assess the structural issues such as fatigue or structure failure. So, the ship motion as well as wave condition is suggested in a conservative manner to design hull structure. Moreover, as shown in equation B.4 and B.5, wave amplitude and frequency is not affect to the dynamic motion of the ship. The response is only related with natural frequency of the ship. Moreover, in order to apply IACS rule, additional prediction method of heave response is required.

B.3   Theoretical Background

Empirical formulae is easy to use at initial assessment of MDA. However, as discussed in previous section, they can provide an over-prediction. In this project, strip method is implemented to estimate wave-induced motion more accurately.

B.3.1   Equation of Motion

As shown in figure B.2, a right-handed co-ordinate system as shown is selected to describe the theoretical background of wave induced motions. For a moving ship at constant speed, U, the wave is observed by the ship using the encounter frequency as shown eq.B.3.1.

$$\omega_{en} = \omega - kU \cos \beta$$

where,

ω: incident wave frequency

k: wave number   (B.6)

U: ship speed

β: relative wave heading
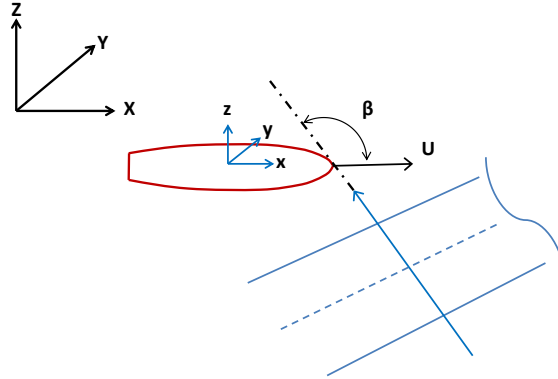
Figure B.2: Coordinate System and Relative Wave Heading

The harmonic motion of the ship due to incoming wave has the same frequency of incident wave. So, the ship motion can be assumed as eq.B.7.

$$x_j = \zeta_j e^{i(\omega_e t + \epsilon_j)}$$

where,

ω_{en}: frequency of motion

$j = 1, 2, 3, 4, 5, 6$: surge, sway, heave, roll, pitch and yaw motion

ζj: motion amplitude

ϵ_j: phase shift

(B.7)

Six degrees of freedom (DOFs) equations of motions of a ship in waves can be described as eq.B.8.

$$\sum_{j=1}^{6}\{(M_{kj} + A_{kj})\ddot{x}_j + B_{kj}\dot{x}_j + C_{kj}x_j\} = X_k$$

where:

$j, k = 1, 2, 3, 4, 5, 6$: surge, sway, heave, roll, pitch and yaw motion direction

$\ddot{x}_j, \dot{x}_j, x_j$: acceleration, velocity and dispacement of harmonic motion   (B.8)

X_k: harmonic wave excitation

M_{kj}: mass or ineria

A_{kj}: added(hydrodynamic) mass or interia

B_{kj}: radiation(hydrodynamic or wave making) damping

C_{kj}: restoring force or moment coefficient

6-DOFs equation of motion can be decoupled into two parts considering typical symmetric shape of the ship[36]. Moreover, surge motion has no significant effect on the minimum water depth problem. The equation of motion can be simplified in terms of heave and pitch as eq.B.9.

$$\begin{bmatrix} M_{33} + A_{33} & A_{35} \\ A_{53} & I_{55} \end{bmatrix}\begin{bmatrix} \ddot{x}_3 \\ \ddot{x}_5 \end{bmatrix} + \begin{bmatrix} B_{33} & B_{35} \\ B_{53} & B_{55} \end{bmatrix}\begin{bmatrix} \dot{x}_3 \\ \dot{x}_5 \end{bmatrix} + \begin{bmatrix} C_{33} & C_{35} \\ C_{53} & C_{55} \end{bmatrix}\begin{bmatrix} x_3 \\ x_5 \end{bmatrix} = \begin{bmatrix} X_3 \\ X_5 \end{bmatrix}$$ (B.9)

Applying eq.B.7, eq.B.9 can be simplified as follows. As a result, the only concern of wave induced motion is to determine hydrodynamic properties such as added mass and wave excitation.

$$\left\{ -\omega_{en}^2 \begin{bmatrix} M_{33} + A_{33} & A_{35} \\ A_{53} & I_{55} \end{bmatrix} + i\omega_{en}\begin{bmatrix} B_{33} & B_{35} \\ B_{53} & B_{55} \end{bmatrix} + \begin{bmatrix} C_{33} & C_{35} \\ C_{53} & C_{55} \end{bmatrix} \right\}\begin{bmatrix} x_3 \\ x_5 \end{bmatrix} = \begin{bmatrix} X_3 \\ X_5 \end{bmatrix}$$ (B.10)

Usually, restoring coefficients are as follows.

$$C33 = -\rho g A_{wl}$$
$$C55 = -\rho g \, V \, GM_L$$
$$C35 = C53 = 0$$
where: (B.11)

A_{wl}: waterplane area

V: submerged volume

B.3.2   Strip Method

To predict hydrodynamic loads on the floating body and simulate wave induced motions, strip method is implemented. Strip method is a popular approximation for typical ships

which are slender and cruising at significant forward speeds [37]. Equation B.12 shows the principle assumption of slender body. Physical meaning of the slender-body approximation is that certain component of the radiation and diffraction potentials is varying slowly along the ship length. As a result, complex 3-dimensional problem like wave loads on the ship can be simplified into 2-dimensional problem. Obviously, the prediction accuracy strongly depends on those slenderness ratios. However, experiments showed that the strip method is effective for predicting the motions of ships with length to breadth ratios(L/B) down to about three.

$$\frac{B}{L}, \frac{T}{L} = O(\epsilon), \ epsilon << 1$$

where:

B: ship beam, L: ship legnth and L: ship length.

(B.12)

With the help of strip method, 3 dimensional hydrodynamic properties can be estimated based on 2 dimensional values. Added mass and radiation damping can be calculated by eq. B.13.

$$A_{33} = \int_L a_{33} \, dx$$

$$A_{35} = -\int_L x \cdot a_{33} - \frac{U}{\omega_{en}^2} \, dx$$

$$A_{53} = -\int_L x \cdot a_{33} + \frac{U}{\omega_{en}^2} \, dx$$

$$A_{55} = \int_L x^2 \cdot a_{33} + \frac{U^2}{\omega_{en}^2} A_{33} \, dx$$

$$B_{33} = \int_L b_{33} \, dx$$

$$B_{35} = -\int_L x \cdot b_{33} + \frac{U}{\omega_{en}^2} \, dx$$

$$B_{53} = -\int_L x \cdot b_{33} - \frac{U}{\omega_{en}^2} \, dx$$

$$B_{55} = \int_L x^2 \cdot b_{33} + \frac{U^2}{\omega_{en}^2} B_{33} \, dx$$

(B.13)

where:

A, B: 3D added mass and radiation damping

a, b: 2D added mass and radiation damping

Wave diffraction force is also approximated by eq.B.14.

$$X_3 = \int_L p \, dx$$
$$X_5 = \int_L -x \cdot p \, dx$$

where:

(B.14)

X_3 and X_5 : wave excitation for heave and pitch

p : wave induced dynamic pressure on 2D section

In addition to the slender-body assumption, strip method assumes that the fluid is an ideal fluid; inviscid, incompressible, and ir-rotational. An ideal fluid is a valid assumption for a wave related problem because inertial effect is dominant. As a result, wave loads can be identified to solve a boundary value problem and find proper potentials. Usually, the total potential can be superposed by three components as eq.B.15.

$$\Phi_{total} = \Phi_I + \Phi_D + \sum_{j=1}^{6} \Phi_{Rj}$$

where, Φ_I: incident wave potential

where, Φ_D: diffraction potential

where, Φ_{Rj}: radiation potential

(B.15)

Each potential in eq.B.15 can be determined by specific boundary conditions, which will be dealt with in the following section.

B.3.3   2D Added Mass and Radiation Damping

Typical cross section of ship looks like figure B.3. When the ship oscillates with a unit amplitude, the displacement will be simplified as eq.B.16.

$$x_j = e^{-i\omega t}$$

(B.16)

Due to the ship motion, the oscillated fluid potential, Φ_j has the same frequency as eq.B.17.

$$\Phi_j = \phi_j e^{i(ky-\omega t)}$$

where:

(B.17)

k = wave number
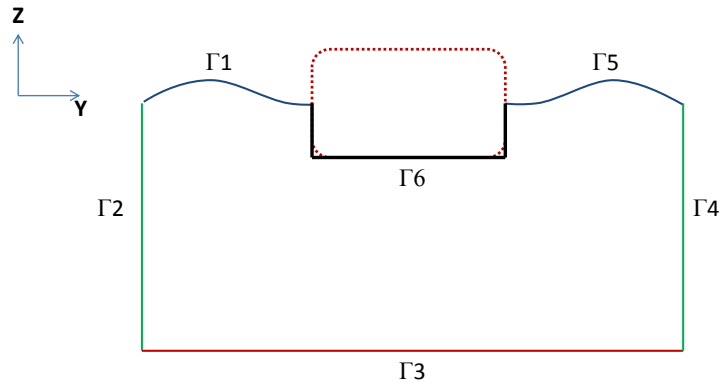
Figure B.3: 2D Hull Section and Boundaries

The radiation potential should satisfy free surface boundary condition(eq.B.18) as well as radiation condition(eq.B.19).

$$\left(\frac{\partial}{\partial n} - \frac{\omega^2}{g}\right)\phi_j = 0 \tag{B.18}$$

$$\left(\frac{\partial}{\partial n} - ik\right)\phi_j = 0 \tag{B.19}$$

For a rigid wall like sea bottom or restrict channel, following boundary condition is applicable.

$$\frac{\partial}{\partial n}\phi_j = 0 \tag{B.20}$$

where: n is surface normal

On the ship, following boundary condition is necessary.

$$\frac{\partial}{\partial n}\Phi_j = n_k \tag{B.21}$$

where: k = 2 for sway or 3 for heave

As a result, added mass and radiation damping is determined by eq. B.22.

$$a_{kj} = \rho\, Re\left[\int_{S_b} \phi_j \cdot n_k\, dS\right]$$

$$b_{kj} = \rho\,\omega\, Im\left[\int_{S_b} \phi_j \cdot n_k\, dS\right]$$

(B.22)

where:

S_b: 2D hull section, $\Gamma 6$

ρ: water density

B.3.4 2D Diffraction Force

Generally, wave excitation force consists of two components. The first part is Froude-Krylov force which is the force introduced by the pressure field generated by undisturbed incoming waves. Froude-Krylov force is easily obtained using incident wave potential of unit amplitude as shown as eq.B.23.

$$\Phi_I(y,z,t) = \frac{igA}{\omega}\frac{\cosh k(z+h)}{\cosh kh}e^{i(ks-\omega t)} = \phi_I e^{i(ks-\omega t)}$$

where :

(B.23)

h: water depth

$s = x \cdot \cos\beta + y \cdot \sin\beta$

The second component is diffraction force which the disturbance caused by the floating body. The diffraction potential,Φ_D, can be determined by solving boundary value problem.

$$\Phi_D = \phi_D e^{i(ks-\omega t)}$$

(B.24)

Diffraction potential of unit amplitude has to satisfy the following boundary condition because there is no flow penetration on the ship surface. Other boundary conditions are the same as those of added mass calculation, eq B.18, B.19 and B.20.

$$\frac{\partial}{\partial n}(\Phi_I + \Phi_D) = 0$$

$$\frac{\partial}{\partial n}(\phi_D) = \frac{-ikg}{\omega\cosh(kh)}\left[i\,\sin(\beta)\,\cosh k(z+h)\cdot n_2 + \sinh k(z+h)\cdot n_3\right]$$

(B.25)

on body surface, $\Gamma 6$

Using incident and diffraction wave potential, the total wave excitation can be calculated by eq. B.26.

$$\begin{aligned} X_k &= \int_{Sb} p \cdot n_k \, ds \\ &= \int_{Sb} -i \, \rho \, \omega_0 \, (\phi_I + \phi_D) \cdot n_k \, ds \end{aligned}$$

(B.26)

B.3.5   Wave-induced Motion

Now, all hydrodynamic properties in eq. B.10 can be estimated based on the strip method. It is note that every potential in the equation is defined with unit amplitude. Thus, the estimated motion response in eq.B.10 is a kind of motion amplification factor under unit amplitude of wave, which is usually called as Response Amplitude Operator (RAO).

B.4   Summary of Wave-induced Motion Prediction Software

B.4.1   Software Package Summary

Based on the strip method theory, wave-induced motion prediction tool is implemented using *MATLAB*^{TM}. Table B.1 introduces the developed script file and its function. Figure B.4 shows the work flow of the package.

Table B.1: Wave-induced Motion Prediction Software Package Content

File Name	Description
AMASS3D.m	Added mass and radiation damping calculation
BEM2D.m	2D BEM module
DIFF3D.m	3D diffraction force calculation
gauss.m	Gaussian quadrature module
GridGen2D.m	2D grid generation module based on piece-wide cubic spline
laplace2d.m	2D Laplace equation solver
offsetReader.m	3D offset data file reader
run_WaveResponse.m	Run example
wavenumber.m	Wave number calculation module
waveResponse.m	Main module to predict wave-induced motion

B.4.2   Analysis Input

Input parameters of the analysis tool are summarized in table B.2. General information of ship such as length, beam and draft is necessary. Environmental parameter such as wave
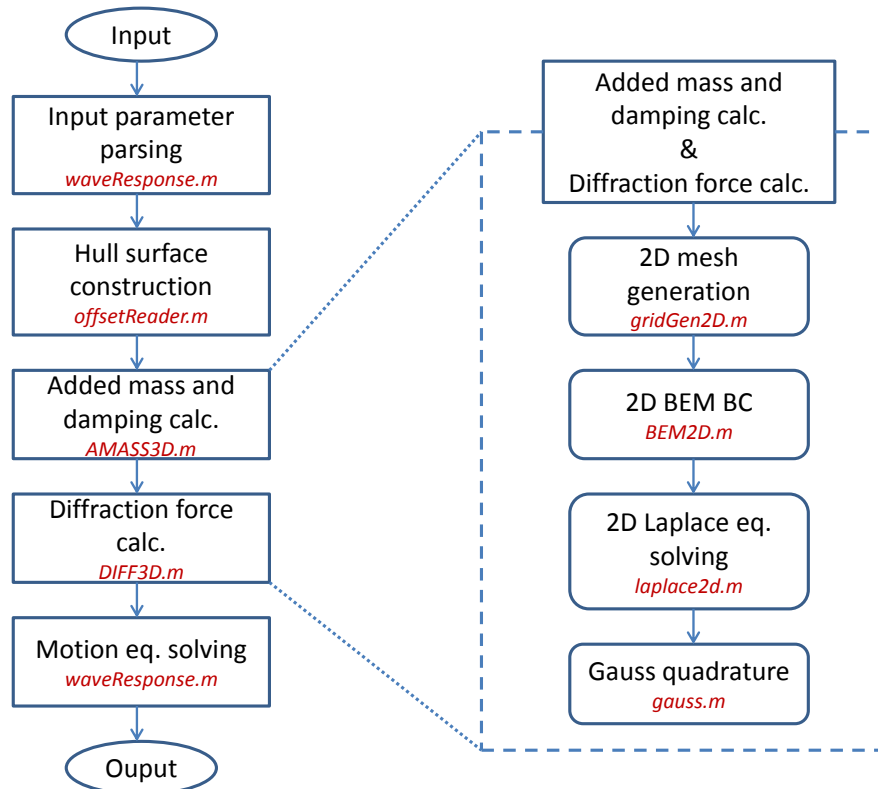
Figure B.4: Work Flow of Developed Strip Method Tool

frequency, heading and depth is also required to predict the wave-induced motion of the ship in the restrict channel. Among these input items, hull geometry is the most critical part to conduct the analysis because it is a time consuming task to convert offset table or hull lines to point sets. The geometry input example is shown as follows.

```
Example of geometry input file

        X Y Z
        ...
        339.0 0.0 7.0
        339.0 0.0 7.1
        339.0 0.1 7.1
        ...
```

Table B.2: Input Data for Wave-induced Motion Prediction

Object	Component	Variable name or input format	Unit
Ship	Hull geometry	External text file of x,y,z points geoFileName	m
	Length	shipLength	m
	Draft	shipDraft	m
	Speed	shipSpeed	m
	Center of gravity	shipKG	m
	Radius of gyration for pitch	shipRadG	m
Wave	Incoming wave frequency	Variable	rad/sec
	Relative wave heading	Variable	rad
Channel	Depth	Variable	m
	Width	Variable	m

B.4.3   Analysis Output

The most important output of the implemented tool is the bow sinkage amplification factor as shown in figure B.5. This bow sink factor is a kind of RAO which is a ratio between motion and incoming wave amplitude. Bow sink is the resultant motion which is coupled response between heave and pitch at bow position.
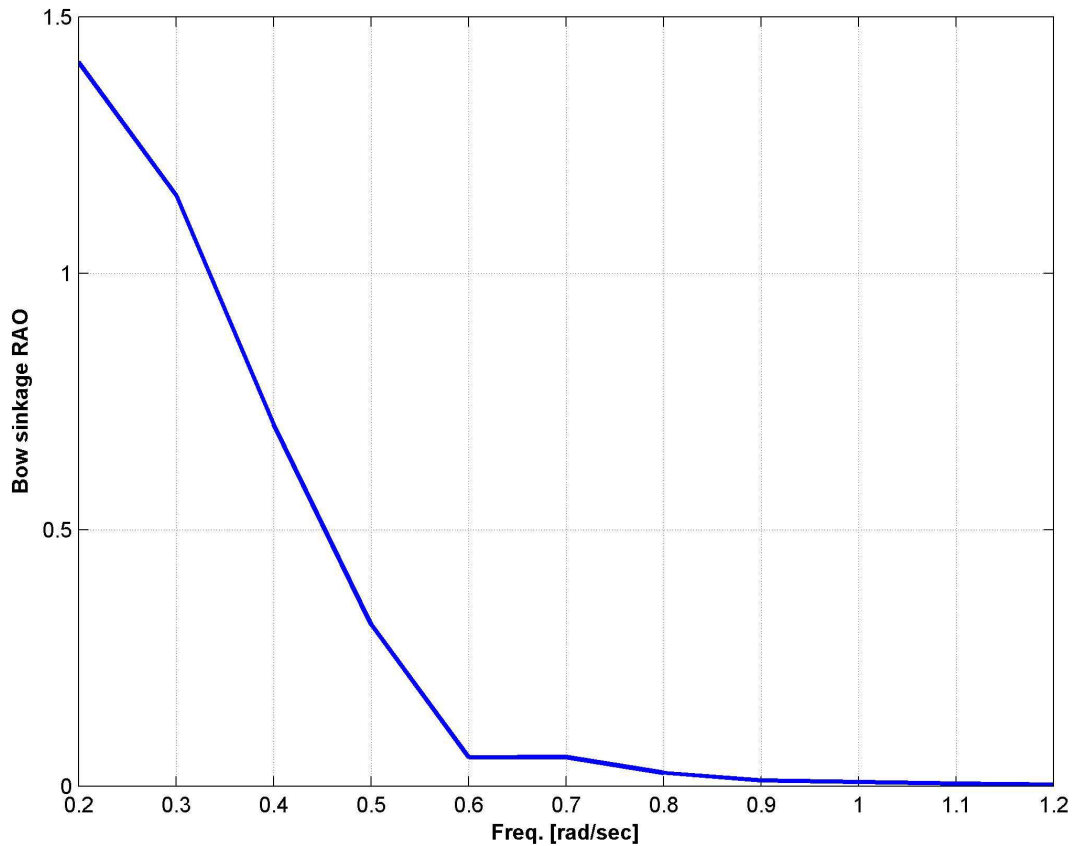
Figure B.5: Typical Result of Bow Sink Amplification Factor
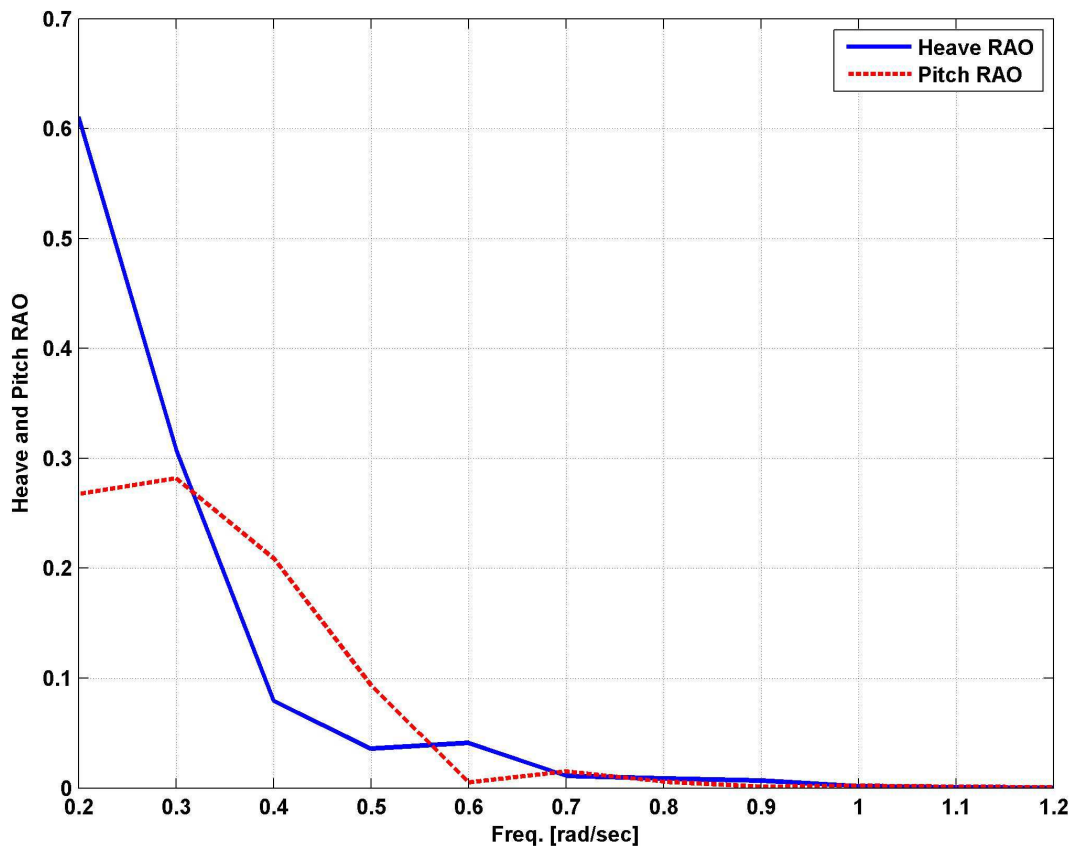
Figure B.6: Typical Result of Heave and Pitch RAO

Figure B.7 shows typical bow sink amplification factor under various wave heading.
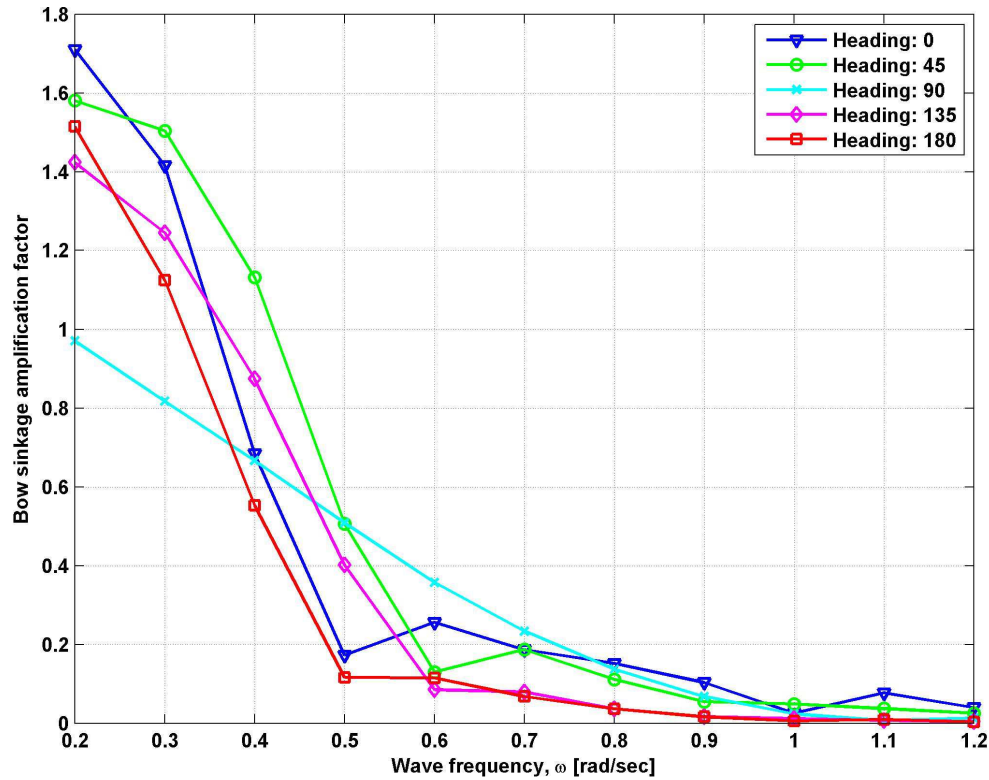
Figure B.7: Bow Sink Amplification Factor for Various Wave Headings with 10 $knot$ of Forward Speed

In addition to the final bow sink ratio, the developed software also support various outputs to check calculation procedure and input parameters as shown in figure B.8 and B.9. Uncoupled heave and pitch RAO can be evaluated like figure B.6
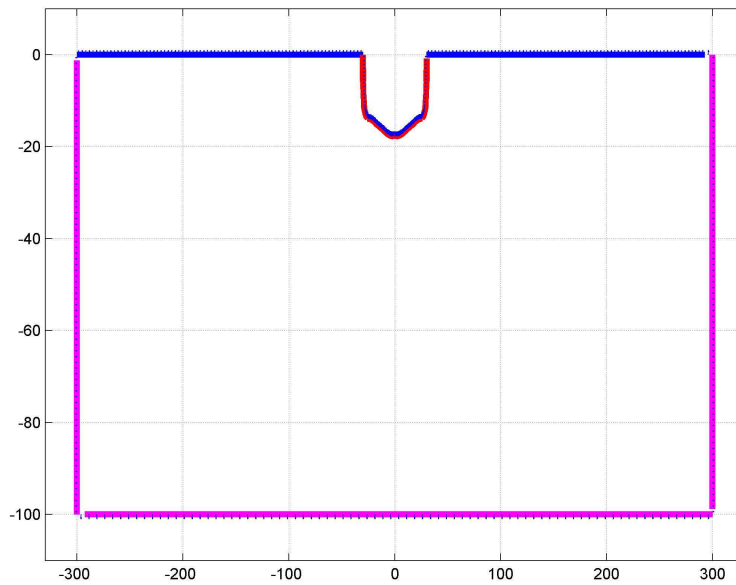
Figure B.8: Typical boundary condition from MATLAB script of BEM2D.m, BEM2D
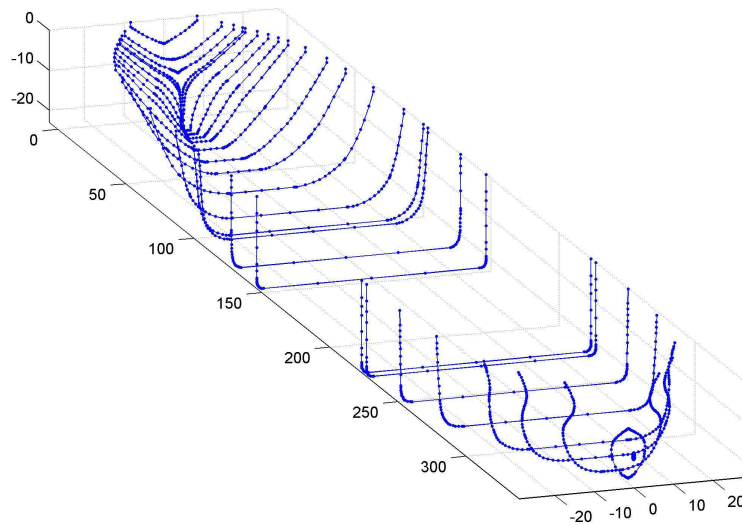
Figure B.9: Typical 3D hull model from MATLAB script of offsetReader.m

B.5   Analysis Result

B.5.1   Added Mass and Damping of Barge

In order to validate the developed tool, added mass and radiation damping for barge ship is compared with *ShipMo3D*™ [33]. ShipMo3D is general sea-keeping analysis tool developed by Defence Research and Development Canada (DRDC). Because ShipMo3D does not support the shallow water analysis, deep water boundary condition is applied to the developed tool. As shown in figure B.10, the results of both analysis agree well with one another.

Table B.3: Test Barge Dimensions

Length	60 m
Beam	10 m
Draft	4 m
Volume	2400 m^3
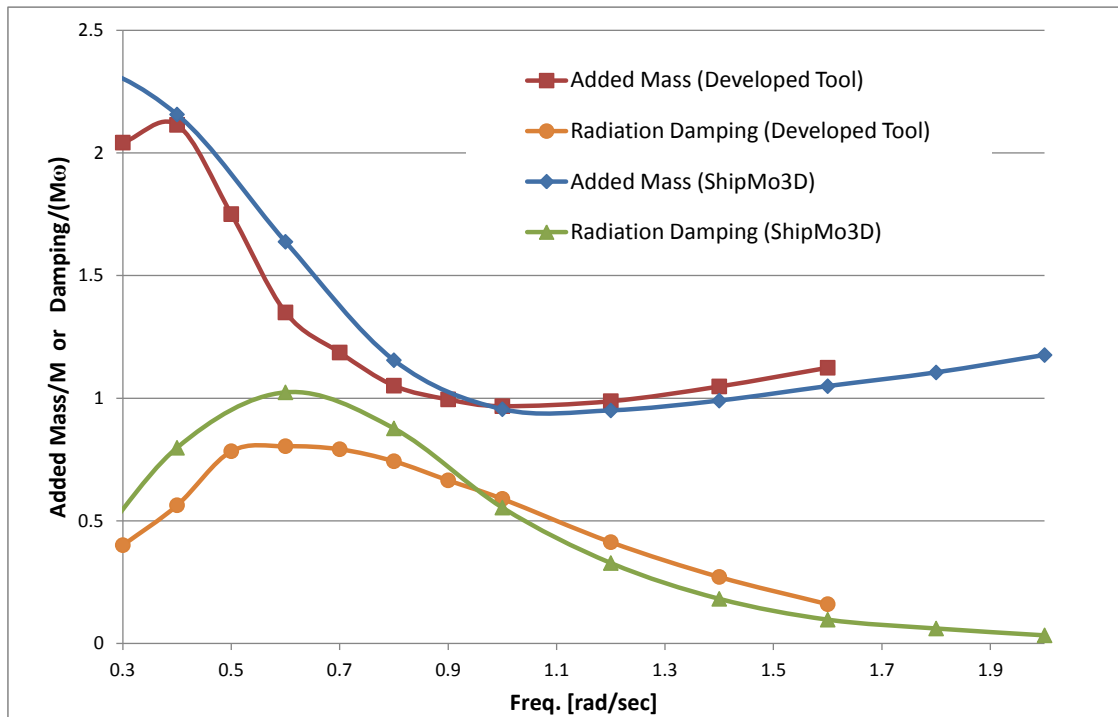
Figure B.10: Added Mass and Radiation Damping Coefficient for Barge

B.5.2 Wave-induced Motion of Generic VLCC

Using the developed wave-induced motion prediction tool, dynamic motion in the open sea is estimated. NRC created a generic VLCC hull to meet the following specification. Operating condition of the ship is assumed as Table B.5.

Table B.4: General Specification of Generic VLCC

Length [m]	345.3
Draft [m]	23.1
Beam [m]	58.1
Volume [m^3]	369,128.0
Block Coeff.	0.8

Table B.5: Environmental Condition

Velocity [$knots$]	10
Wave heading	head sea (180 °) and 150 °
Water depth [m]	100

The Japan Fairway guidance usually suggests two components: roll-heave and pitch-heave. Generally, for a huge ship like VLCC, pitch-heave coupled motion is more dominant that roll-heave case. Pitch-heave motion is selected for the comparative study. As shown figure B.11 and B.12, non-dimensional variable $\sqrt{L_{ship}/L_{wave}}$ is used to represent the relative wave characteristics. IACS JTP rule also suggests wave-induced motion. However, it is not included in this case study, because it does not provide heave motion.
As shown in figure B.11, every estimation method gives a similar trend qualitatively. Around 0.8, both empirical formulae give a larger value than the developed tool. This difference is supposed to correspond to the different hull shape between the developed tool and empirical formula. As mentioned in the previous section, Jensen's method assumes that the ship is a box shaped barge, which can cause a larger pitch motion eventually. Also, Japan Fairway Guideline assumes that single typical graph of wave-induced motion can be applied to every kind or every type of ships. The typical response of Japan Fairway is supposed to give the conservative result. Thus, it is supposed that empirical formulae give an over-estimated result compared with the numerical method.

B.5.3 Comparison with Kitimat study

In Kitimat study[26], dynamic motion in open sea is assessed using IACS JTP rule. In order to apply IACS JTP rule prediction result to Fig. B.11 and B.12, additional assumption is necessary. The first one is wave height. The second information is heave response or heave RAO because it is not provided in IACS rule. From Kitimat study (2010) [26], this
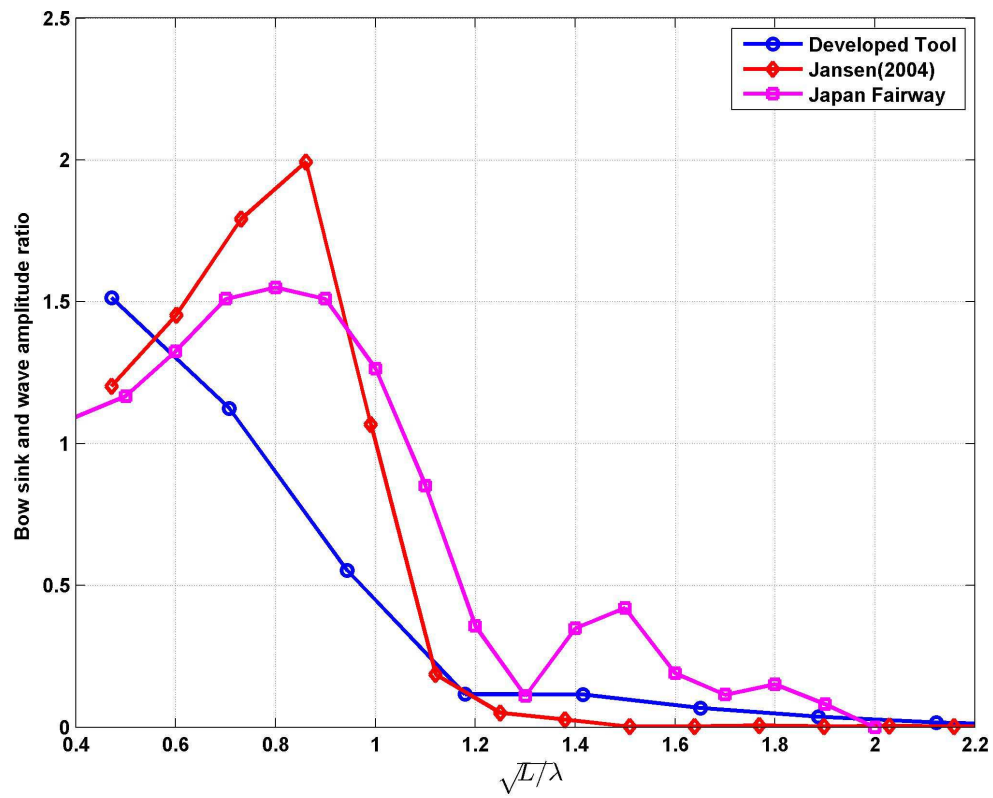
Figure B.11: Ratio Between Bow Sink and Wave Amplitude with Head sea
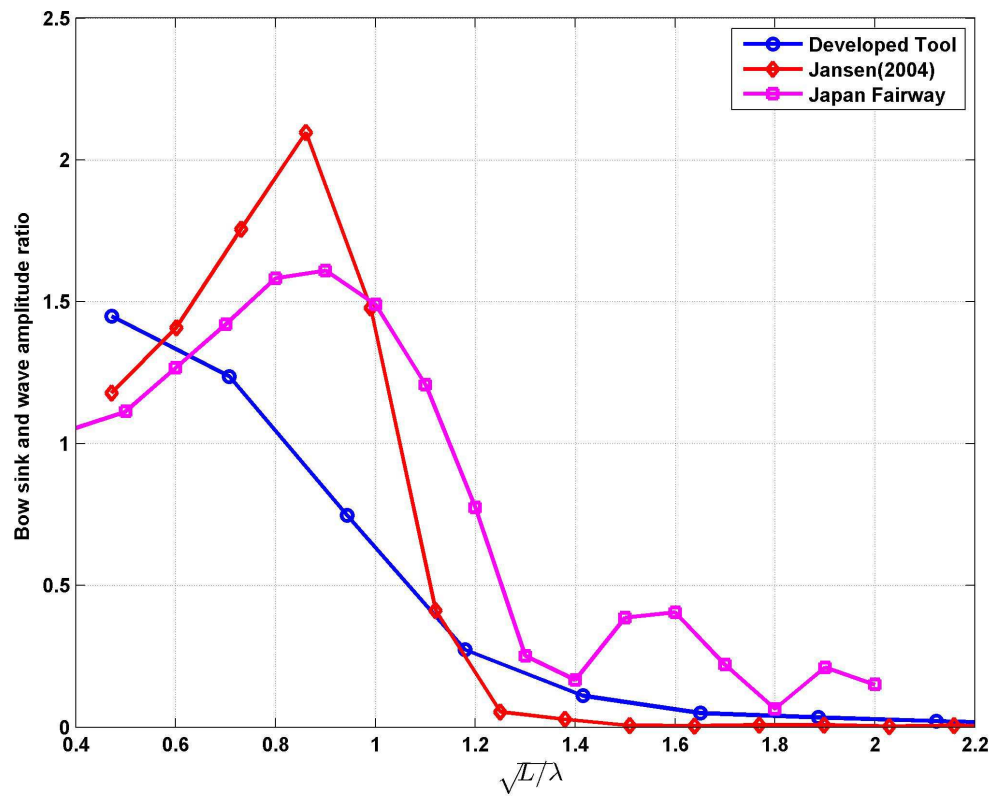
Figure B.12: Ratio Between Bow Sink and Wave Amplitude with Quatering sea, $130°$

information can be referred as Table B.6. When assuming the significant wave heights and heave RAO, the wave-induced motion is predicted as Fig. B.13 and Fig. B.13.

Table B.6: Additional Assumptions for IACS JTP Rule

Significant wave heights	15 m
Max. heave RAO	1.5
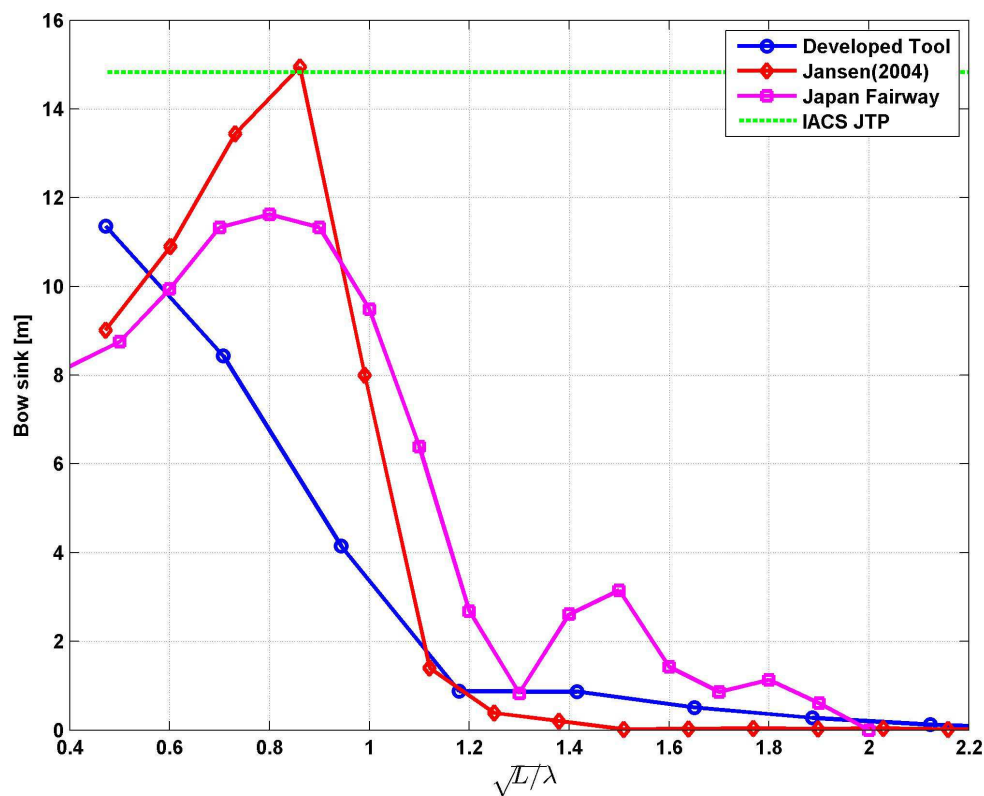
Figure B.13: Bow Sink in 15 m of Significant Wave Height with Head Sea

As shown in Fig. B.13 and B.13, IACS rule provides only one single maximum value. This kind of a maximum value evaluation is very effective to the designing process, which should consider the extreme loading condition. However, it provides single extreme value, which can not be used to realistic operation or reasonable motion is sea way.

Kitimat study report [26] also mentioned about the wave-induced motion in coastal areas. In the report, the wave condition in coastal areas is suggested like Table B.7.
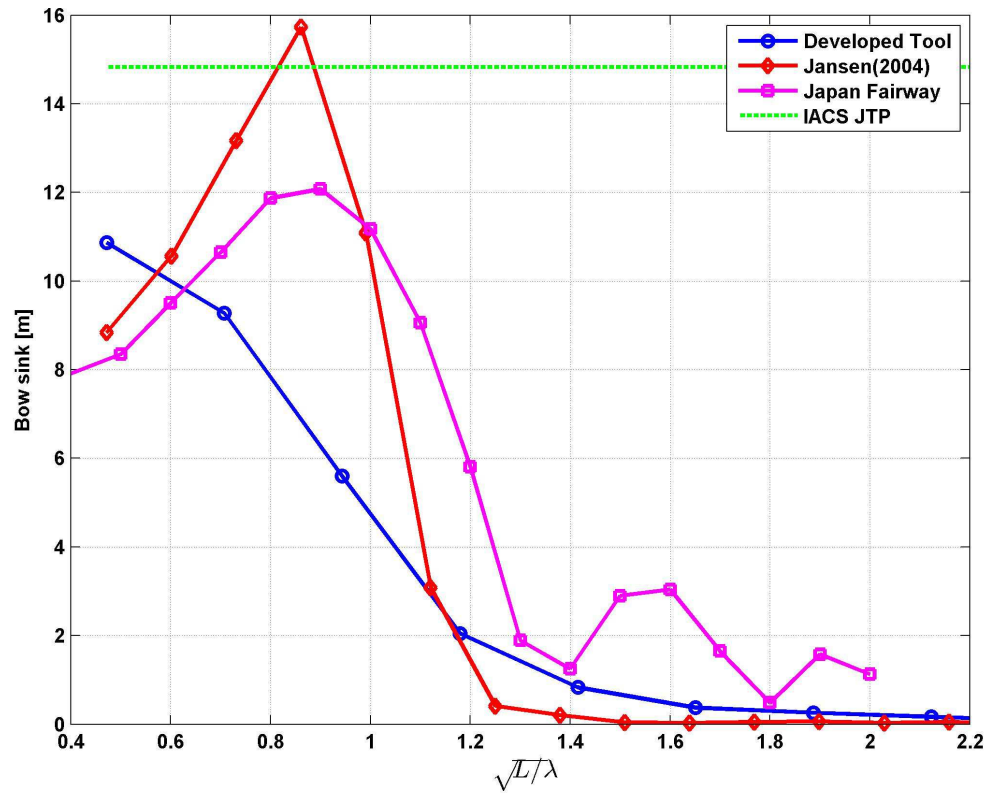
Figure B.14: Bow Sink in 15 m of Significant Wave Heights with Quartering sea, 130°

Table B.7: Wave Condition of Coastal Areas in Kitimat Study

Wave height [m]	2
Wave period [sec]	5
Wave freq. [rad/sec]	1.3
Wave length [m]	39
$\sqrt{L_{ship}/L_{wave}}$	3.2

In Kitimat study, the combined vertical displacement in coastal areas is reported as 8.4 m. Using Fig. B.12, every estimation method gives the motion response below 1 m. Obviously, the big difference of wave-induced motion between open sea and coastal area comes from wave height and period, which is too small to excite the big ship like VLCC as mentioned in the report[26]. The developed tool is basically providing the ratio between motion and wave amplitude. As a result, the accuracy of the wave data has a large influence on how realistic the results are.

B.5.4   Wave-induced Motion in Shallow Water

General sea-keeping software does not consider the restrict channel. Using the developed tool, wave-induced motion in shallow water is simulated. As shown in Fig. B.15, wave-induced motion becomes smaller in shallower water. Around 0.2 rad/s of wave frequency, it is supposed that the numerical error due to the extreme long wave corresponding wave length is around 1300 m.
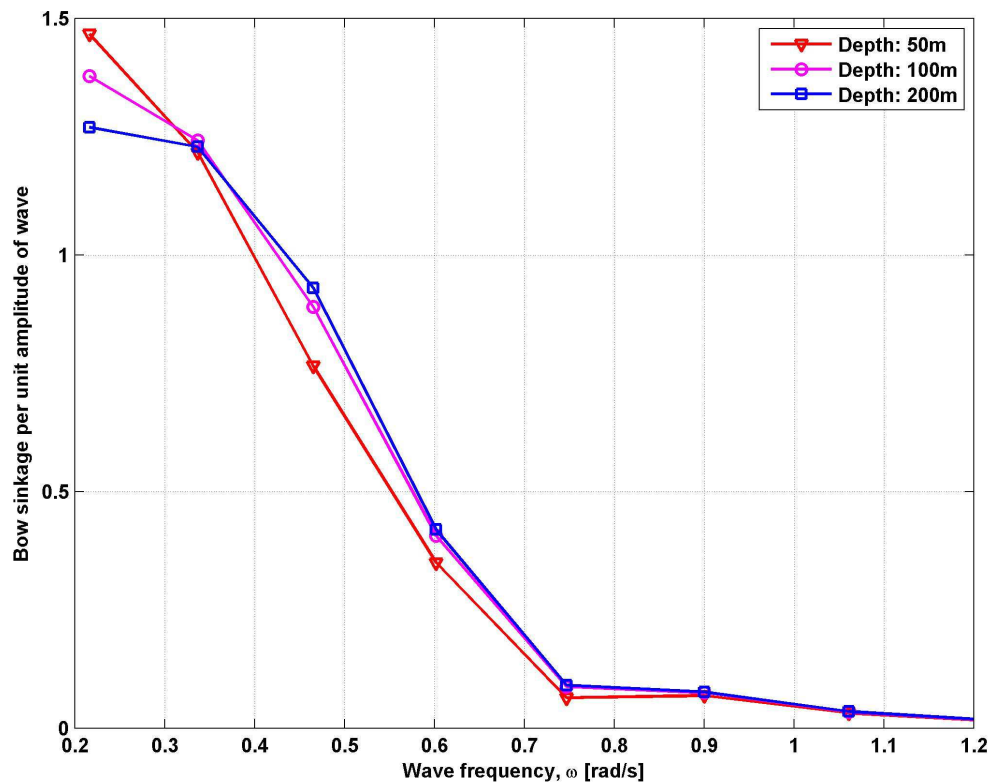
Figure B.15: Bow Sink Amplification Factor in Various Depths with 135° of Wave Heading

Unfortunately, quantitative validation data to confirm shallow water simulation is not reported since there was no full-scale or model-scale data available for comparison. However, it is supposed that the trend of decreasing motion in shallower water is well agreed with similar research of Kim [34].

B.6   Discussion and Summary

Wave-induced prediction tool for ships in restricted channel is developed using *MATLAB*[TM].
Typical simulation result shows that the strip method tool provides a reasonable prediction
of wave-induced motion. Important outcomes can be summarized as follows.

- Empirical formula is quick and easy prediction method, but it can give an over-prediction in wave response.

- Numerical tool can provide more realistic value, but it needs more input data and processing time.

- Numerical tool can predict more accurate wave motion and more realistic MDA guide-line.

- Validation data in shallow water is necessary to confirm the accuracy of the developed strip method tool quantitatively.

- Accurate wave environmental data such as wave frequency and heading is necessary to decide the wave-induced motion contribution to MDA assessment.

C SHIP SQUAT

C.1 Purpose

The purpose of this report is to present the results of a preliminary investigation into the capability, applicability, advantages, disadvantages and limitations of each of the various formulae for predicting ship squat that are available in the open literature, and, their agreement with model-scale or full-scale data where available.

C.2 Introduction

The purpose of this section is to provide a simple introduction as to what is "ship squat".

It is a well-known phenomenon that a ship travelling in (transiting into) shallow waters will experience (i) a reduction in forward speed (at the same propeller RPM, engine setting), (ii) a vertical sinkage, and, (iii) a change in trim angle. As a result, the ship and will sink bodily and the underkeel clearance (UKC) will be reduced. Depending on the shape of the hull, the combination of sinkage Δz and change in the angle of trim $\Delta \theta$ may make either the bow or the stern come close to, or touch, the seabed or bottom of the waterway.

With the economics of marine transportation demanding increased sizes of ships and because increasing the draft of a ship is the least expensive dimension to increase, it becomes increasingly important to learn how to evaluate these shallow-water effects so that safe speeds and safe UKC can be prescribed for navigation in both shallow waters and restricted channels in order to avoid both ship-bottom and channel-bottom damage, which can be expensive. In this report any reduction in the UKC has two components, the vertical sinkage Δz of the whole ship (which is measured positive downward at the centre of gravity, CG, or at the centre of flotation, CF), and a lowering (or rising) of the bow or stern due to the change in trim angle $\Delta \theta$.

In Reference [38], the 22nd ITTC Manoeuvring Committee report (1999), page 20, provides a definition of squat. The quotation is from Tuck who defines squat as follows: "Squat is not a change of draft (...). It is an overall lowering of the ship together with the water in the neighbourhood of the ship. Hence it is almost unseen in the open sea, where it is nevertheless present. However, squat is mainly of concern in restricted water (...)".

In [40] Constantine says "When a ship passes along a canal or other restricted waterway, it has been observed that the distance between the keel of the ship and the canal bottom decreases as the speed increases, and, in fact, on occasions the ship has been known to strike the bottom. This phenomena is known as 'squatting'.".

In the introduction to section 26.1 on page 724 of Chapter 26 in [4], Briggs et al describe "ship squat" as follows. When a ship travels through shallow water it undergoes changes

in its vertical position (relative to the seabed) due to (a) hydrodynamic forces and moments produced by the flow of water around and under the ship's hull, and, (b) wave-induced motions of heave, pitch and roll. The focus of this report is (a) which is the mechanism which produces "ship squat". For the purposes of this report, squat is the reduction in under-keel clearance (UKC) from (i) when the vessel at rest in calm water, to (ii) when the vessel is underway and there is flow around and under the ship's hull. The forward motion of the ship pushes water ahead of the ship (in the form of a bow wave) and this water must subsequently pass along the sides of the ship and under the keel. The motion of this water induces a velocity relative to the ship that produces a water-level depression (drawdown) along the sides of the ship, as shown diagramatically in Figure C.1 and in the photograph in Figure C.2. A stern wave is also produced. As a result of (a) this water-surface depression, (b) the bow wave, and, (c) the stern wave, the changes in the distribution of buoyant force about the hull produce changes in the hydrostatic and hydrodynamic forces and moments which support the weight of the ship. This phenomena produces a downward vertical force (sinkage, positive downward) and a moment about the transverse axis through the centre of flotation (trim, positive bow up) that can produce different values of squat at the bow and stern. This combination of sinkage and trim is called "ship squat". Since the weight of the ship remains constant, the displaced volume of the ship remains the same, thus the ship's draft does not change. Simply put, the water-surface itself is now closer to the seabed so the ship is now closer to the seabed and the UKC has been reduced. It is observed that these effects increase with increasing forward speed, thus the UKC decreases with increasing forward speed. This effect is experienced in deep water (as noted above in the quotation from Tuck) but is difficult to observe and measure. The effect of shallow water, and, the effect of river or channel banks, increases the magnitude of this sinkage and change in trim angle, at all forward speeds. These effects apply to both self-propelled ships and towed barges.

C.3   Background, Definitions, Diagrams etc.

There are several ship-geometry parameters which are used in the descriptions and formulae which follow. Here L_{pp} is the length between perpendiculars, as shown in Figure C.12; also shown is the ship's draft T, the ship's beam (or breadth) b, the ship's transverse vertical-plane cross-sectional area A_m, and, the ship's longitudinal horizontal-plane 'waterplane area' A_{wp}. From those lengths and areas are formed the ship's non-dimensional coefficients C_b, C_m and C_{wp}. The channel parameters W, H, H_t and θ are shown in Figures C.5, C.6 and C.7. Table C.8 on page 150 provides example values of C_b, C_m and C_{wp} for seven naval vessels and 21 commercial ships.

Table C.9 on page 153 provides descriptions, units and an indication of the first place in this document where each symbol occurs.

In this Appendix, the notation (n) indicates the number of an equation, while [n] indicates
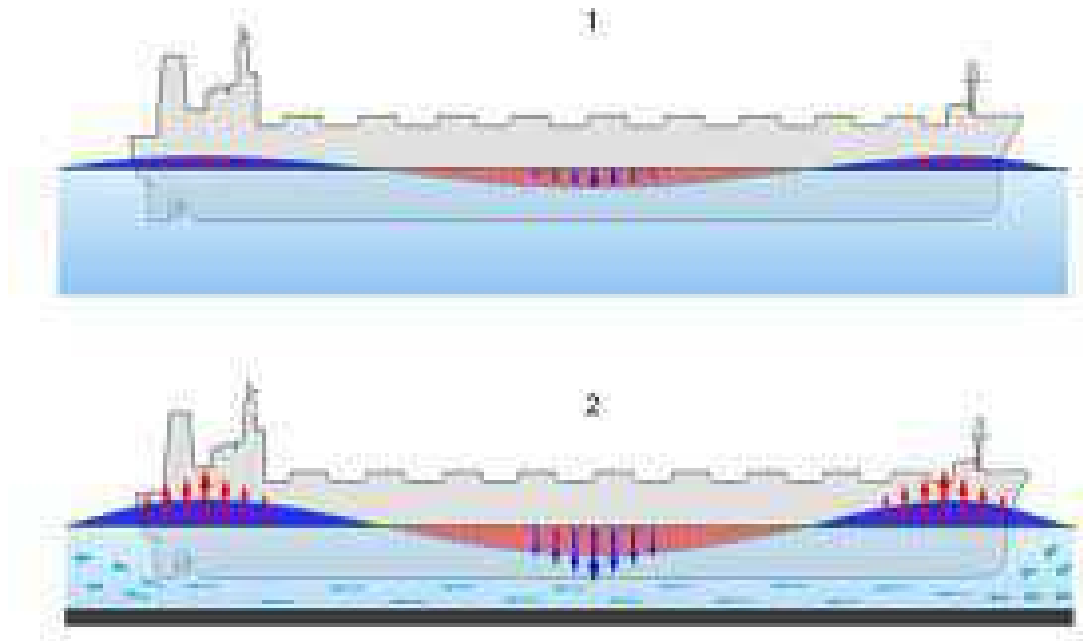
Figure C.1: Bow wave, water-surface drawdown and stern wave in unrestricted and
shallow water; the ship is travelling from left to right.

Figure C.2: Transfennica showing bow wave, water-surface drawdown and stern wave
produced at 20 kt with 10 m under-keel clearance.

the number of a document in the References Section on page 56.
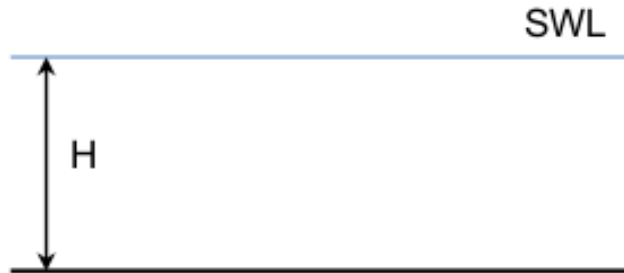
Figure C.3: Unrestricted uniform-depth shallow water

C.3.1   A ship in unrestricted uniform-depth shallow water

Figure C.3 shows an example of what is known as unrestricted uniform-depth shallow water of depth H as measured from the still-water level (SWL) to the bottom of the seabed or waterway. Figure C.4 shows the principal dimensions of a vertical-plane transverse cross-section of a ship operating in shallow water, the beam (breadth) b and the draft T. For the purposes of sinkage and trim changes, it is conventional to choose the cross-section of the ship which is maximum, thus usually amidship, since this will give the smallest gap between the keel of the ship and the bottom of the waterway, and, between the sides of the ship and the banks of the waterway.

There are various formulae which predict this sinkage and change in trim angle. Some of these formulae are based on analytical methods, some are semi-empirical (they are based on analytical methods with corrections provided from model-scale tests or full-scale measurements), some a purely empirical, some are the result of regression methods applied to data from model-scale tests or full-scale measurements, and so on.
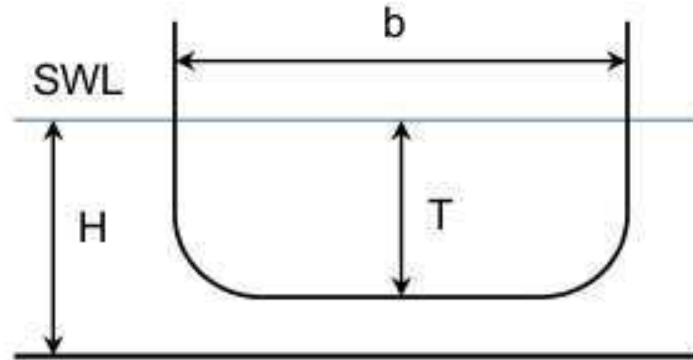
Figure C.4: A ship in unrestricted uniform-depth shallow water

Table C.1: Parameters for Ship Squat Predictions in Unrestricted Shallow Waterways

	Ship					Water		Other	
	∇	L_{pp}	T	b	C_b	V	H	g	W_{eff}
Tuck 1966	-	y	-	-	-	y	y	y	-
Eryuzlu et al 1994	-	-	y	-	-	y	y	y	-
Hooft 1974	y	y	-	-	-	y	y	y	-
ICORELS 1980	y	y	-	-	-	y	y	y	-
Huuska & Guliev 1976	y	y	-	-	-	y	y	y	-
Eryuzlu & Hausser 1978	-	-	y	y	-	y	y	y	-
Millward 1990	-	y	-	y	y	y	y	y	-
Millward 1992	-	y	y	-	y	y	y	y	-
Norrbin 1986	-	y	y	y	y	y	y	-	-
Yoshimura 2002	-	y	y	y	y	y	y	y	-
Romisch 1989	-	y	y	y	y	y	y	y	-
Ankudinov 2009	-	y	y	y	y	y	y	y	-
Barrass 2006	-	-	y	y	y	y	y	-	y

The details of the origin and limitations of each formula are given in the references. Table C.1 summarizes which parameters are used in each particular shallow-water formula. In this table, as in Figure C.4, b is the maximum breadth of the ship, T is the draft (which depends on whether the ship is fully-loaded, partially-loaded or empty), and H is the water depth. Other ship dimensions include L_{pp}, the waterline length at draft condition T; C_b is the volumetric block coefficient at draft condition T etc.

These formulae tend to express the sinkage and trim changes in terms of the ratios (H/T), (L/H) and (b/W_{eff}) where W_{eff}, as defined by Barrass, is an "effective width of water" at the water surface.

The following section contains the formulae which are valid and for use only in unrestricted uniform-depth shallow-water conditions.

C.3.2   A ship in a confined waterway

Figures C.5 to C.8 show typical examples of confined waterways.
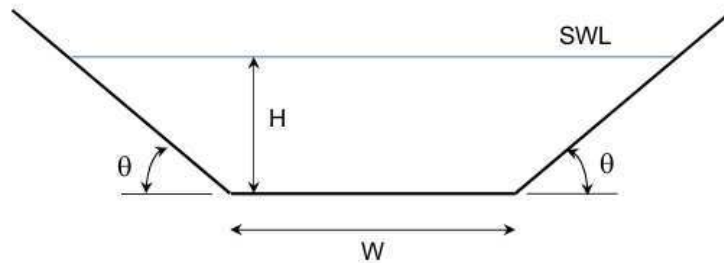
Figure C.5: A trapezoidal channel

Figures C.8, C.9 and C.10 show a ship placed on the longitudinal centreline of a channel of rectangular cross-section. The purpose of this figure is to introduce two cross-sectional area parameters which are used in many of the formulae for predicting the sinkage and trim change which occurs in confined channels. As mentioned above, the ship is drawn with the dimensions of its maximum vertical-plane lateral cross-section since this will give the smallest gap between the keel of the ship and the bottom of the waterway.
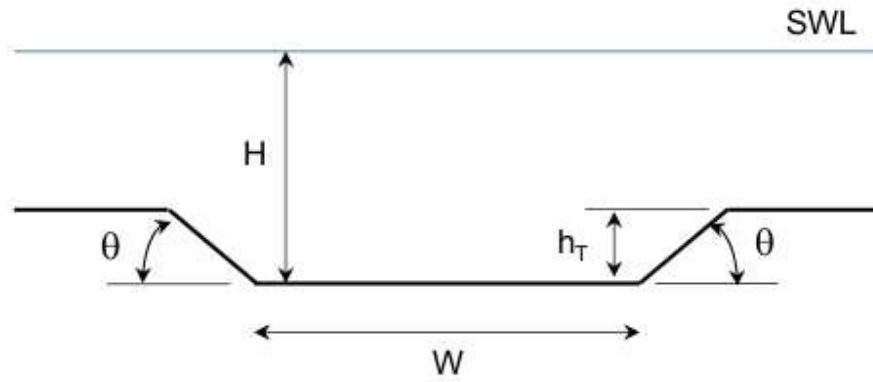
Figure C.6: Channel with trench of trapezoidal cross-section
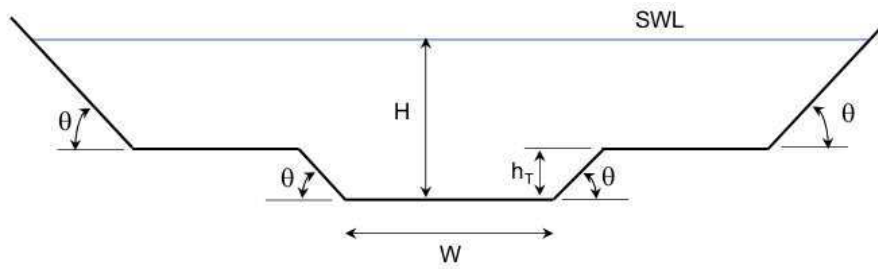
Figure C.7: Channel with trapezoidal cross-section and trapezoidal trench
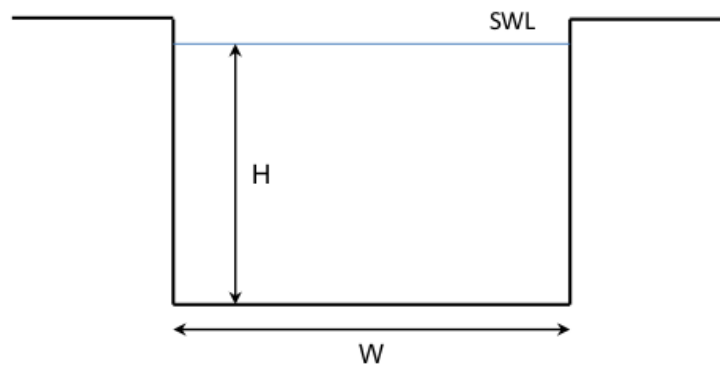
Figure C.8: A rectangular channel or lock
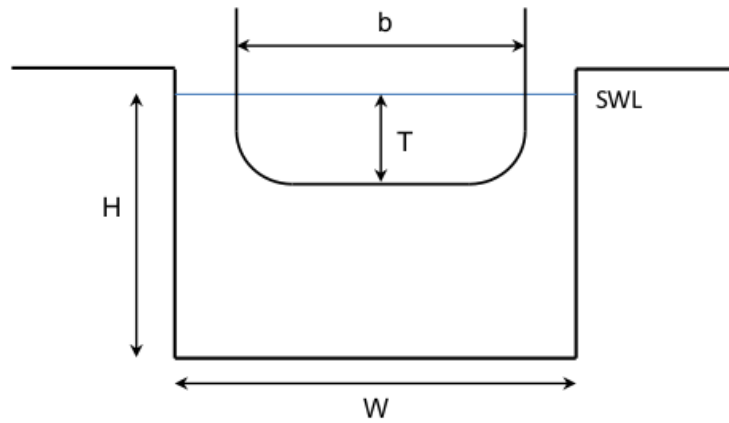
Figure C.9: A rectangular channel with a ship
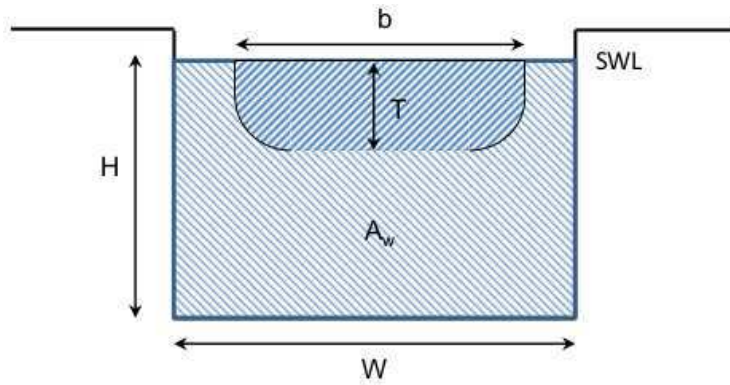
Figure C.10: A rectangular channel with a ship, A_m and A_w defined

Figure C.10 shows a ship in a rectangular channel but only the submerged portion of the ship. The cross-sectional area delimited by the maximum breadth b and the draft T defines the maximum cross-sectional area A_m; here A_m is given by the product of b and T, multiplied by a constant of the order of 0.9 due to the corner-radius of the hull; see Table C.8. For the example ship in the later figures, this parameter, C_m has the value 0.998 since, in proportion to b and T the corner-radius of the hull is small. The cross-sectional area of the empty channel, A_c, is the product of the water-depth H and the channel width W. The cross-section of the surrounding water, A_w, is the difference between A_c and A_m. The ratio of A_m to A_w is used as the confinement factor or blockage ratio S. As it turns out, the larger is the confinement S the greater are the sinkage and change in trim angle, for a given ship forward speed V.

Figure C.11(a) shows a ship at rest in a confined trapezoidal channel with bottom-width W; here the water-depth is H. In Figure C.11(b) the ship is moving at constant forward speed V; here the drawdown of the water surface is given by Δz and the water-depth is therefore $H - \Delta z$. Note that ship's draft has not changed; it remains as T in both Figure C.11(a) and C.11(b). However the UKC has been reduced from H-T in (a) to $H - \Delta z - T$ in (b). Thus the cross-section of the surrounding water in (b) is less than in (a) so the confinement factor S for the sinkage and trim calculations must use the value of A_w in (b).

Figure C.12 assists in providing definitions for the ship parameters L_{pp}, T, b, A_m and A_{wp}.
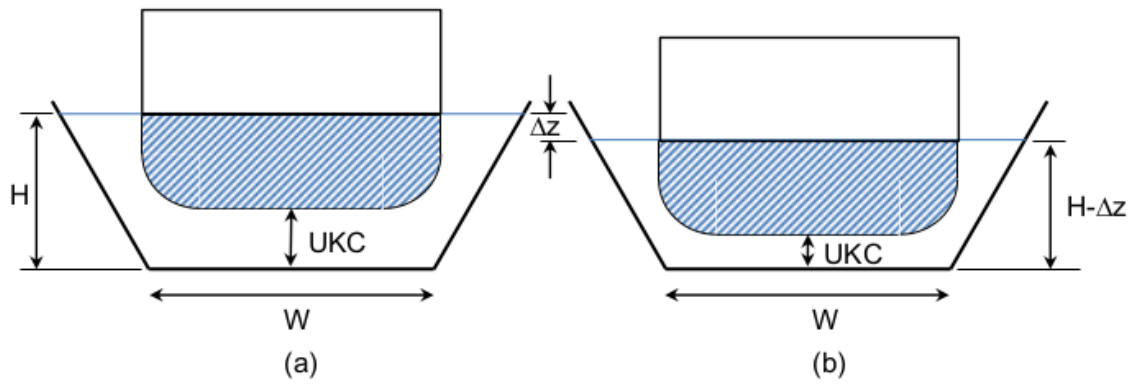
Figure C.11: Definition of drawdown and squat
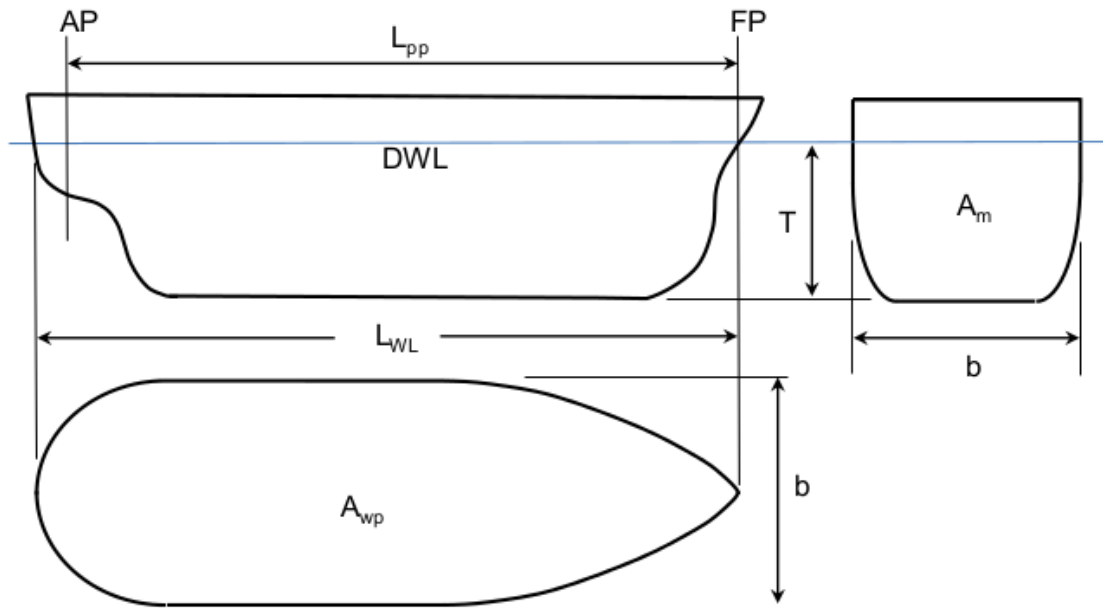
Figure C.12: Definition diagram for ship particulars

C.4 Some Formulae for Predicting Squat in Unrestricted Uniform-depth Shallow Water

The beginnings of the study of ship squat can be traced back to Horn (1937), Havelock (1939), Schijf (1949) and Constantine (1960) to name a few. Other details of the early history of analytical developments in ship squat can be found in Gourlay [54].

There are few full-scale measurements but notable reported measurements took place in the St. Lawrence Seaway as reported by Tothill in [42, 43], by Stocks et al in [49], in the Panama Canal by Briggs et al in [57] and in [45], and, in the Elbe River by Dunker in [60].

Some of the ship squat formulae, since they are empirical and not necessarily strictly non-dimensional, require the ship's speed V to be given in nautical miles per hour [kt] rather than metres per second [m/s]. If so, the former is indicated by V_k and the latter by either V or V_s.

In many of the formulae, a Froude Number based on water depth is used, and this is defined as

$$F_{nh} = \frac{V_s}{\sqrt{g \cdot H}}$$ (C.1)

Table C.2 indicates via the abbreviations 'U', 'R' and 'C' which formulae apply to the conditions of (i) unrestricted, uniform-depth shallow-water, (ii) restricted trenched-channels, and, (iii) trapezoidal or rectangular canals.

Table C.2: Capabilites of various ship squat formulae for unrestricted (U), restricted (R) and canal (C) waterways

Formula	Bow			Stern		
	U	R	C	U	R	C
Tuck 1966	y	-	-	-	-	-
Eryuzlu et al 1994	y	y	y	-	-	-
Hooft 1974	y	-	-	-	-	-
ICORELS 1980	y	-	-	-	-	-
Huuska & Guliev 1976	y	y	y	-	-	-
Eryuzlu & Hausser 1978	y	-	-	-	-	-
Millward 1990	y	-	-	-	-	-
Millward 1992	y	-	-	-	-	-
Norrbin 1986	y	-	-	-	-	-
Yoshimura 2009	y	y	y	-	-	-
Romisch 1989	y	y	y	y	y	y
Ankudinov 2009	y	y	y	y	y	y
Barrass 2006	y	y	y	y	y	y

103

Table C.3: Constraints on Parameters for Various Squat Formulae

Formula	C_b	Constraints H/T	L_{pp}/H	Configuration U	R	C
Tuck 1966						
Eryuzlu et al 1994	≥ 0.8	1.1 to 2.5	-	y	y	-
Hooft 1974	-	-	-	y	-	-
ICORELS 1980	-	-	-	y	-	-
Huuska & Guliev 1976	-	1.1 to 2.0	-			
Eryuzlu & Hausser 1978	≥ 0.8	1.08 to 2.75	-	-	y	y
Millward 1990	0.44 to 0.83	-	6 to 12	y	-	-
Millward 1992			6 to 12	y	-	-
Norrbin 1986				y	-	-
Yoshimura 2002						
Romisch 1989		1.19 to 2.25		y	y	y
Ankudinov 2009						
Barrass 2006	0.55 to 0.85	1.1 to 1.4	-	y	y	y

Table C.3 outlines some of the restrictions for each formula, in terms of the range of C_b, range of depths, and, hull-length to water-depth ratio. Constraints based on Froude Number are given in the text adjacent to a particular formula.

C.4.1   Tothill 1966

In 1966 the NRC in conjunction with the St. Lawrence Seaway Authority performed both scale-model experiments with two ships at NRC. Both squat and steering performance were measured at various speeds, and passing maneuvers of the two models were investigated. Full-scale measurements of ship squat for 190 ships were performed at Caughnawaga by the St. Lawrence Seaway Authority. The full-scale data were compared with the theoretical drop of water level due to the passage of the ships and were found to agree within acceptable limits, as did the measurements from the model-scale experiments. The theory therefore permits estimation of squat, critical speeds, and safe speed limits imposed by considerations of water depth and draft, for any ship in any canal. Information concerning the development of Tothill's analytical model for ship squat, and, concerning the ship-model experiments and full-scale measurements are contained in [42, 43].

C.4.2   Tuck 1966

$$\Delta z_b = L_{pp} \cdot C_t \cdot \frac{F_{nh}^2}{\sqrt{1 - F_{nh}^2}} \tag{C.2}$$

where C_t is Tuck's ship form factor with typical value 0.02.

C.4.3 Hooft 1974

$$\Delta z_b = 1.96 \cdot \left(\frac{\nabla}{L_{pp}^2}\right) \cdot \frac{F_{nh}^2}{\sqrt{1 - F_{nh}^2}} \tag{C.3}$$

This formula uses the displaced volume ∇, L_{pp}, g, H and V so it is one of the simplest to apply. The constant 1.96 is used as a typical value but values from 1.9 to 2.03 are sometimes used [67]. This formula is not applicable to restricted channels. It is not mentioned in [44] how this formula was validated.

C.4.4 Huuska and Guliev 1976

$$\Delta z_b = 2.4 \cdot \left(\frac{\nabla}{L_{pp}^2}\right) \cdot \frac{F_{nh}^2}{\sqrt{1 - F_{nh}^2}} \tag{C.4}$$

Thus this formula uses the displaced volume ∇, L_{pp}, g, H and V. It is not mentioned in [44] how this formula was validated however it is stated that this formula should not be used for F_{nh} greater than 0.7.

C.4.5 Eryuzlu and Hausser 1978

$$\Delta z_b = 0.113 \cdot b \cdot \left(\frac{T}{H}\right)^{0.27} \cdot F_{nh}^{1.8} \tag{C.5}$$

thus this formula uses T, H, b, g and V. Table 2 on page 8 of [44] says it is not used for restricted channels or canals. This formula has been validated with model-scale measurements with large, fully-loaded, self-propelled tanker models.

C.4.6 ICORELS 1980

$$\Delta z_b = 2.4 \cdot \left(\frac{\nabla}{L_{pp}^2}\right) \cdot \frac{F_{nh}^2}{\sqrt{1 - F_{nh}^2}} \tag{C.6}$$

which is effectively the same as the Huuska and Galiev (1976) formula and the Hooft (1974) formula with a larger constant. The PIANC (1997) document notes that the constant 2.4 is sometimes replaced with the value 1.75 for ships with large C_b values. This formula uses the displaced volume ∇, L_{pp}, g, H and V so it is one of the simplest to apply. It is not mentioned in [44] how this formula was validated.

C.4.7 Norrbin 1986

$$\Delta z_b = \left(\frac{C_b}{15}\right) \cdot \left(\frac{b}{L_{pp}}\right) \cdot \left(\frac{T}{H}\right) \cdot V_k^2 \tag{C.7}$$

105

thus this formula uses C_b, L_{pp}, b, H, T and V. It is not mentioned in [44] how this formula was validated however it is stated that this formula should not be used for F_{nh} greater than 0.4.

C.4.8   Römisch 1989

For unrestricted conditions the Römisch (1989) formulae permit us to calculate the bow squat using

$$\Delta z_b = C_V \cdot C_F \cdot K_{\Delta T} \cdot T \tag{C.8}$$

and to calculate the stern squat using

$$\Delta z_s = C_V \cdot K_{\Delta T} \cdot T \tag{C.9}$$

For the bow and stern squat we need

$$V_{cr} = C \cdot K_{ch} \tag{C.10}$$

for unrestricted conditions and where

$$K_{ch} = 0.58 \cdot \left[\left(\frac{H}{T} \right) \cdot \left(\frac{L_{pp}}{b} \right) \right]^{0.125} \tag{C.11}$$

and

$$C = \sqrt{g \cdot H}. \tag{C.12}$$

The value of C_V comes from

$$C_V = 8 \cdot \left(\frac{V_s}{V_{cr}} \right)^2 \left[\left(\frac{V_s}{V_{cr}} - 0.5 \right)^4 + 0.0625 \right] \tag{C.13}$$

and the value of C_F comes from

$$C_F = 100 \cdot \left(\frac{b \cdot C_b}{L_{pp}} \right)^2 \tag{C.14}$$

for calculating the bow squat, and, $K_{\Delta T}$ comes from

$$K_{\Delta T} = 0.155 \cdot \sqrt{\frac{H}{T}} \tag{C.15}$$

Thus these formulae for the squat under unrestricted conditions use only V, C_b, L_{pp}, b, H, T and g. Note that K_{ch} contains both the effects of water depth (H/T) and the ship size (L_{pp}/b). C_V contains only ship-speed effects; C_F contains only the ship parameters b, L_{pp} and C_b. The Römisch formulae were validated using model-scale measurements of bow and stern squat using three channel configurations.

C.4.9 Millward 1990

$$\Delta z_b = (\frac{L_{pp}}{100}) \cdot \left(15 \cdot C_b \cdot (\frac{b}{L_{pp}}) - 0.55 \right) \cdot \frac{F_{nh}^2}{(1 - 0.9 \cdot F_{nh})} \qquad (C.16)$$

thus this formula uses L_{pp}, C_b, b, V, g and H and not T. This formula was validated with towed models in a towing tank where the width was approximately twice the L_{pp}. This formula has a tendency to predict large squat values; see Figures C.13 to C.17 for the VLCC in Section C.5.1.

C.4.10 Millward 1992

$$\Delta z_b = (\frac{L_{pp}}{100}) \cdot \left(61.7 \cdot C_b \cdot (\frac{T}{L_{pp}}) - 0.6 \right) \cdot \frac{F_{nh}^2}{\sqrt{1 - F_{nh}^2}} \qquad (C.17)$$

thus this formula uses L_{pp}, C_b, T, V, g and H and not b.

C.4.11 Eryuzlu et al 1994

$$\Delta z_b = 0.298 \cdot \left(\frac{H^2}{T} \right) \cdot \left(\frac{V_s}{\sqrt{g \cdot T}} \right)^{2.289} \cdot \left(\frac{T}{H} \right)^{2.972} \qquad (C.18)$$

Thus for open-water conditions, this formula uses only the four parameters H, T, g and V_s. This formula can be applied for open-water conditions only if the ratio of W_{eff}/b, ss defined below in (C.22), is greater than 9.61. This formula (and its modifications for restricted channels) has been validated with both model-scale and full-scale measurements on cargo ships and bulk carriers with bulbous bows in both unrestricted conditions and in restricted channels.

C.4.12 Yoshimura 2002

$$\Delta z_b = \left[\left(0.7 + 1.5(\frac{T}{H}) \right) \left(\frac{b \cdot C_b}{L_{pp}} \right) + 15(\frac{T}{H}) \left(\frac{b \cdot C_b}{L_{pp}} \right)^3 \right] \left(\frac{V_s^2}{g} \right) \qquad (C.19)$$

thus this formula uses T, H, C_b, b, L_{pp}, V_s and g. It is not mentioned in [44] how this formula was validated.

C.4.13 Barrass 1979, 1981

For unrestricted conditions Barrass initially proposed to use

$$\Delta z_b = \left(\frac{C_b}{30} \right) \cdot S_2^{\frac{2}{3}} \cdot V_k^{2.08} \qquad (C.20)$$

with

$$A_c = H \cdot W_{eff} \qquad (C.21)$$

107

where W_{eff} is the effective 'width of influence' [m]. Here

$$W_{eff} = [7.7 + 45 \cdot (1 - C_{wp})^2] \cdot b \tag{C.22}$$

as long as W_{eff}/b > 8. So this formula uses C_b, C_{wp}, W_{eff}/b, V_k, g, H, T since A_m is approximately $0.98 \cdot b \cdot T$ or more precisely

$$A_m = C_m \cdot b \cdot T \tag{C.23}$$

then the blockage ratio S is found from

$$S = A_m/A_c = \frac{b \cdot T}{H \cdot W_{eff}} = (\frac{b}{W_{eff}}) \cdot (\frac{T}{H}) \tag{C.24}$$

so H appears only through S; then

$$S_2 = A_m/A_w = A_m/(A_c - A_m) = S/(1 - S) \tag{C.25}$$

also contains the ratio (T/H). This squat formula has been validated with full-scale measurements.

C.4.14   Barrass 2004

By 2004 Barrass had modified his empirical formula to [47] provide the maximum sinkage [m] in open water using

$$\delta_{max} = \frac{C_b \cdot S^{0.81} \cdot V_k^{2.08}}{20} \tag{C.26}$$

where V_k is the vessel forward speed [kt]. However in this version the effective 'width of influence' [m] is given by

$$W_{eff} = \left(\frac{7.04}{C_b^{0.85}}\right) \cdot b \tag{C.27}$$

and the corresponding value of S comes from (C.24) above. In this version δ_{max} is assigned to the bow if $C_b > 0.7$ and to the stern if $C_b < 0.7$.

C.4.15   Barrass 2006

By 2006 Barrass had modified his empirical formula [48] so that he retains the use of (C.26) for δ_{max} while modifying the definition of W_{eff} to be

$$W_{eff} = [7.7 + 20 \cdot (1 - C_b)^2] \cdot b \tag{C.28}$$

Again the corresponding value of S comes from (C.24) above.

C.4.16   Barrass 2009

Since 2009 various authors appear to be using what Barrass in [47] and in [48] referred to as his "short-cut" formula

$$\delta_{max} = \frac{C_b \cdot V_k^2}{100} \tag{C.29}$$

which is valid for 1.1 < H/T < 1.4 so no value for W_{eff} or S is required. Apparently this formulation is based on analysis of over 600 laboratory and prototype measurements for all three channel types. Again, δ_{max} is assigned to the bow if $C_b > 0.7$ and to the stern if $C_b < 0.7$.

C.4.17   Ankudinov 2009

At the MARSIM 2000 conference V.Ankudinov proposed that the formula for maximum squat in shallow water should be based on the midpoint sinkage S_m and vessel trim. The Ankudinov method has undergone considerable revision as new data were collected and compared. The most recent modifications from a study of ship squat in the St. Lawrence Seaway [49] were made in April 2009 and are included in the formulation which is given below. See [45] for the details of how the Ankudinov method is formulated.

The Ankudinov prediction uses some of the most comprehensive, but also the most complicated formulae, for predicting ship squat. These components include factors to account for the effects of the ship and channel. The restriction on Depth Froude Number F_{nh}, is that these formulae are valid for $F_{nh} < 0.6$.
The maximum ship squat S_{max} is a function of two main components: the vessel midpoint sinkage S_m and the vessel trim, $Trim$, given by

$$S_{max} = L_{pp} \cdot (S_m \pm 0.5 \cdot Trim) \tag{C.30}$$

The maximum squat S_{max} can occur at the bow or stern depending on the value of $Trim$.

C.4.17.1   Vessel sinkage

The vessel midship sinkage S_m is given by

$$S_m = (1 + K_P^S) \cdot P_{Hu} \cdot P_{F_{nh}} \cdot P_{+h/T} \tag{C.31}$$

where the ship, water depth and channel parameters in (C.31) are described below. The *propeller parameter* K_P^S is given by

$$K_P^S = \left\{ \begin{array}{l} 0.15 \ \text{ for a single propeller} \\ 0.13 \ \text{ for twin propellers} \end{array} \right\} \tag{C.32}$$

109

The *ship hull parameter* P_{Hu} is given by

$$P_{Hu} = 1.70 \cdot C_b \cdot \left(\frac{b \cdot T}{L_{pp}^2} \right) + 0.004 \cdot C_b^2 \tag{C.33}$$

The *ship forward speed parameter* $P_{F_{nh}}$ is given by

$$P_{F_{nh}} = F_{nh}^{(1.8 + 0.4 \cdot F_{nh})} \tag{C.34}$$

which is used as a numerical approximation to the term $F_{nh}^2 / \sqrt{1 - F_{nh}^2}$ that is used in many of the PIANC empirical squat formulae. Here F_{nh} is the *depth-based Froude Number* given by

$$F_{nh} = \frac{V_s}{\sqrt{g \cdot H}} \tag{C.35}$$

where V_s is the ship forward speed [m/s], H is the water depth [m], and, g is the acceleration due to gravity, 9.81 m/s^2. The *water depth effect parameter* $P_{+h/T}$ is given by

$$P_{+h/T} = 1.0 + \frac{0.35}{(H/T)^2} \tag{C.36}$$

C.4.17.2   Vessel trim

The second main component in the MARSIM 2000 ship squat formula is the vessel trim which is given by

$$Trim = -1.70 \cdot P_{Hu} \cdot P_{F_{nh}} \cdot P_{h/T} \cdot K_{Tr} \tag{C.37}$$

In addition to the two parameters P_{Hu} and $P_{F_{nh}}$ already described above for the vessel midship sinkage formula (C.31), the trim formula also includes the parameters $P_{h/T}$ and K_{Tr}. Here $P_{h/T}$ quantifies the effect of water-depth and vessel speed, while K_{Tr} quantifies the effects of (i) vessel trim, (ii) the ship's propellers, (iii) the shape of the bow (conventional or bulbous), (iv) the type of stern (conventional or transom), and, (v) the initial trim condition when the ship is stationary in calm water. The *vessel trim parameter* $P_{h/T}$ accounts for the reduction in trim due to the action of the propeller while in shallow water, and is given by

$$P_{h/T} = 1 - \exp \left[\frac{2.5(1 - H/T)}{F_{nh}} \right] \tag{C.38}$$

The *trim coefficient* K_{Tr} is a function of many factors and is given by

$$K_{Tr} = C_b^{n_{Tr}} - 0.15 \cdot K_P^S - K_P^T - K_B^T - K_{Tr}^T - K_{T1}^T \tag{C.39}$$

The first factor in (C.39), $C_b^{n_{Tr}}$, is the result of raising the block coefficient C_b to the power n_{Tr}. This *trim exponent* n_{Tr} for the unrestricted waterway case is given by

$$n_{Tr} = 2 + 0.8 \cdot \left(\frac{1}{C_b} \right) \tag{C.40}$$

The next two factors in (C.39) define the effect of the propeller(s) on the vessel trim. The first factor, K_P^S is the same as the *propeller parameter* for the miship sinkage given in (C.31). The second factor, K_P^T, is the *propeller trim parameter* which is given by

$$K_P^T = \begin{cases} 0.15 & \text{for a single propeller} \\ 0.20 & \text{for twin propellers} \end{cases} \qquad \text{(C.41)}$$

The last group of three factors K_B^T, K_{Tr}^T and K_{T1}^T define the effects of the bulbous bow, stern transom and initial trim, respectively, on the vessel trim. Here the *bulbous bow factor* K_B^T is given by

$$K_B^T = \begin{cases} 0.10 & \text{for a bulbous bow} \\ 0.00 & \text{for a conventional bow} \end{cases} \qquad \text{(C.42)}$$

The *stern transom factor* K_{Tr}^T is given by

$$K_{Tr}^T = \begin{cases} 0.10 \cdot \left(\dfrac{B_{Tr}}{b} \right) \approx 0.04 & \text{for a stern transom} \\ 0.0 & \text{for a conventional stern} \end{cases} \qquad \text{(C.43)}$$

where B_{Tr} is the *stern transom width* and is typically 0.4 times the ship's beam b, although values as high as 0.7 time b have been used. The *initial trim effect factor* K_{T1}^T is given by

$$K_{T1}^T = \frac{(T_{ap} - T_{fp})}{(T_{ap} + T_{fp}} \qquad \text{(C.44)}$$

where T_{ap} is the static draft at the stern (or aft perpendicular), and, T_{fp} is the static draft at the bow (or forward perpendicular) when the ship is stationary in calm water.

C.5 Examples for an Unrestricted Waterway

The largest proposed vessel that will dock at the Kitimat Terminal is a VLCC with a length (L_{pp}) of 336 m, maximum beam b of 60 m and maximum draft T (when fully-loaded) of 23.1 m. The block coefficient C_b for this vessel is expected to be about 0.81 and the waterplane area coefficient C_{wp} to be about 0.89.

C.5.1 Effects of H/T on the squat predictions for a VLCC

The following graphs show the predictions from ten different squat formulae from Section C.4 for unrestricted uniform-depth open-water conditions. For the fully-loaded draft condition, predictions are made for five water depths 25.4, 27.7, 30.0, 32.3 and 34.7 m corresponding to depth-to-draft-ratios (H/T) of 1.1, 1.2, 1.3, 1.4 and 1.5.

Within each graph, Figures C.13 to C.17, the first nine curves are for bow squat; the tenth curve is for stern squat. For this ship, at this draft loading, for these five water depths, at all speeds, the bow squat is predicted by the Römisch formula to be about double the stern squat.

Also shown in Figures C.13 to C.17 via the thick black dashed line is the "mean-of-ten-formulae" curve. At each ship speed V the average of the ten predictions was used to construct the "mean-of-ten-formulae" curve. Next, at each speed V the deviation of each of the ten curves from the "mean-of-ten-formulae" curve in order to obtain the "one sigma" values. Finally two solid black curves are plotted; the upper one represents the "mean-plus-one-sigma" values while the lower one represents the "mean-minus-one-sigma" values.

In Figures C.13 to C.17, for all speeds and all five values of (H/T), the dashed red Millward(2) formula predicts the largest squat, and, the solid red Eryuzlu-Hausser formula predicts the smallest squat. Both of these curves lies outside the "one-sigma" band surrounding the "mean-of-ten-formulae" curve.

Figure C.13: Results for a VLCC in open water for water-depth to draft ratio 1.10

In Figure C.13 for (H/T) of 1.10 and for speeds less than 14.5 kt, the dashed blue Millward(1) curve lies below the "mean-plus-one-sigma" curve. For (H/T) of 1.10 and for all speeds up to 16 kt, the dashed cyan curve for Römisch stern squat lies below the "mean-minus-one-sigma" curve.

Fig 14, VLCC_open_shallow_water_squat_calculations_30sep13.m

Figure C.14: Results for a VLCC in open water for water-depth to draft ratio 1.20

In Figure C.14 for (H/T) of 1.20 and for all speeds less than 15.5 kt, the dashed blue Millward(1) curve lies below the "mean-plus-one-sigma" curve. For (H/T) of 1.20 and for all speeds up to 16 kt, the dashed cyan curve for Römisch stern squat lies below the "mean-minus-one-sigma" curve.

Figure C.15: Results for a VLCC in open water for water-depth to draft ratio 1.30

In Figure C.15 for (H/T) of 1.30 and for speeds less than 16 kt, the dashed blue Millward(1) curve lies below the "mean-plus-one-sigma" curve. For (H/T) of 1.30 and for all speeds up to 16 kt, the dashed cyan curve for Römisch stern squat lies below the "mean-minus-one-sigma" curve.
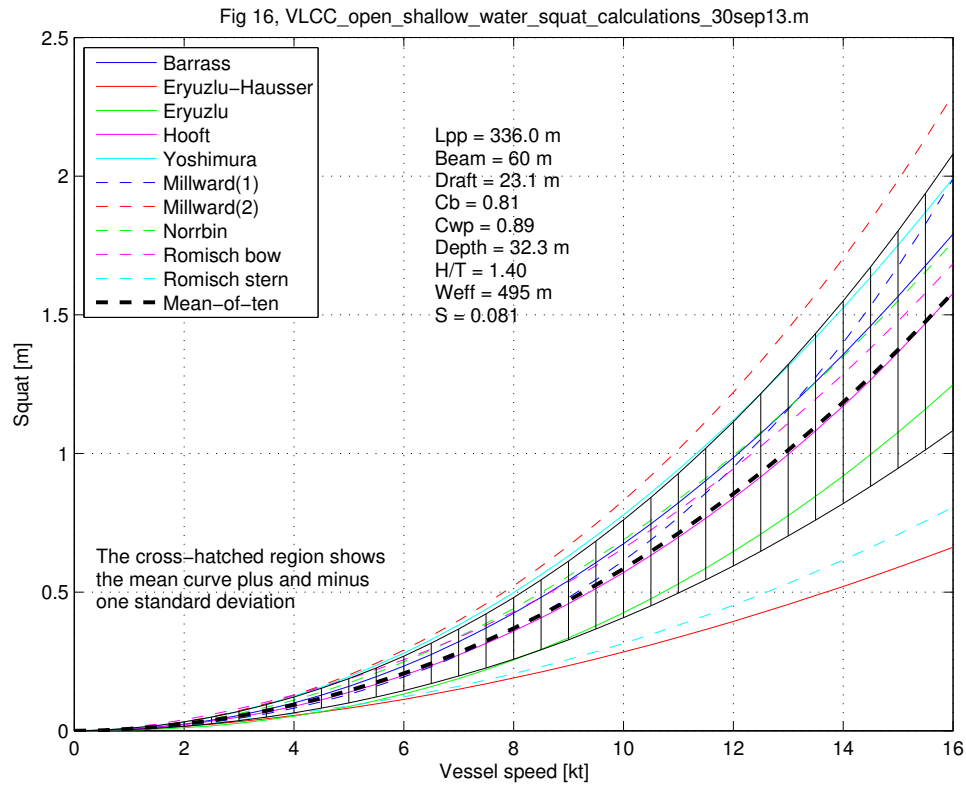
Figure C.16: Results for a VLCC in open water for water-depth to draft ratio 1.40

In Figure C.16 for (H/T) of 1.40 only the dashed red Millward(2) curve, the solid red Eryuzlu-Hausser curve and the dashed cyan Römisch stern squat curve lie outside the "mean-plus-and-minus-one-sigma" band.
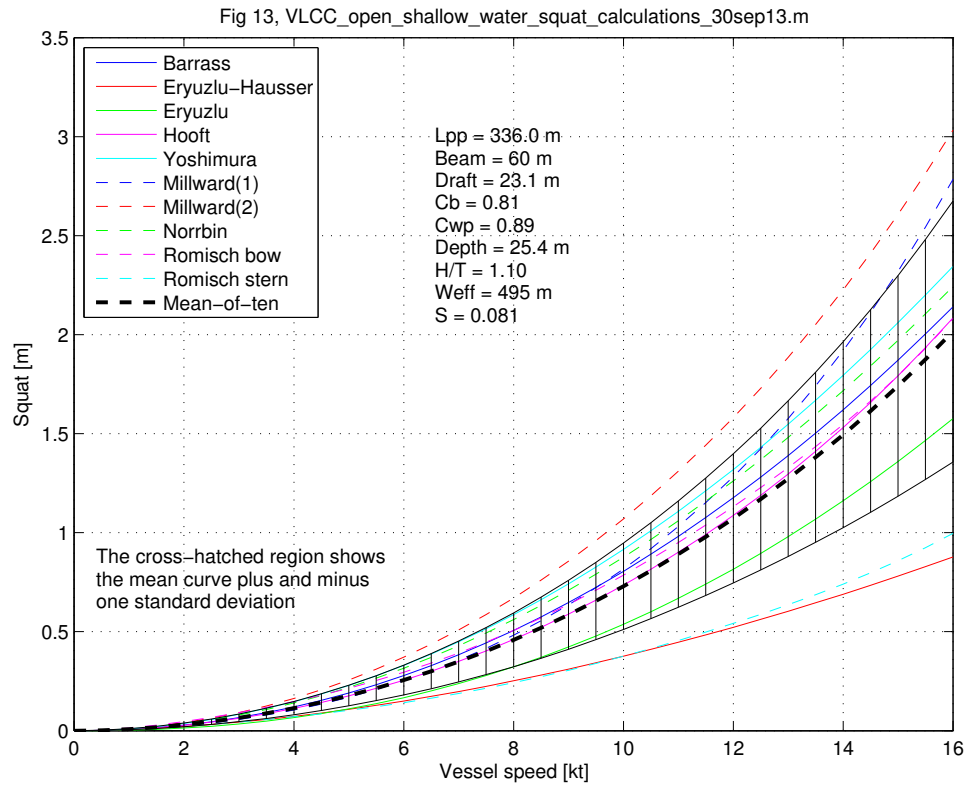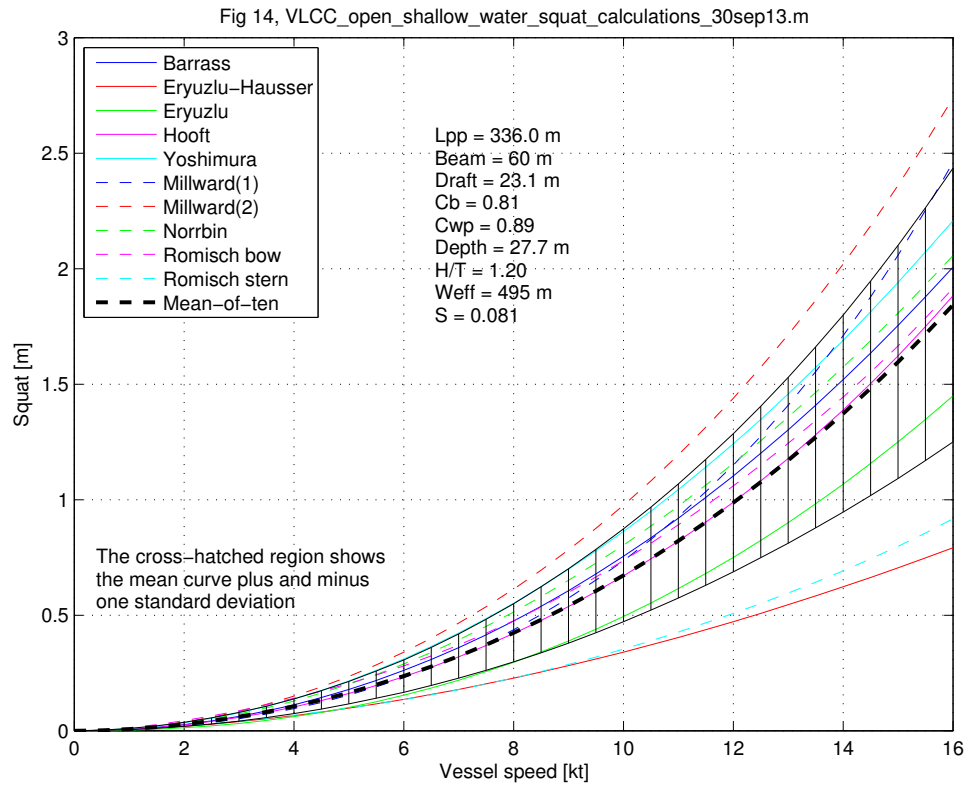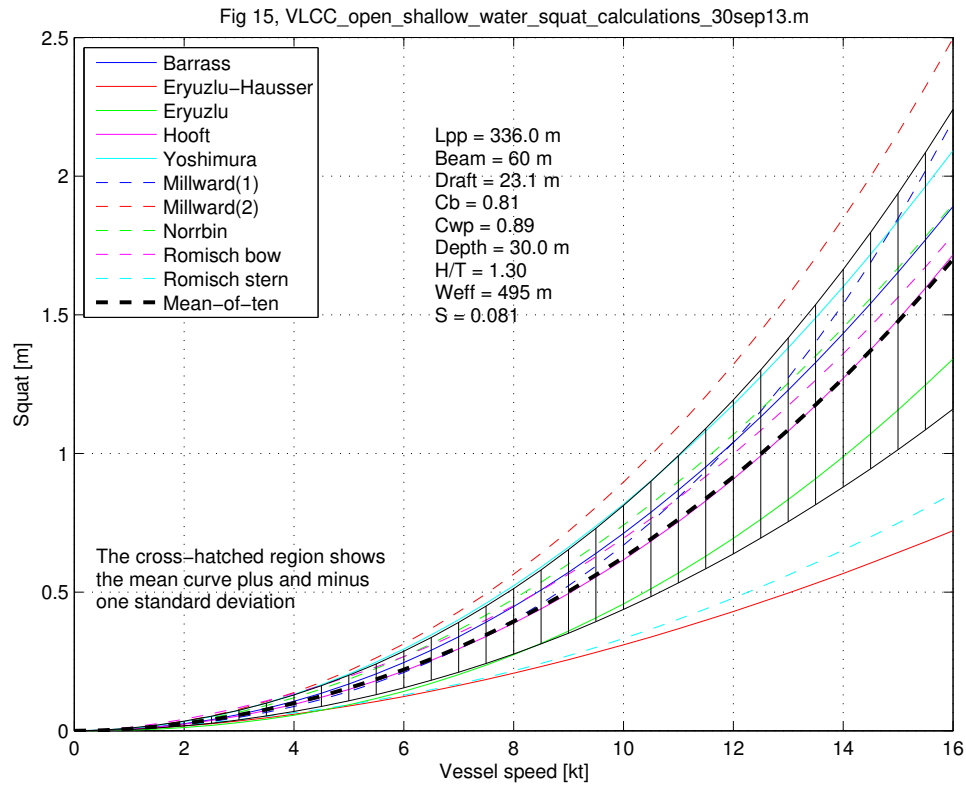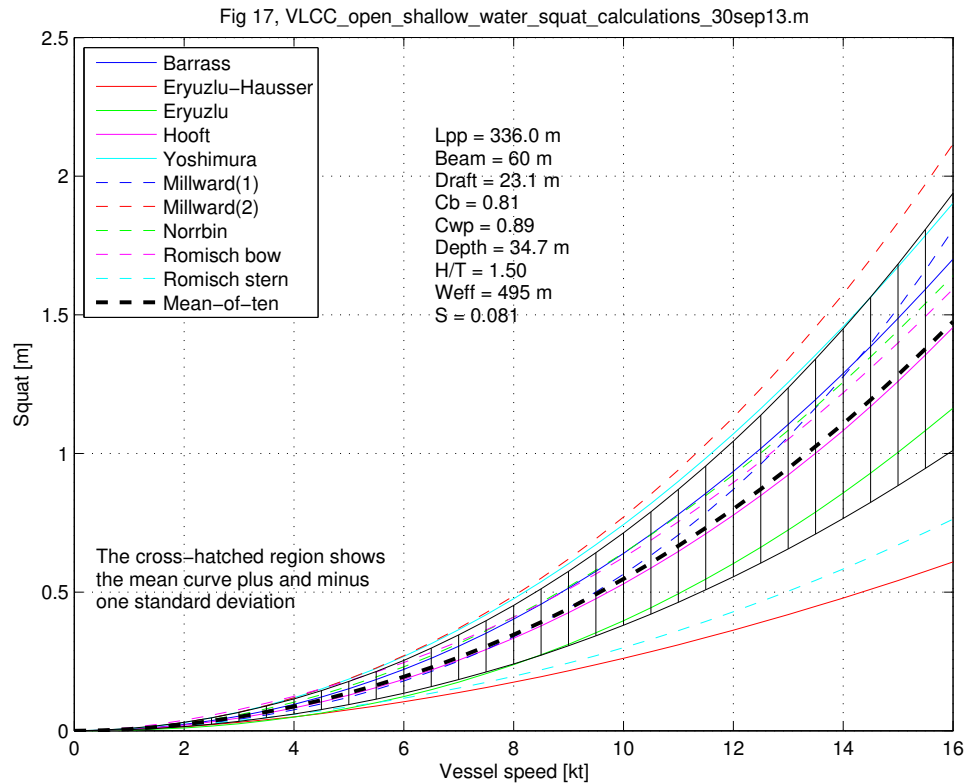
Figure C.17: Results for a VLCC in open water for water-depth to draft ratio 1.50

In Figure C.17 for (H/T) of 1.50 for speeds less than 14.5 kt, the solid cyan Yoshimura prediction lies above the "mean-plus-one-sigma" curve.

From Figures C.13 to C.17 we conclude from the mean curves that

(a) the mean values of the predicted squat from ten different formulae tend to be proportional to the square of the ship's forward speed, and,

(b) for the range 1.1 < (H/T) < 1.5, for all ship speeds less than 14.5 kt, seven of the ten prediction curves fall within the "mean-plus-and-minus-one-sigma" band.

The prediction which tracks the open-water mean curve most closely is the solid magenta curve for the Hooft formula. An advantage of the Hooft formula for unrestricted uniform-depth shallow water is that it depends only on the displaced volume of the ship, the ship's length L_{pp}, and the depth-based Froude Number so such a predictor is simple to compute. Unfortunately the value of the displaced volume is not always readily available for a particular loading condition of a given ship. If values of the displaced volume for several loading

117

conditions for each ship can be determined, a table or chart of squat values based on the Hooft formula, applicable to sailing in shallow open-water conditions, could be provided for each ship.

C.5.2   Consideration of the TERMPOL report squat predictions for a VLCC
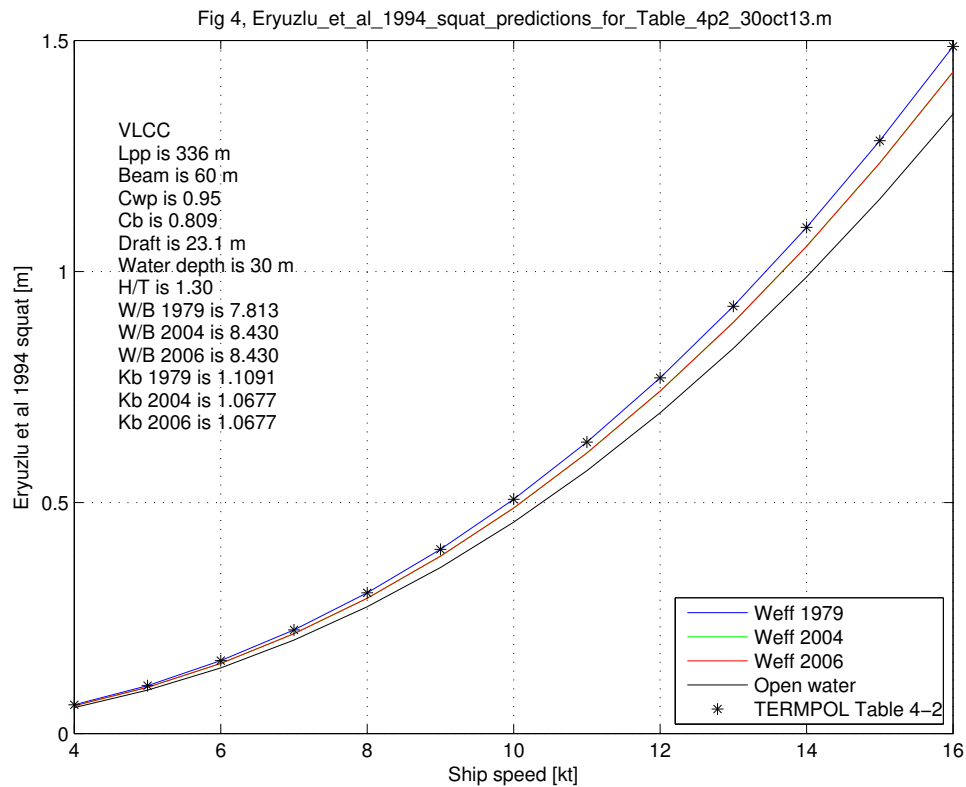
Figure C.18: Bow squat versus ship speed for several W_{eff} values for a VLCC in open-water conditions with H/T of 1.30

The TERMPOL report (Kitimat study [26]) uses the Eryuzlu et al 1994 formula to predict the bow squat of a VLCC in unrestricted uniform-depth shallow-water condtions. To that end it uses W_{eff} based on the ship's waterplane area coefficient C_{wp} from (C.22), so that expression produces a value of W_{eff}/b of 7.81 so this is a lateral restriction consideration and the open-water requirement of $W_{eff}/b > 9.61$ does not apply and the value for K_b of unity cannot be used. Thus we must use

$$K_b = 3.1/\sqrt{Weff/b} = 1.1091 \tag{C.45}$$

118

then the bow squat is given by

$$\Delta z_b = 0.298 \cdot (H^2/T) \cdot [(\frac{V_s}{\sqrt{g \cdot T}})^{2.289}] \cdot [(\frac{H}{T})^{-2.972}] \cdot K_b \qquad \text{(C.46)}$$

and these two expressions provide the values in Table 4-2 on page 4-5 of the report [26].

Thus the Eryuzlu et al 1994 formula for K_b in (C.45) includes only the lateral restriction effect of W_{eff}/b for the open-water condition, and not any vertical restriction effect due to the water-depth to draft ratio H/T. Note that the definition of the blockage ratio

$$S = \frac{A_s}{A_c} = \frac{(b \cdot T)}{(W_{eff} \cdot H)} = (\frac{b}{W_{eff}}) \cdot (\frac{T}{H}) \qquad \text{(C.47)}$$

for open-water conditions includes both the lateral-restriction and vertical-restriction effects; the blockage ratio S is used in other 'correction' factors with other formulae in order to model the effects of restriction in confined channels, but not in the factor K_b in the Eryuzlu et al 1994 formula.

In summary, we see that the Eryuzlu formula (C.46) includes only the vertical-restriction effects (in terms of H and T) in the first three terms, while the lateral-restriction effects are captured in the fourth term K_b.

In Figure C.18 the four curves show the effect of using different values of W_{eff} the effective width of channel in the calculation of K_b. Here the blue curve shows the predicted values for shallow open water for this VLCC when using Barrass' original 1979 expression

$$W_{eff}/b = F_b = 7.7 + 45 \cdot [(1 - C_{wp})^2] \qquad \text{(C.48)}$$

The green curve shows the predicted values when using Barrass' 2004 expression

$$F_b = 7.04/C_b^{0.85} \qquad \text{(C.49)}$$

The red curve shows the predicted values when using Barrass' 2006 expression

$$F_b = 7.7 + 20 \cdot [(1 - C_b)^2] \qquad \text{(C.50)}$$

It just so happens that for this C_b value of 0.81, the values of F_b from the 2004 and 2006 expressions are numerically identical, hence the red curve lies on top of the green curve thus the green curve is not visible. The black curve is the result from using the open-water predictor, that is, equation (C.46) with K_b set to unity.

The results show that the ratio of the values of the Eryuzlu bow squat prediction with $K_b(1979)$ to the Eryuzlu bow squat open water predictions are a constant 1.1091, at all speeds.

The results show that the ratio of the values of the Eryuzlu bow squat prediction with K_b(2004) to the Eryuzlu bow squat open water predictions are a constant 1.0677, at all speeds.

The results show that the ratio of the values of the Eryuzlu bow squat prediction with K_b(2006) to the Eryuzlu bow squat open water predictions are a constant 1.0677, at all speeds.

The ratio of 1.1091 to 1.0677 is 1.0388 so the effect of changing from the 1979 to 2004 (or 2006) expression for W_{eff} provides a 3.9 % decrease in the calculated squat. At 12 kt this represents a squat increase of about 29 cm in going from the green or red curve to the blue curve. Since C_b is 0.81, Barrass will predict that the maximum squat will occur at the bow. As a fraction of L_{pp} of 336 m, this 29 cm is probably negligible and is within the one to five cm accuracy of the vertical DGPS measurements in the Panama Canal experiments reported in [45].

From these results we conclude that:

 a. The open-water results which ignore any lateral 'width of influence' effect are given correctly by the black curve which effectively uses unity for K_b in formula (C.46).

 b. The open-water results which include the lateral 'width of influence' effect are given correctly by the other three curves which each use a different value of W_{eff} and thus a different value for K_b. The three Barrass expressions for W_{eff} used are given in (C.48), (C.49) and (C.50) above.

 c. The results which include the use of K_b, confirm that the bow squat is directly proportional to the value of K_b, at all speeds.

C.6 Formulae for Trapezoidal Canals

Referring to Figure C.11, in the context of the derivations by Tothill, Vermeer, Constantine, Dand and Ferguson and others, it is the 2D vertical-plane cross-sectional shape of the ship (relative to the vertical-plane cross-sectional shape of the channel in which the ship operates) which produces the narrow gap between the keel and the channel bottom which causes the flow speed-up and hence the drawdown of the water-surface. Thus we would expect squat prediction formulae to contain factors such as (a) the water-depth-to-draft ratio (H/T), and, (b) the ship-beam-to-channel-bottom-width ratio (b/W). Only when 3D effects are incorporated into a squat formula would the ship length L_{pp} appears in ratios such as (L_{pp}/b), (L_{pp}/T), (L_{pp}/H) and (L_{pp}/W). Similarly parameters which represent the underwater shape of the hull such as the displaced volume of the ship ∇, the block coefficient C_b, and the waterplane area A_{wp}, are additional 3D effects which could be included.

For trapezoidal canals, see Figures C.6 and C.11. Here the canal bottom-width is W and the reciprocal of the side-slope of the banks is given by $n = cot(\theta)$ where θ is the angle of the side-bank measured from the horizontal. The cross-sectional area A_c of the canal when is full of water of depth H is given by

$$A_c = H \cdot (W + n \cdot H) \tag{C.51}$$

The blockage ratio S is then given approximately by

$$S = \frac{A_s}{A_c} = \frac{b \cdot T}{H \cdot (W + n \cdot H)} \tag{C.52}$$

or more precisely by

$$S = \frac{A_s}{A_c} = \frac{C_m \cdot b \cdot T}{H \cdot (W + n \cdot H)} \tag{C.53}$$

if the midship area coefficient C_m is known. Table C.8 shows that typical values for C_m are 0.996 for a VLCC and as low as 0.85 for a naval vessel with a V-shaped hull.

C.6.1   Huuska and Guliev 1976

The Huuska (1976) and Guliev (1971, 1973) formula is an extension of the Hooft formula for its use with restricted channels and canals, so it is written as

$$\Delta z_b = 2.4 \cdot \left(\frac{\nabla}{L_{pp}^2} \right) \cdot \frac{F_{nh}^2}{\sqrt{1 - F_{nh}^2}} \cdot K_s \tag{C.54}$$

In general this formula should not be used for F_{nh} greater than 0.7. For a trapezoidal canal the value of K_s is given by

$$K_s = 7.45 \cdot S + 0.76 \tag{C.55}$$

where S is calculated using either (C.52) or (C.53) above.

C.6.2   Eryuzlu et al 1994

For a trapezoidal canal, the same formula applies, namely

$$\Delta z_b = 0.298 \cdot (H^2/T) \cdot [(\frac{V_s}{\sqrt{g \cdot T}})^{2.289}] \cdot [(\frac{H}{T})^{-2.972}] \cdot K_b \tag{C.56}$$

where K_b is a correction factor which accounts for the geometry of the trapezoidal canal. Here

$$K_b = 3.1/\sqrt{W/b} \tag{C.57}$$

when W/b < 9.61, and,

$$K_b = 1 \tag{C.58}$$

when W/b > 9.61. Here W is the width of the bottom of the trapezoidal canal.

C.6.3 Römisch 1989

For a trapezoidal canal, Römisch again uses his equation (C.8) for the bow squat and equation (C.9) for the stern squat. However for a trapezoidal canal the formula for V_{cr} becomes

$$V_{cr} = C \cdot K_c \tag{C.59}$$

where the value of K_c is given by

$$K_c = 0.2306 \cdot log_e(\frac{1}{S}) + 0.0447 \tag{C.60}$$

where S is given above by (C.52) or (C.53). All the remaining expressions stay the same as in Section C.4.8.

C.6.4 Barrass 2006

In neither his 2004 book nor his 2006 book does Barrass provide a specific formula for a trapezoidal canal. For a rectangular river section he uses a factor K which is given by

$$K = 6 \cdot S + 0.4 \tag{C.61}$$

where S is given above by (C.52) or (C.53). This value of K is then used with

$$\delta_{max} = K \cdot \left(\frac{C_b}{100}\right) \cdot V_k^2 \tag{C.62}$$

for the maximum sinkage. The implication seems to be that for the same values of S and K, the predicted sinkage will be the same whether the ship is in a rectangular river section or in a trapezoidal canal.

C.6.5 Barrass 2009

In [57] on page 18 in equations (1) and (2), and, in [45] on page 78 in equations (21) and (22), it is shown that by 2007 Barrass had modified his empirical formula for medium-width river sections to become

$$\delta_{max} = \frac{K \cdot C_b \cdot V_k^2}{100} \tag{C.63}$$

with

$$K = 5.74 \cdot S^{0.76} \tag{C.64}$$

with $1 < K < 2$. Again δ_{max} is assigned to the bow if $C_b > 0.7$ and to the stern if $C_b < 0.7$. Apparently this version of Barrass' channel coefficient, K, is based on analysis of over 600 laboratory and prototype measurements for all three channel types. Here [57] and [45] confirm that for a trapezoidal canal, S is given by either (C.52) or (C.53) on page 121. The lower limit for K is for an S-value of 0.10 while the upper limit for K is for an S-value of 0.25. The implication seems to be that for the same values of S and K, the predicted sinkage will be the same whether the ship is in a medium-width river or in a trapezoidal canal.

C.6.6   Ankudinov 2009

For a trapezoidal canal, the blockage ratio S is again the ratio A_s/A_c which is the fraction of the cross-sectional area of the waterway A_c which is occupied by the ship's underwater midships transverse vertical-plane cross-sectional area A_s. Thus

$$S = A_s/A_c = \frac{(b \cdot T)}{H(W + nH)} \tag{C.65}$$

so we need to know the values for the width W of the bottom of the canal, and n, the reciprocal of the side-slope of the canal banks. Then

$$S_h = C_b \cdot S \cdot \left(\frac{T}{H}\right) \tag{C.66}$$

then the *channel effects parameter* P_{Ch1} is given by

$$P_{Ch1} = 1 + 10 \cdot S_h - 1.5 \cdot (1 + S_h) \cdot \sqrt{S_h} \tag{C.67}$$

Also need to define and include P_{Ch2} since it was unity for the unrestricted waterway case. The *channel effect trim correction parameter* P_{Ch2} is given by

$$P_{Ch2} = 1 - 5 \cdot S_h \tag{C.68}$$

Also need to redefine n_{Tr} to include the effect of the new value for P_{Ch1} since the new value of the *trim exponent* n_{Tr} is given by

$$n_{Tr} = 2 + 0.8 \cdot \left(\frac{P_{Ch1}}{C_b}\right) \tag{C.69}$$

Finally the expression for the vessel midship sinkage S_m becomes

$$S_m = (1 + K_P^S) \cdot P_{Hu} \cdot P_{F_{nh}} \cdot P_{+h/T} \cdot P_{Ch1} \tag{C.70}$$

and the expression for the vessel trim becomes

$$Trim = -1.70 \cdot P_{Hu} \cdot P_{F_{nh}} \cdot P_{h/T} \cdot K_{Tr} \cdot P_{Ch2} \tag{C.71}$$

for a trapezoidal canal.

C.6.7   Yoshimura 2009

In [45] at the bottom of page 79 a modification is provided which is implied by the text to be in [46] but is not actually in that document. This modification is to change V_s to V_e in Yoshimura's open-water expression (C.19) on page 107 so as to be able to incorporate the effects of a confining channel.

$$V_e = \frac{V_s}{(1 - S)} \tag{C.72}$$

where the value of S is given for a trapezoidal canal by (C.52) or (C.53) above. The final expression for the bow squat is therefore

$$\Delta z_b = \left[\left(0.7 + 1.5(\frac{T}{H}) \right) \left(\frac{b \cdot C_b}{L_{pp}} \right) + 15(\frac{T}{H}) \left(\frac{b \cdot C_b}{L_{pp}} \right)^3 \right] \left(\frac{V_e^2}{g} \right) \qquad (C.73)$$

C.7   Examples for Trapezoidal Canals

Reference [45] provides information about DGPS measurements of the squat of four ships which transited the Gaillard Cut section of the Panama Canal in December 1997 and April 1998.

Table C.4 provides values for the five parameters which describe the four ships and their transit conditions.

Table C.4: Particulars for the four ships in the Panama Canal measurements

Ship	Ship Particulars				
	L_{pp}	b	T_{fp}	T_{ap}	C_b
Elbe Panamax tanker	222	32.2	11.3	11.3	0.84
Global Challenger Panamax bulk carrier	216	32.3	11.7	11.8	0.83
Majestic Maersk Panamax container ship	284.5	32.2	11.8	11.8	0.63
OOCL Fair container ship	227	32.2	9.8	10.6	0.65

In the above table of parameters, T_{fp} is the initial draft (when stationary) at the forward perpendicular; T_{ap} is the initial draft (when stationary) at the aft perpendicular; the difference between these two numbers determines whether the ship is initially at a "level keel" condition, or, it has an initial non-zero trim angle.

Given the DGPS measurements of bow squat for the Elbe tanker (as an example) in Figure 2 of that paper, it can be seen that there is considerable scatter in the data, in the sense that at any given vessel speed there are multiple measured values, and, the measured values do not cluster closely around a single trend line. Reference [45] on page 75 mentions that the minimum water depths apply to the centre 91 m section of the canal, not to the full bottom-width of the canal; all the squat formulae for canals assume a trapezoidal cross-section with a constant-depth portion of width W at the bottom. Page 75 states that "the vertical accuracy of the DGPS measurements was of the order to 1 to 5 cm". Page 75 also mentions that "a larger source of uncertainty is the measurement of water levels and depth".

Reference [45] says that the four ships represent 2878 individual measurements of squat, either at the bow or the stern, depending on the ship. Thirty-one values of the vessel speed

were scaled from Figure 3 of that paper, and, 31 values of measured squat from the plots in Figures 6, 7, 8 and 9 at those speeds. These 31 values were taken at the grid points which correspond to distances 1000 feet (305 m) apart. Based on the average ship speed through this 9.1 km portion of the Panama Canal, these 31 values correspond to one measurement taken every minute. In these calculations the Barrass 2009 formulas in (C.63) and (C.64) on page 122 were used.

All the following predictions used the same (constant) values of the water depth H (13.05 m), width of the channel bottom W (152 m) and side-slope parameter n of 1.88 which were reported in [45]. Thus the only variables were the specific geometric parameters for each ship, as well as the initial (zero-speed) draft and trim condition.

Table C.5: Goodness of fit for squat predictors to DGPS measurements, Panama Canal

Squat Formula	Elbe SSE	SSE Rank	Global SSE	SSE Rank	Majestic SSE	SSE Rank	OOCL SSE	SSE Rank	Sum of Ranks	Sum of Ranks*
Ankudinov	0.707	5	3.516	5	0.585	2	0.112	1	13	3.25
Barrass3	0.110	1	0.510	1	0.373	1	0.253	2	5	1.25
Eryuzlu	1.141	6	4.498	6					12	6
Huuska & Guliev	0.189	2	3.437	4					6	3
Romisch	0.266	3	0.759	2	2.148	3	0.357	3	11	2.75
Yoshimura	0.268	4	1.052	3					7	3.5
Sum of SSE	2.681		13.772		3.106		0.722			
SSE/N	0.45		2.30		1.04		0.24			

Table C.5 provides statistical information which pertains to Figures C.19, C.20, C.21 and C.22 for the Elbe tanker, Global Challenger bulk carrier, Majestic Maersk and OOCL Fair container ships, respectively. In each figure six curves of predicted ship squat are shown, along with the sampled full-scale DGPS measurements.

In Table C.5, SSE represents the sum of the squares of the deviations of the DGPS measurements of squat from the predicted values of squat, at each measured vessel speed. The lower the value of the SSE, the closer the predicted values correspond to the measured values. For the Elbe and Global ships, since $C_b > 0.7$, the measured and predicted squat is at the bow. For the Majestic and OOCL, since $C_b < 0.7$, the measured and predicted squat is at the stern.

Most of the formulae in Section C.6 predict the squat at the bow of the ship. Some formulae predict the squat at both the bow and the stern, as well as the trim (Ankudinov, Barrass, Römisch) so only those three should be used for predictions for the two container ships.

In terms of overall usefulness for predicting the squat of ships which transit the Panama Canal, the column labelled 'SSE Rank' in Table C.5 shows that the Barrass squat formula has the smallest SSE for three out of four ships. To judge whether or not the Barrass formula is more useful than the others (a) in unrestricted shallow waterways, or, (b) in non-canal restricted waterways, will require access to measurements of full-scale squat for those two waterways.

Apparently the Eryuzlu formula is used extensively for prediction of squat of ships which transit the St. Lawrence Seaway. Clearly the Eryuzlu formula, which is valid only for $C_b > 0.8$ and can predict only bow squat, is not appropriate for predicting the squat of ships which squat by the stern in the Panama Canal. Even for the Elbe tanker and Global Challenger bulk carrier, the Eryuzlu formula grossly underpredicts their bow squat in the Panama Canal.

Other formulae were not used in [45] and were not used in this section since some of these formulae can only predict ship squat in unrestricted shallow waterways and are thus not applicable to restricted waterways (trapezoidal canals) such as the Panama Canal. The omitted formulae include those by Tuck (1966), Hooft (1974), ICORELS (1980), Eryuzlu and Hausser (1978), Millward (1990, 1992) and Norrbin (1986).

In Table C.5 the columns for the Majestic Maersk and OOCL Fair container ships have only the SSE values for the three formula which predict stern squat. The bottom row of this table contains the sum of the six (or three) SSE values, divided by the number of formulae used (six or three); these four values show that the OOCL Fair container ship has the closest agreement between the measured and predicted values of squat. The column labelled "Sum of Ranks" contains the sum of the individual rankings for each formula, across the

four ships. The last column contains the value of "Sum of Ranks" divided by the number of ships to which that formula was applied. These values show that the Barrass formula provides the lowest SSE for all four ships when they operate in the Panama Canal. The second-most-useful formula for these four ships in the Panama Canal is the Römisch formula. Unfortunately, although the Ankudinov formula is perhaps the "most recent" formula, and, the formula which includes the largest number of ship parameters, the Ankudinov formulation does not provide the best agreement (the lowest SSE) for these four ships in the Panama Canal.
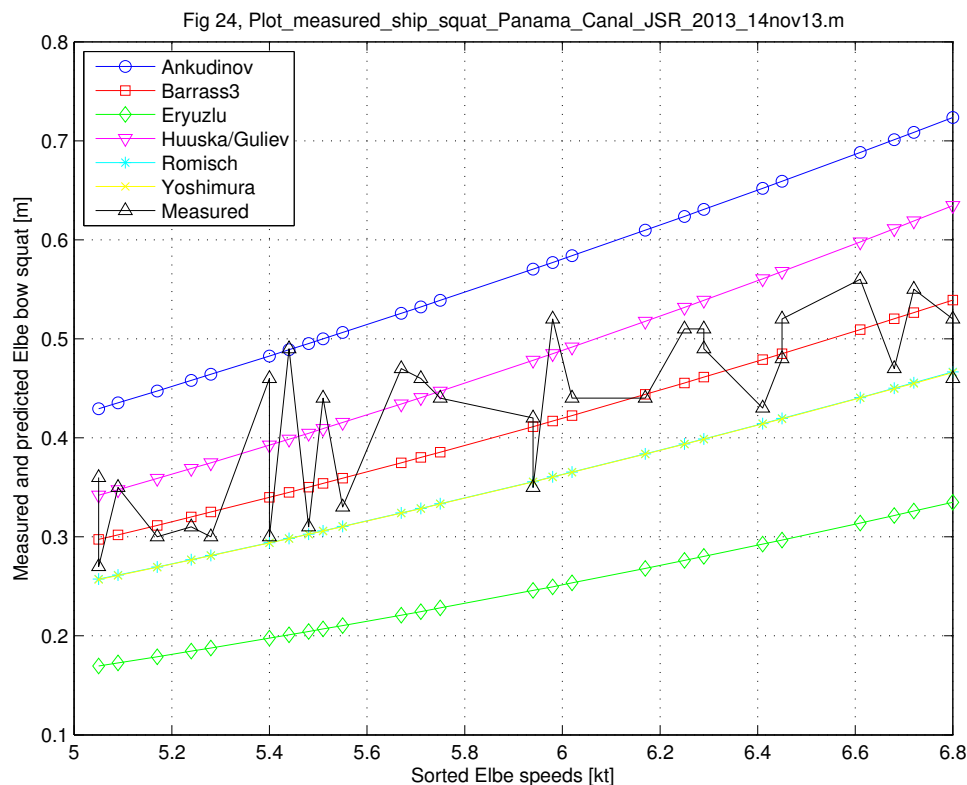
Figure C.19: Elbe tanker, bow squat measurements and predictions, Panama Canal

Figure C.19 shows the sampled full-scale measurements of bow squat for the Elbe tanker. These data-points have been ordered according to the vessel speed which occurred at the same instant as the DGPS squat measurement was performed. Also shown is the curve which represents the average of the six bow-squat prediction values at each vessel speed. This figure shows that for the Elbe tanker, the six prediction curves do straddle the measured values of bow squat. The cyan Römisch curve and the yellow Yoshimura curves are

essentially coincident so they appear as a single light-green curve.
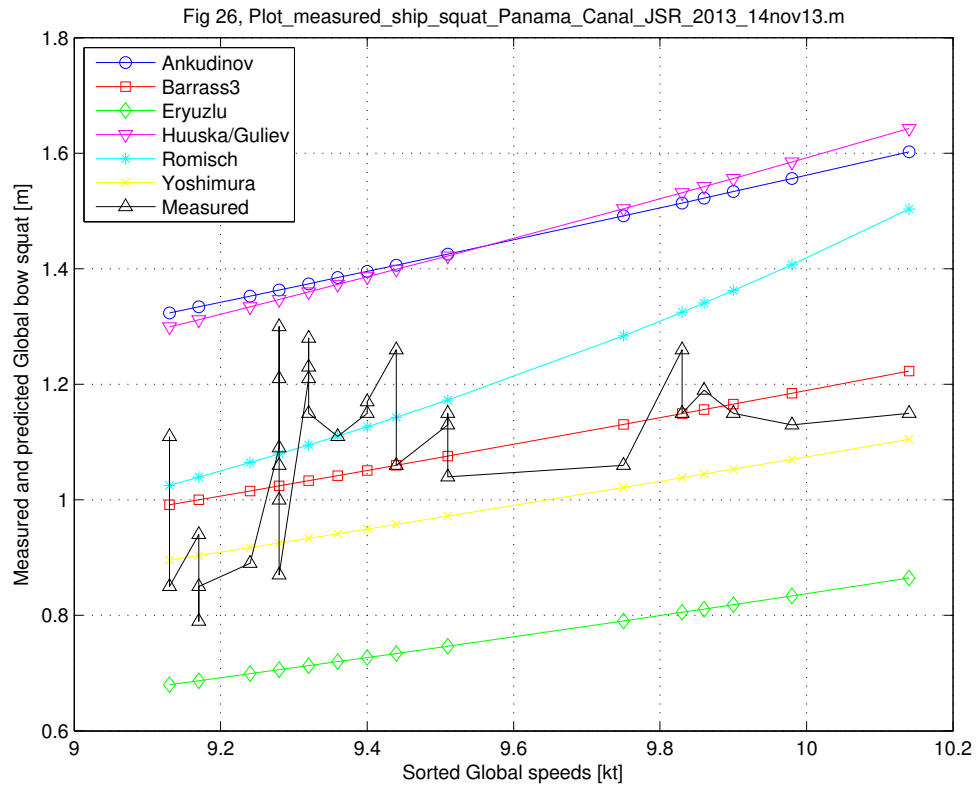
Figure C.20: Global Challenger bulk carrier, bow squat measurements and predictions, Panama Canal

Figure C.20 shows the corresponding measured values for the bow squat of the Global Challenger bulk carrier. Also shown is the curve which represents the average of the six bow-squat prediction values at each vessel speed. This figure shows that for the Global Challenger bulk carrier, the six prediction curves do straddle the measured values of bow squat.

Fig 28, Plot_measured_ship_squat_Panama_Canal_JSR_2013_14nov13.m

Figure C.21: Majestic Maersk container ship, stern squat measurements and predictions, Panama Canal

Figure C.21 shows the corresponding measured values for the stern squat of the Majestic Maersk container ship. Also shown is the curve which represents the average of the three stern-squat prediction values at each vessel speed. For this ship the average curve tends to follow the measured values quite well even though the range of measured vessel speeds (relative to the other three ships) is quite large at almost 4.4 kt. This figure shows that for the Majestic Maersk container ship, five of the six prediction curves pass through the bulk of the measurements of stern squat. The Yoshimura curve is predicting the bow squat, which is not what the measurements represent. Also, although they are predicting bow squat, the Eryuzlu and Huuska-Guliev curves tend to follow the trend of the measurements. Note that above about 10 kt, the Römisch stern predictions diverge sharply from the trend in the measurements.

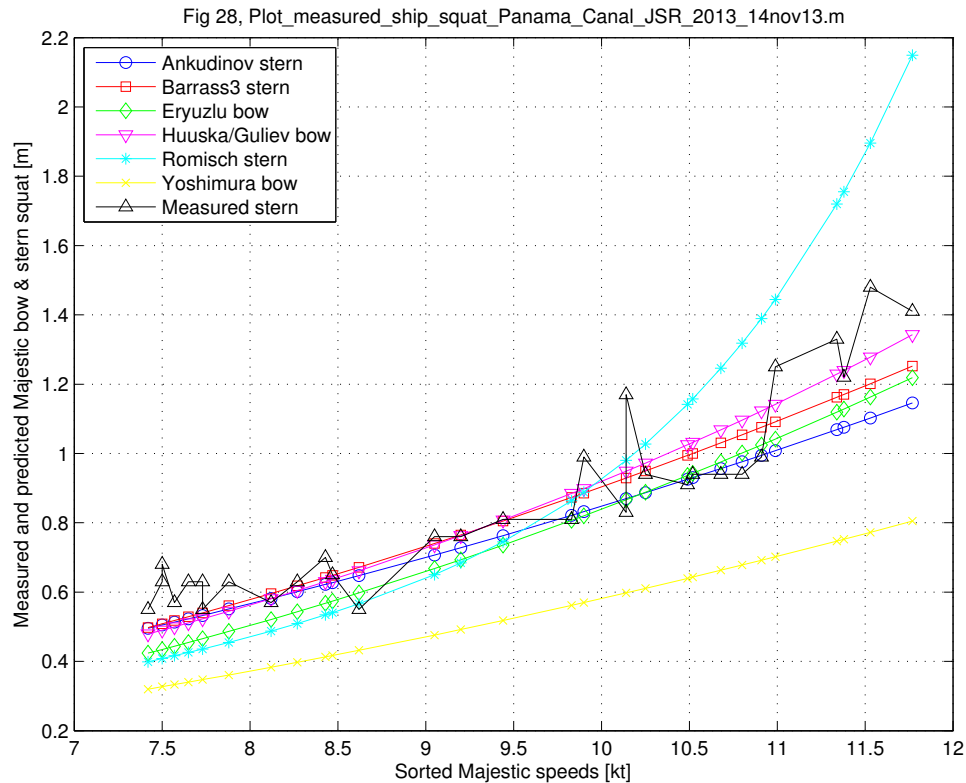Fig 30, Plot_measured_ship_squat_Panama_Canal_JSR_2013_14nov13.m
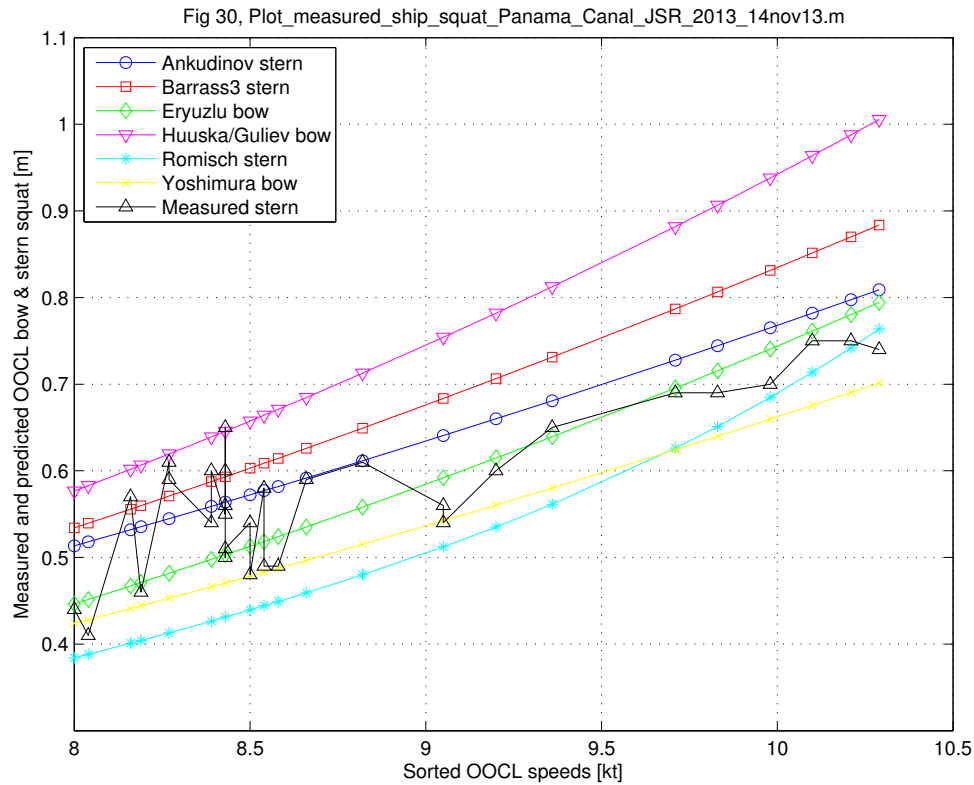
Figure C.22: OOCL Fair container ship, stern squat measurements and predictions,
Panama Canal

Figure C.22 shows the corresponding measured values for the stern squat of the OOCL
Fair container ship. Also shown is the curve which represents the average of the three
stern-squat prediction values at each vessel speed. For this ship the average curve tends
to follow the measured values quite well. Because the range of measured speeds was
small at about 2.3 kt, the sum of the SSE values for this ship was the smallest of the corre-
sponding sums for the four ships. This figure shows that for the OOCL Fair container ship,
the three stern-squat prediction curves straddle the measurements of stern squat.
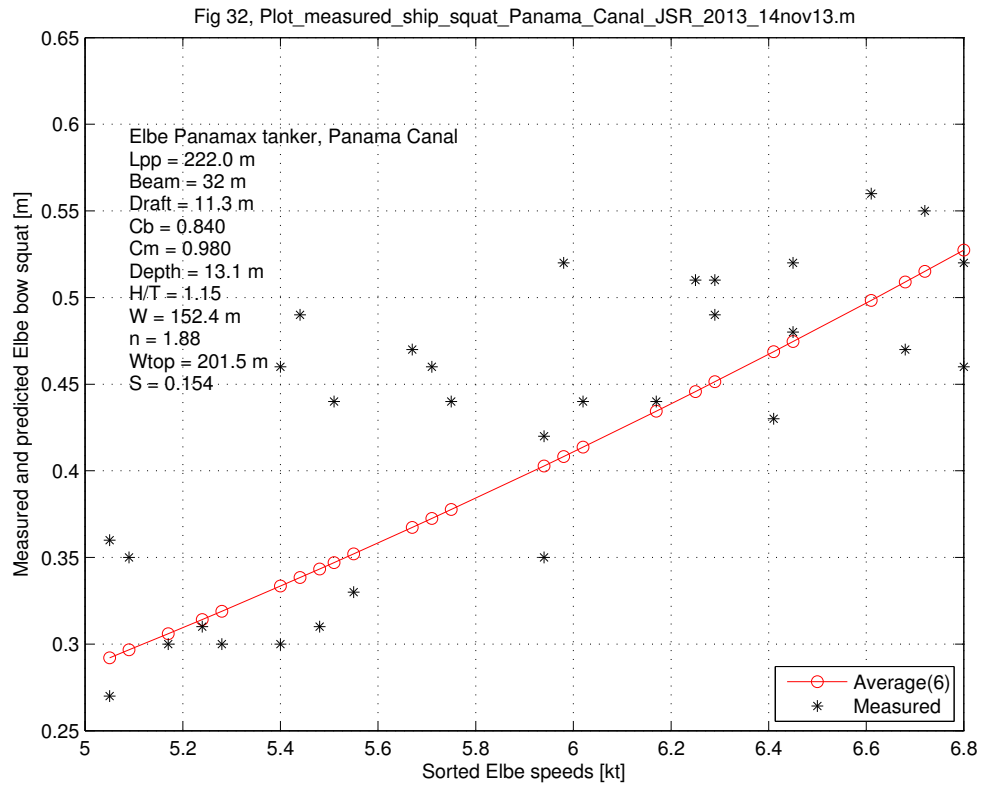
Figure C.23: Elbe tanker, bow squat measurements and average of six predictions, Panama Canal

Figure C.23 shows the bow-squat measurements for the Elbe tanker along with the average of the six bow-squat predictions.
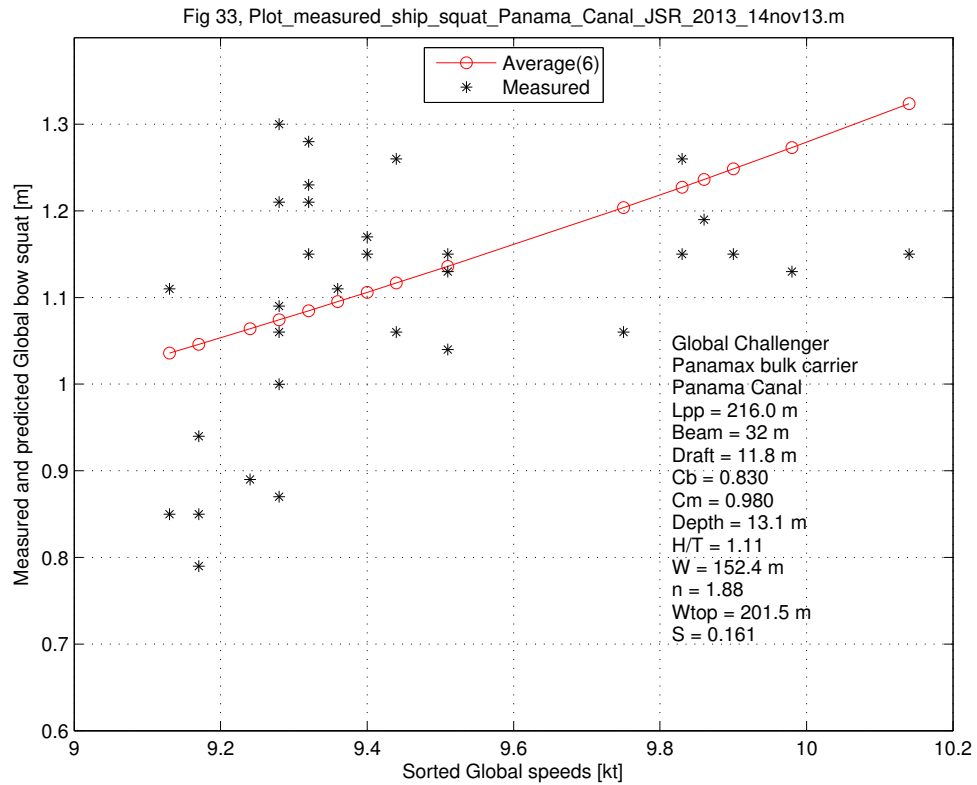
Figure C.24: Global Challenger bulk carrier, bow squat measurements and average of six predictions, Panama Canal

Figure C.24 shows the bow-squat measurements for the Global Challenger bulk carrier along with the average of the six bow-squat predictions.

133

Fig 34, Plot_measured_ship_squat_Panama_Canal_JSR_2013_14nov13.m

Majestic Maersk, Panama Canal
Lpp = 284.7 m
Beam = 32 m
Draft = 11.8 m
Cb = 0.633
Cm = 0.980
Depth = 13.1 m
H/T = 1.11
W = 152.4 m
n = 1.88
Wtop = 201.5 m
S = 0.161
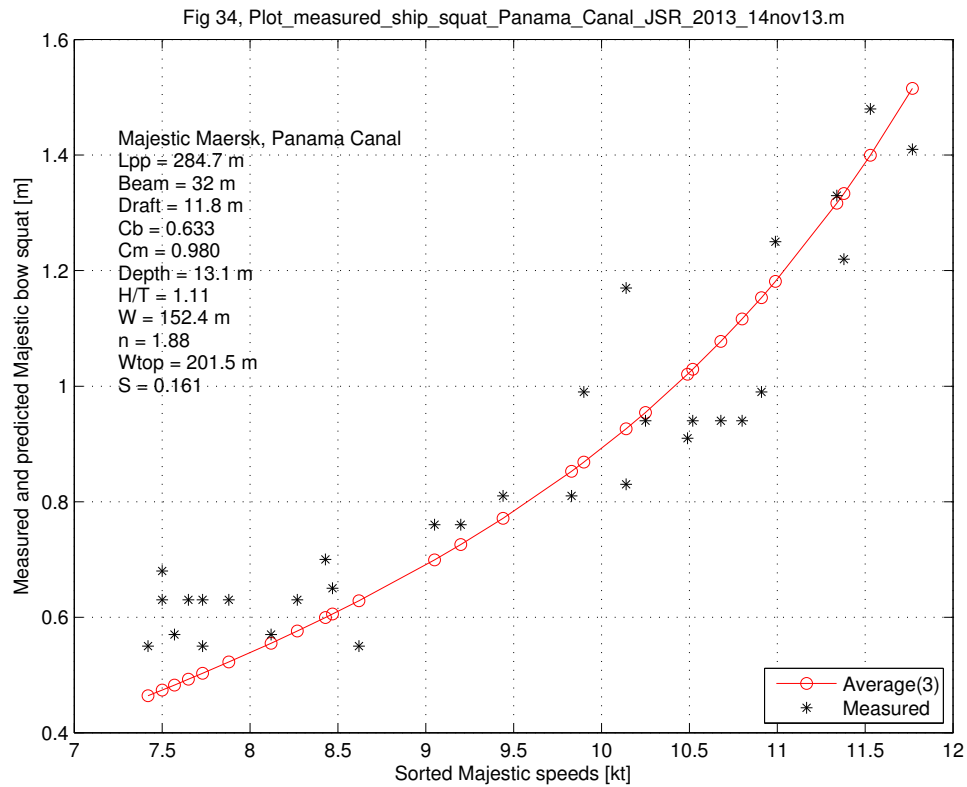
Figure C.25: Majestic Maersk container ship, stern squat measurements and average of three predictions, Panama Canal

Figure C.25 shows the stern-squat measurements for the Majestic Maersk container ship along with the average of the three stern-squat predictions.

Fig 35, Plot_measured_ship_squat_Panama_Canal_JSR_2013_14nov13.m
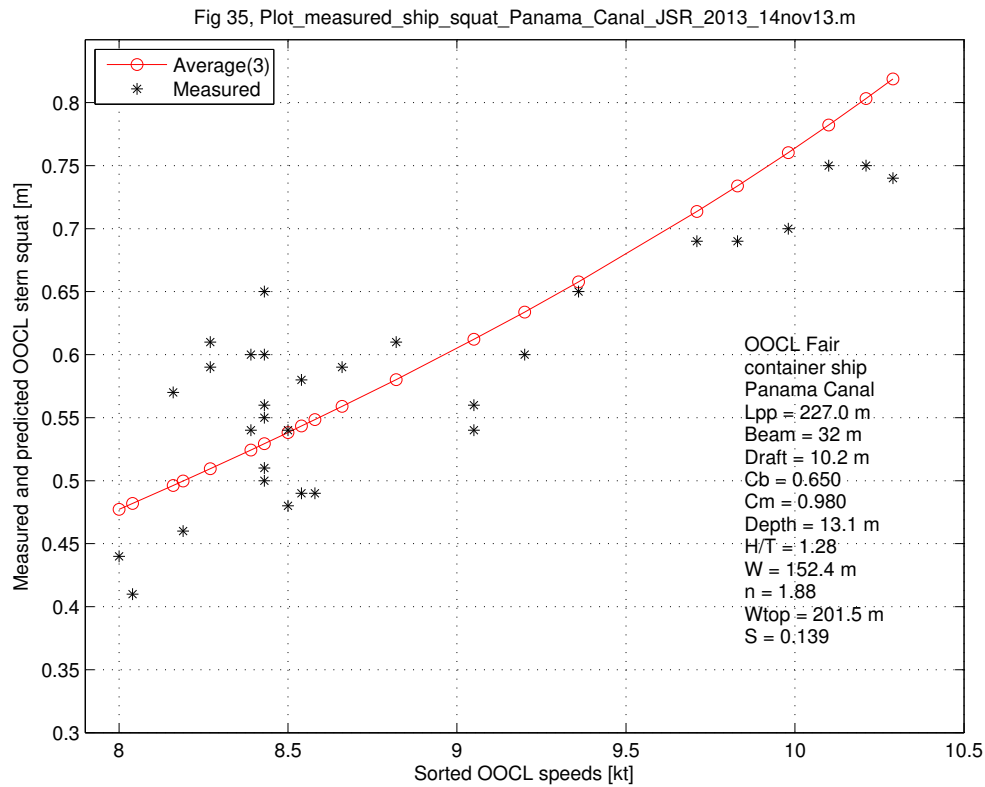
Figure C.26: OOCL Fair container ship, stern squat measurements and average of three predictions, Panama Canal

Figure C.26 shows the stern-squat measurements for the OOCL Fair container ship along with the average of the three stern-squat predictions.

C.8   Formulae for Trenched Channels

In this section we show five sets of formulae which are applicable for predicting ship squat in trenched channels.

C.8.1   Römisch 1989

For a trenched channel, Römisch again uses his equation (C.8) for the bow squat and equation (C.9) for the stern squat. Here we introduce the trench height H_t and calculate the corresponding value of V_{cr} using V_{cr} from

$$V_{cr} = C_{mT} \cdot \left[K_{ch} \cdot \left(1 - \frac{H_t}{H} \right) + K_c \cdot (\frac{H_t}{H}) \right] \tag{C.74}$$

135

with the celerity in the trenched channel C_{mT} given by

$$C_{mT} = \sqrt{g \cdot H_{mT}}$$ (C.75)

This celerity in turn depends on the effective water depth in the trenched channel H_{mT} from

$$H_{mT} = H - \frac{H_t}{H} \cdot (H - H_m)$$ (C.76)

with mean water depth H_m from

$$H_m = \frac{A_c}{W_{top}}$$ (C.77)

The mean water depth H_m is a standard hydraulic parameter which is required only for restricted waters and canals. For use in these formulae, W_{top} is the projected width of the trapezoidal cross-section of the channel at the SWL (as shown in Figure C.6 where the sides of the trench are projected upward to the SWL); W_{top} is given by

$$W_{top} = W + 2 \cdot n \cdot H$$ (C.78)

Here A_c is the cross-sectional area of the trenched channel so it is given by the product of the total depth H and the mean of the top width W_{top} and the bottom width W, thus

$$\overline{W} = W + n \cdot H$$ (C.79)

and

$$A_c = \overline{W} \cdot H = H \cdot (W + n \cdot H)$$ (C.80)

The blockage ratio S is then given approximately by

$$S = \frac{A_s}{A_c} = \frac{b \cdot T}{\overline{W} \cdot H} = (\frac{b}{\overline{W}}) \cdot (\frac{T}{H})$$ (C.81)

or more precisely by

$$S = \frac{A_s}{A_c} = C_m \cdot (\frac{b}{\overline{W}}) \cdot (\frac{T}{H})$$ (C.82)

if the midship area coefficient C_m is known. As before we get K_{ch} from (C.11) and K_c from (C.60). We next calculate V_{cr} from (C.74) then calculate Δz_b using (C.8) and Δz_s using (C.9).

C.8.2   Barrass 2006

In neither his 2004 book nor his 2006 book does Barrass provide a specific formula for calculating the blockage ratio S for a trenched channel. For a rectangular river section he uses a factor K which is given by (C.61). The implication seems to be that for the same values of S and K, the predicted sinkage will be the same whether the ship is in a rectangular river section or a trapezoidal canal or a trenched channel.

C.8.3   Barrass 2009

It may be useful for trenched channels to use Barrass' 2009 version of the channel coefficient K given in (C.64) on page 122 with his formula for δ_{max} in (C.63). Again we need a method for calculating the blockage ratio S for a trenched channel as identified above in Section C.8.2.

C.8.4   Ankudinov 2009

For a trenched channel, we need to include the trench-height parameter H_t then the blockage ratio S_h is modified to include the effect of H_t/H and this is formulated as

$$S_h = C_b \cdot S \cdot (\frac{T}{H}) \cdot (\frac{H_t}{H}) \tag{C.83}$$

Then the new values for P_{Ch1} and P_{Ch2} and n_{Tr} need to be calculated using (C.67), (C.68) and (C.69) respectively as for the trapezoidal canal. Finally the expressions (C.70) and (C.71) above for the vessel midship sinkage S_m and vessel trim, respectively, are used to calculate the response in the trenched channel.

C.8.5   Yoshimura 2009

How to use the V_e version in (C.73) and apply it to a trenched channel if there is no geometric diagram or expression provided for calculating S for a trenched channel? Page 32 of the Japan Fairway document [7] says that for trenched channels of the type shown in Figure C.7 the depth of the outer water is D_{out} and the depth of the fairway is D hence h_1 is used as the ratio of D_{out} to D. The value H_t in Figures C.6 and C.7 is simply $D - D_{out}$. From h_1 the value h_f is defined to be a correction coefficient where

$$h_f = \exp\left[\frac{-2 \cdot h_1}{(1 - h_1)}\right] \tag{C.84}$$

An alternative might be to use the same value of W_{top} as one would for an open-water calculation, then use Figure C.6 to define the cross-sectional area of the trenched channel A_c; this would have the advantage that one could see immediately the effect of the ratio (H_t/H) on the blockage ratio S. A third possibility might be to look carefully at Ankudinov's approach in (C.83) for S_h to see if that modified S, or a variant, might be usable; this approach might require plotting Römisch's $S(A_c)$ versus Ankudinov's S_h to see if there is a usable relationship. An extension of this sort for Yoshimura's squat formula (C.73) could be explored in a future phase of this project.

C.8.6   Huuska and Guliev 1976

The Huuska and Guliev formulation for a trenched channel is the only formulation which relates specifically to tests which were performed with five variants in the height H_t of the

trench; see [50]. For a trenched channel the value of K_s for (C.54) is, instead of (C.55), given by

$$K_s = 7.45 \cdot s_1 + 0.76 \qquad\qquad (C.85)$$

when the blockage factor s_1 is greater than 0.03, and by

$$s_1 = \frac{S}{K_1} \qquad\qquad (C.86)$$

Again S is the ratio of A_s to A_c used above in (C.52) or (C.53) for the trapezoidal canal. In their experiments, the results measured for the trenched channel were expressed as a multiple of the results measured for the trapezoidal canal with the same bottom-width W and side-slope factor n. Here the correction factor K_1 is given by Guliev's plot of K_1 versus S for different trench-height ratios H_t/H shown in Figure C.13. A curve-fit fit of these values is given by

$$K_1 = 1 + a_1 \cdot S + a_2 \cdot S^2 + a_3 \cdot S^3 \qquad\qquad (C.87)$$

valid for $0 < S < 0.25$. Thus in this approach, one calculates S using (C.81) or (C.82) based on W_{top} as in (C.78) being the projected width of the trapezoidal cross-section of the channel at the SWL (as shown in Figure C.6 where the sides of the trench are projected upward to the SWL) and $\overline{W}$ in (C.79) and A_c in (C.80). Given the requisite value of the ratio H_t/H and the calculated value of S, one can interpolate between the curves in Figure C.13 to obtain a suitable value for K_1. Finally (C.86) is used to find s_1 and (C.85) is used to find K_s for use in (C.54) on page 121 to obtain an estimate of the bow squat.
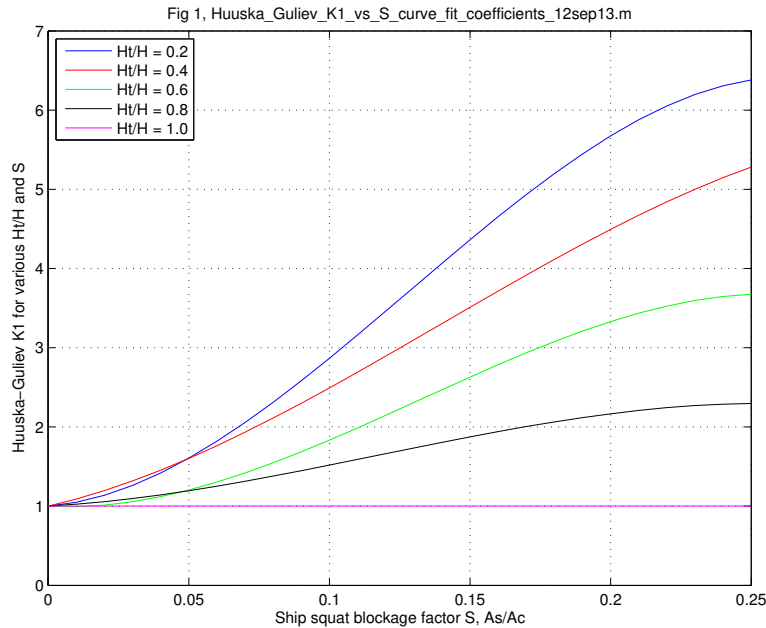
Figure C.27: Curves of K_1 versus blockage ratio S for trenched channels for the Huuska-Guliev formula

In the Appendix to [41] there is a graph and a table of values for the coefficients a_1 to a_3 for each of the five values of H_t/H. That table is repeated below as Table C.6 and it forms the basis for the five curves shown in Figure C.27.

Table C.6: Values of curve-fit coefficients for Huuska and Guliev $K_1(S)$

Ht/H	a_1	a_2	a_3
0.2	2.7704	214.87	-559.42
0.4	8.0885	89.87	-214.88
0.6	-1.9528	137.6	-347.93
0.8	1.9453	45.325	-129.48
1.0	1.0	1.0	1.0

C.9   Examples for Trenched Channels

The Panama Canal expansion project (also called the Third Set of Locks Project) will double the capacity of the Panama Canal by 2015 by creating a new lane of traffic and allowing more and larger ships to transit. At present there are no examples of predictions for

trenched channels but some are planned using the dimesions of the channel modifications (widening and deepening) of the Panama Canal.

It is proposed that in Figure C.6 for trenched channels that the same value of W_{top} should be used as in a corresponding calculation for open-water conditions. In this approach one could immediately see the effect of the ratio (H_t/H) on the blockage ratio S. This approach and examples could be investigated in a future phase of this project.

C.10   Sensitivity Analyses

One metric for the scatter in the 31 scaled "measurements" for the squat of each ship in the Panama Canal is the SST, which is the sum of the squares of the deviations of each of the 31 squat measurements from the mean value of the squat measurements. For the Elbe tanker the value of SST is 0.22 m; for the Global Challenger bulk carrier the SST is 0.56 m; for the Majestic Maersk container ship the SST is 2.20 m, and, for the OOCL Fair container ship the SST is 0.24 m. However the range of measured speeds was not the same for all four ships, so if one divides by the speed range [kt] one gets Elbe 0.12, Global Challenger 0.55, Majestic Maersk 0.51 and OOCL 0.11, so OOCL has "smallest scatter".

In [57] near the bottom of page 9 it says that there are "channel area variations at each measurement location along the Panama Canal". In [45] on page 75 it is stated that "a large source of error or uncertainty is in the measurements of water levels and depth". Thus it is possible that variations in the bathymetry of the canal affected the measurements of full-scale squat.

For this reason it was decided to explore whether variations in the water depth H, variations in the width of the channel bottom W, and, variations in the side-slope parameter n might account for the scatter in the squat measurements.

Given the performance of the Barrass predictions in Section C.7 concerning the full-scale DGPS measurements of ship squat in the Panama Canal, it was decided to explore whether or not the Barrass formula could be used to show whether such changes in H, W and n could explain the observed scatter in the DGPS measurements of ship squat.

Initially the effects of increasing (or decreasing) the water depth H by 10 percent, the width of the channel bottom W by 10 percent, and, the value of the side-slope parameter n by 10 percent were considered. The purpose was to determine whether or not such variations in these parameters could produce prediction curves which would "bracket" the measured values of either bow or stern squat.

Figure C.28 shows seven curves which represent the effects of changing the value of only one of these three parameters at a time, on the predicted bow squat of the Elbe tanker. In
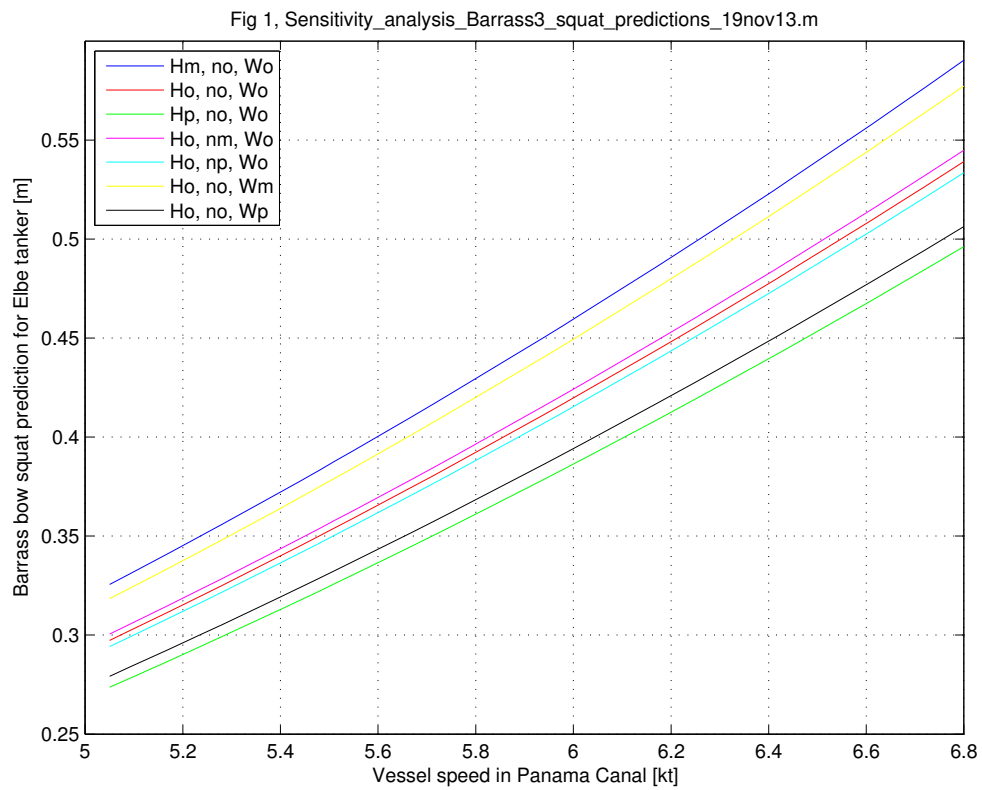
Figure C.28: Elbe tanker, Barrass squat sensitivity based on variations in parameters of a trapezoidal canal

this figure, the red curve is the original curve for (Ho,no,Wo). The strongest effect is that of changing H by 10 percent. The squat curve shifts upward from the red curve to the blue curve when the water depth H is decreased. When H is increased, the squat decreases to the green curve. The blue curve shows that a 10 percent decrease in H produces a 9.49 percent increase in squat, at all speeds. The green curve shows that a 10 percent increase in H produces a 8.64 percent decrease in squat, at all speeds.

Figure C.28 also shows that the second strongest effect is that of changing W by 10 percent. The squat curve shifts upward from the red curve to the yellow curve when the width of the bottom of the channel W is decreased. When W is increased, the squat curve shifts downward from the red curve to the black curve. The yellow curve shows that a 10 percent decrease in W produces a 7.09 percent increase in squat, at all speeds. The black curve shows that a 10 percent increase in W produces a 6.48 percent decrease in squat, at all speeds.

Figure C.28 also shows that the smallest effect is that of changing the reciprocal of the side-slope n by 10 percent. The squat curve shifts upward from the red curve to the magenta curve when n is decreased since the channel cross-sectional area A_c decreases and the blockage factor S increases. When n is increased, the channel cross-sectional area A_c increases and the blockage factor S decreases so the squat curve shifts downward from the red curve to the cyan curve. The magenta curve shows that a 10 percent decrease in n produces a 1.07 percent increase in squat, at all speeds. The cyan curves shows that a 10 percent increase in n produces a 1.05 percent decrease in squat, at all speeds.

For the Barrass prediction curves for the Elbe tanker shown in Figure C.29 , it was found that by (a) increasing the water depth H by 10 percent and increasing the width of the channel bottom W by 10 percent, and, (b) reducing the water depth H by 10 percent and reducing the width of the channel bottom W by 20 percent, two curves could be constructed which would contain 27 of 31 measured values of bow squat. This shows that natural variations of this magnitude of these two parameters might explain the scatter in the measured values of bow squat for this ship.

How likely is the channel bottom width W to increase (or decrease) by 10 percent along the Gaillard Cut? Probably this is the most likely effect.

How likely is the channel side-slope parameter n to increase (or decrease) by 10 percent along the Gaillard Cut? Since $n = \cot(\theta)$, a ten percent increase in n from 1.88 to 2.068 would require a decrease in the side-slope angle (measured from the horizontal) from 28.0 to 25.8 degrees, an 8.5 percent change. Would mud-slides or rock-slides produce such a change in the angle of repose of the side-bank material?

The answers to these questions as to whether such variations in water depth, channel
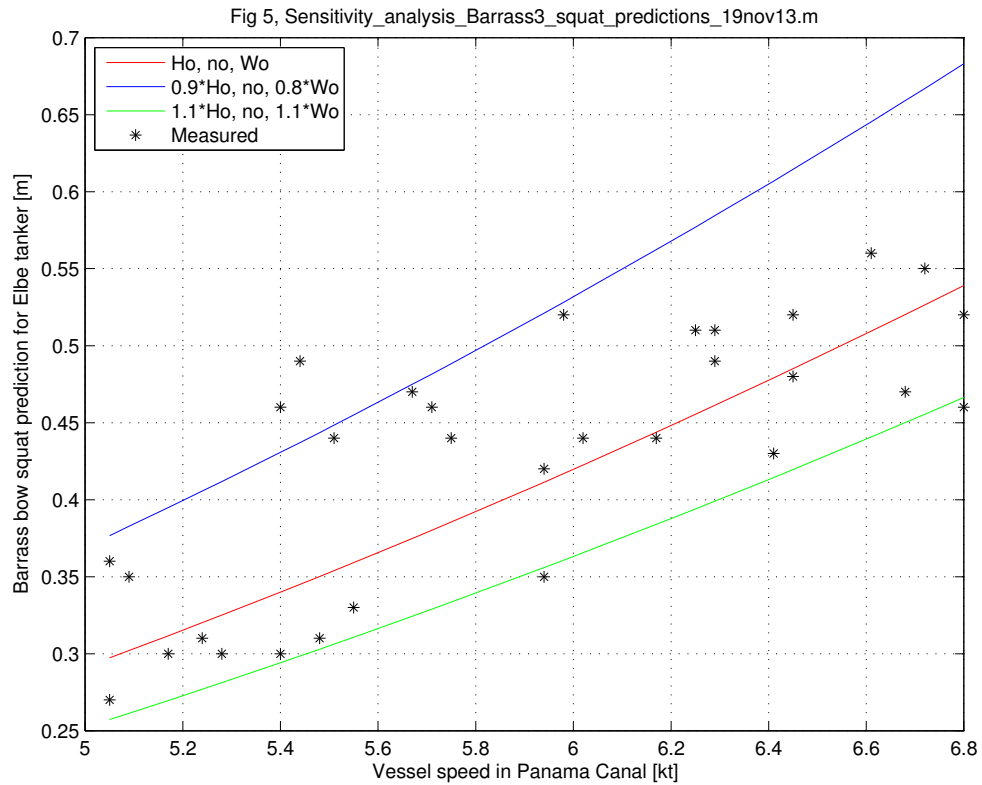
Figure C.29: Elbe tanker, squat measurements and range of Barrass predictions based on variations in parameters of a trapezoidal canal

width and side-slope actually occur in the Gaillard Cut portion of the Panama Canal, and, whether these variations can be correlated with the stations at which the DGPS measurements were made, could be considered in a future phase of the NRIM project, if NRC can gain access to relevant bathymetric data for that canal.

C.11   Other Verifications

Included here are four graphs which show the effect of changing the 'width of influence' W_{eff} in the predictions for unrestricted uniform-depth shallow-water conditions. The purpose of this examination is to determine how sensitive such open-water results are to the assumed 'width of waterway' at the SWL. The results of this analysis will indicate what sort of accuracy is required in bathymetric and map-based channel-width measurements for future squat simulations.

Figure C.30: Predictions for VLCC bow squat for various values of the river width of influence W_{eff}

Figure C.30 shows how the 'breadth of water' (BoW) (aka 'width of influence' W_{eff}) affects the predicted bow squat (using the Barrass short-cut formula for open-water squat from either page 153 of [47] or page 334 of [48] for a VLCC for water-depth to draft ratio (H/T) of 1.10 in an unrestricted uniform-depth shallow-water condition. Figure C.31 shows the stern squat for the same ship under the same conditions. Figure C.32 shows the trim angle for the same ship under the same conditions.
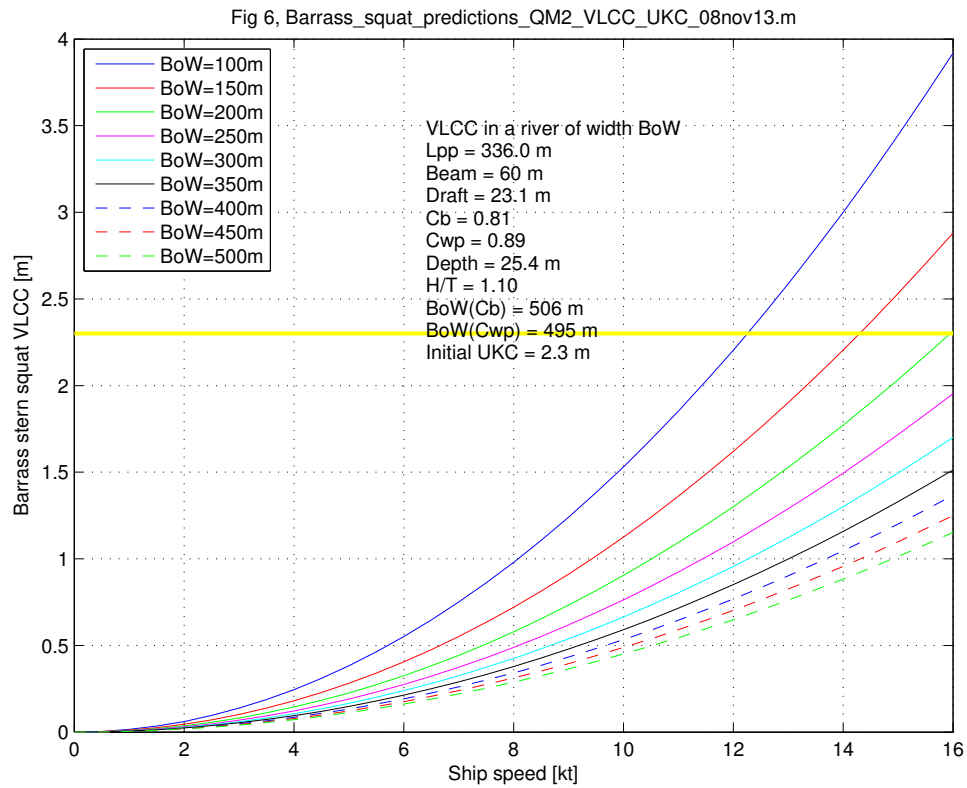
Figure C.31: Predictions for VLCC stern squat for various values of the river width of influence W_{eff}

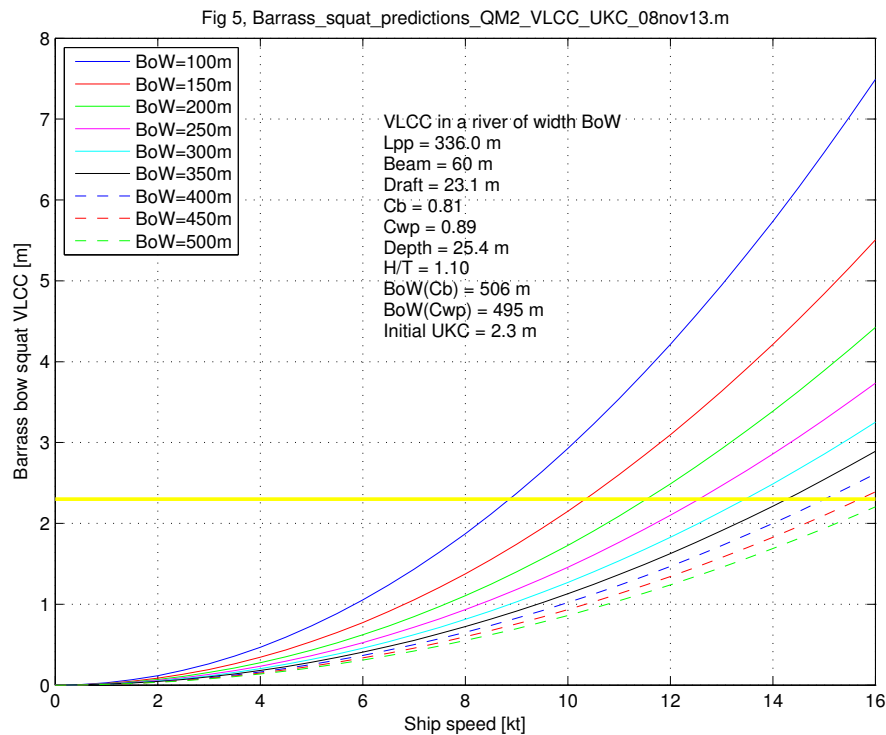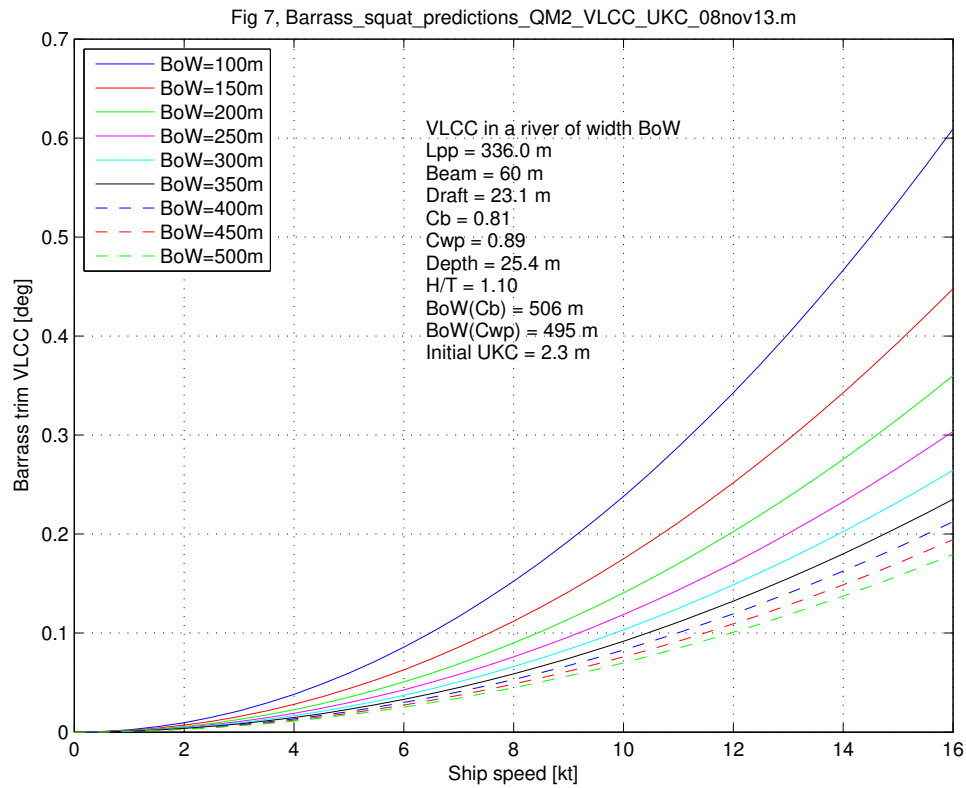Figure C.32: Predictions for VLCC trim angle for various values of the river width of influence W_{eff}
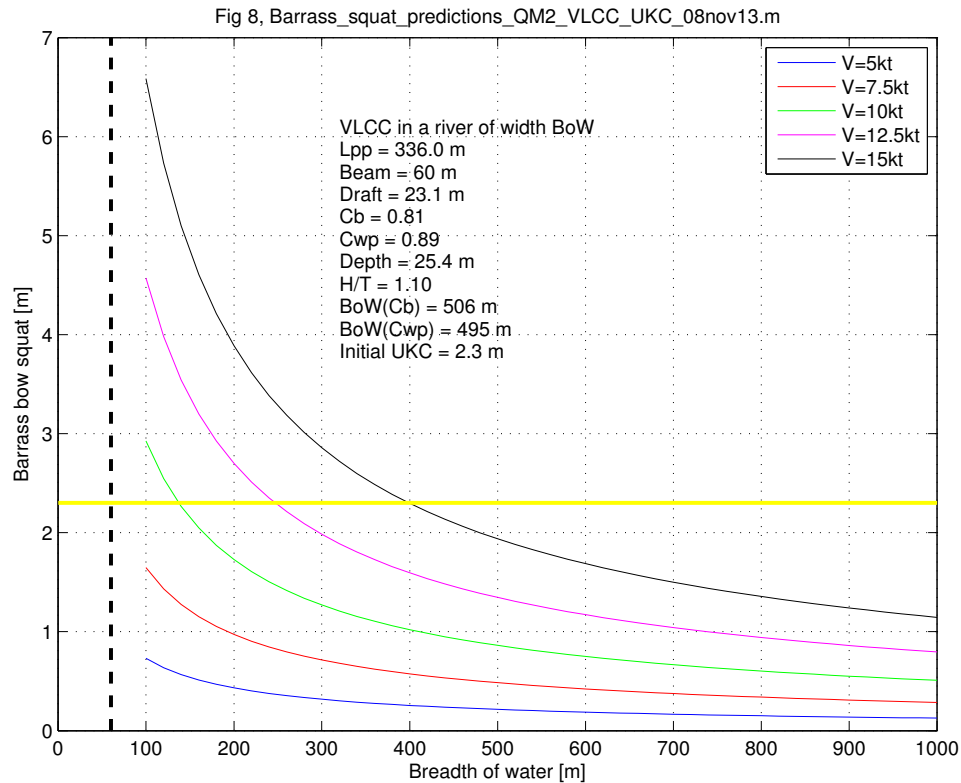
Figure C.33: Predictions for VLCC bow squat for various values of speed and river width of influence W_{eff}

Figure C.33 shows the bow squat plotted versus increasing 'BoW' for five different values of constant speed. In each curve the in UKC is show as a horizontal line so that where a squat curve intersects this horizontal line indicates that bow-grounding or stern-grounding is likely to occur. Equation (C.24) shows that the blockage ratio S is inversely proportional to the 'BoW'. But with an exponent for S such as 0.81 in equation (C.26), ultimately the squat is inversely proportional to W_{eff} to the 0.81 power. Thus a ten-percent increase in W_{eff} produces about a seven-percent decrease in the predicted squat.

C.12 Regression Analysis

We expect that squat prediction formulae should contain factors such as (a) the water-depth-to-draft ratio (H/T), and, (b) the ship-beam-to-channel-width ratio (b/W). Only when 3D effects are incorporated into a squat formula would the ship length L_{pp} appear in ratios such as (L_{pp}/b), (L_{pp}/T), (L_{pp}/H) and (L_{pp}/W). Similarly parameters which represent the underwater shape of the hull such as the displaced volume of the ship ∇, the block coefficient C_b, the transverse vertical-plane cross-sectional area A_s, and, the waterplane area A_{wp}, are additional 3D effects which could be included. From the perspective of the waterway, clearly the water-depth H and width of the canal bottom W and the height of the trench H_t should enter in ratios such as H/T, Ht/H and W/b and others.

All these parameters (and more) have been included in previous statistical regression analyses of both model-scale and full-scale squat measurements; notable recent examples are [51] and [52] and [53]. The results of such analyses are not included in this report at this time but may be considered in a later phase of this project.

C.13 Observations, Cautions, Conclusions

Since the volume of water ∇ which is displaced by a ship's hull is given by

$$\nabla = C_b \cdot b \cdot T \cdot L_{pp} \tag{C.88}$$

it is seen that in open water conditions the Hooft, Huuska and Guliev, ICORELS, Norrbin and Ankudinov formulae, as well as both Millward formulae and all four Barrass formulae, all predict that the bow squat is directly proportional to the value of the ship's block coefficient C_b. The Römisch formula has the bow squat proportional to the square of C_b while Yoshimura has the bow squat proportional to the sum of a term which is proportional to C_b and a term which is proportional to C_b cubed. Thus it is important to know the value

Table C.7: Mean and standard deviation for C_b for a large number of ships of eight types

Type	Mean	Sigma	Range
Passenger ship	0.591	0.0595	0.53 to 0.65
Pure car carrier	0.594	0.0665	0.53 to 0.66
Roll-on, Roll-off ship	0.667	0.0939	0.57 to 0.76
Container ship	0.668	0.0472	0.62 to 0.72
LNG ship	0.716	0.0399	0.68 to 0.76
LPG ship	0.737	0.0620	0.67 to 0.80
Cargo ship	0.804	0.0712	0.73 to 0.88
Oil tanker	0.824	0.0381	0.79 to 0.86

of this parameter for each ship with some certainty. The Japan Fairway documentation

provides some guidance as to what value of C_b applies to eight types of ships, as shown in Table C.7, along with the values of the standard deviation of the variation of C_b about the stated average value. The last column in this table contains the likely range of values for C_b based on the 'mean $\pm$ one sigma'.

The Barrass (1979, 1981) formula for W_{eff} requires the value of the ship's waterplane area coefficient C_{wp} in equation (C.22), and, similarly the exact formula for the ship's midship transverse vertical-plane cross-sectional area A_m requires knowledge of the ship's midship area coefficient C_m. Table C.8 provides typical values for those coefficients for seven types of naval vessels and 21 types of commercial vessels.

As a result of this preliminary investigation, it is not possible to recommend the use of any particular formula for any particular type of ship for any particular configuration of a waterway. Until these predictive formulae can be validated either through comparison with full-scale or model-scale measurements of the changes in ship sinkage and trim due to shallow-water and bank-confinement effects, the NRC will not be in a position to make such recommendations.

Table C.8: Typical Coefficients of Form for Various Types of Ships

Type of Ship	Block Coefficient C_b	Midship Area Coefficient C_m	Waterplane Area Coefficient C_{wp}
Navy Ships			
Aircraft Carrier (CV-59 Class)	0.578	0.984	0.729
Battleship (BB-61 Class)	0.594	1.000	0.694
Cruiser (CGN-38 Class)	0.510	0.810	0.780
Destroyer (DD-963 Class)	0.510	0.850	0.760
Frigate (FFG-7 Class)	0.470	0.770	0.750
Replentishment Ship (AOR-1 Class)	0.652	0.981	0.777
Salvage Tug (ARS-50 Class)	0.542	0.908	0.791
Commercial Vessels			
General Cargo (slow-speed)	0.800	0.992	0.880
General Cargo (medium-speed)	0.700	0.980	0.810
General Cargo (high-speed)	0.576	0.972	0.695
Tanker (35,000-ton DWT)	0.757	0.978	0.845
Large Tanker (76,000-ton DWT)	0.802	0.997	0.874
VLCC (250,000 ton DWT)	0.842	0.996	0.916
Container Ship	0.600	0.970	0.740
RO-RO	0.568	0.972	0.671
Ore Carrier	0.808	0.995	0.883
Great Lakes Bulk Carrier	0.900	0.995	0.950
Passenger Liner	0.530	0.956	0.690
Barge Carrier	0.570	0.950	0.820
Large Car Ferry	0.530	0.910	0.680
Ocean Tug, Trawler	0.550	0.833	0.850
Offshore Supply Vessel	0.660	0.906	0.892
Harbour Tug	0.585	0.892	0.800
Ocean Power Yacht (76 m LWL)	0.565	0.938	0.724
Large Passenger Ship	0.710	0.973	0.980
RMS Titanic	0.684	0.970	0.766
Cruise Ship (design project)	0.605	0.981	0.835
Cruise Ship (STX Class 2006)	0.655	0.989	0.850

C.14   Recommendations for Further Work

1. Develop appropriate diagrams and geometrical descriptions for several configurations of trenched channels. The purpose is to simplify and make available specific expressions for calculating the cross-sectional area of such channels, so as to simplify the calculation of the blockage ratio S for such channels. The intent is to provide a smooth transition in S from trenched, trapezoidal and rectangular channels to unrestricted waterways.

2. At present there are no examples in this report of predictions for trenched channels but some are planned using the dimensions of the channel modifications (widening and deepening) of the Panama Canal. This work could be performed in a future phase of this project.

3. If access could be provided to full-scale measurements of squat in the St. Lawrence Seaway as reported in [42, 43] and in [49], and, in the Panama Canal as reported in [57] and [45], then validation of many of the formulae used in this preliminary investigation could begin to take place.

4. When using existing squat formulae, the GUI for NRIM could provide a choice of averaging across multiple formulae at each vessel speed. Perhaps the plots of predicted squat versus vessel speed include (i) the mean curve and (ii) a band of width plus-and-minus one standard deviation based on the range of predicted values at each vessel speed. This item could be investigated in a future phase of this project.

Table C.9: Table of symbols, descriptions and units

Symbol	Description	Units	Definition or Equation
A_c	Cross-sectional area of the water in a channel without the ship being present	m^2	21
A_m, A_s	Transverse, vertical-plane cross-sectional area of the ship	m^2	23
A_w	The difference between the cross-sectional area of the channel and the ship, $A_c - A_m$	m^2	25
b	Ship's beam (breadth)	m^2	-
C_b	Ship's block coefficient	-	-
C_m	Ship's midship area coefficient	-	-
C_{wp}	Ship's waterplane area coefficient	-	-
F_{nh}	Froude Number based on ship's forward speed and water depth	-	1
g	Acceleration due to gravity	m/s^2	9.81
H	Overall depth of the waterway	m	Figs C.3 to C.11
H_t	Height of the trench measured from the bottom of the channel	m	Figs C.6, C.7
K	Barrass channel coefficient	-	57, 60
K_b	Eryuzlu correction factor for channel width	-	41
K_s	Huuska and Guliev correction factor for ship blockage	-	51
K_1	Huuska and Guliev correction factor for channel trench-height	-	83
L_{pp}	Ship's length between perpendiculars		Fig C.12
n	Reciprocal of channel bank side-slope, n = run/rise = $\cot(\theta)$	-	Figs C.5, C.6, C.7
S	Blockage ratio, S = A_s/A_c	-	24
S_2	Modified blockage ratio, $S_2 = S/(1-S)$	-	25
T	Ship's draft	m	Fig C.12
V	Ship's forward speed	m/s	-
V_{cr}	Ship's critical speed in Romisch formulae	m/s	10
V_e	Ship's forward speed in Yoshimura formula	m/s	68
V_k	Ship's forward speed	knot	Page 103
V_s	Ship's forward speed	m/s	Page 103
W	Width of bottom of canal or channel	m	Figs C.5 to C.11

W_{eff}	Effective width-of-influence at the still water level (SWL)	m	22, 27, 28
W_{top}	Effective width-of-influence at the SWL in a trenched channel	m	74
$\overline{W}$	Mean width of a trenched channel based on W_{top}	m	75

Greek Symbols

δ_{max}	Maximum sinkage due to squat effect	m	26
Δz_b	Bow squat	m	2
∇	Volume of water displaced by the ship's hull	m^3	84
θ	Angle of the side-bank of a channel, measured from the horizontal	deg	Figs C.5, C.6, C.6